On the Convexity and Reliability of the Bethe Free Energy Approximation

Harald Leisenberger

HARALD.LEISENBERGER@TUGRAZ.AT

Signal Processing and Speech Communication Laboratory Graz University of Technology Graz, Austria

Christian Knoll

CHRISTIAN.KNOLL@TUGRAZ.AT

Signal Processing and Speech Communication Laboratory Graz University of Technology Graz, Austria

Franz Pernkopf

PERNKOPF@TUGRAZ.AT

Signal Processing and Speech Communication Laboratory Graz University of Technology Graz, Austria

Abstract

The Bethe free energy approximation provides an effective way for relaxing NP-hard problems of probabilistic inference. However, its accuracy depends on the model parameters and particularly degrades if a phase transition in the model occurs. In this work, we analyze when the Bethe approximation is reliable and how this can be verified. We argue and show by experiment that it is mostly accurate if it is convex on a submanifold of its domain, the 'Bethe box'. For verifying its convexity, we derive two sufficient conditions that are based on the definiteness properties of the Bethe Hessian matrix: the first uses the concept of diagonal dominance, and the second decomposes the Bethe Hessian matrix into a sum of sparse matrices and characterizes the definiteness properties of the individual matrices in that sum. These theoretical results provide a simple way to estimate the critical phase transition temperature of a model. As a practical contribution we propose BETHE-MIN, a projected quasi-Newton method to efficiently find a minimum of the Bethe free energy.

Keywords: Variational Inference, Bethe Free Energy Approximation, Probabilistic Graphical Models, Quantum Mechanics, Mathematical Foundations of Machine Learning.

1 Introduction

Statistical models from quantum mechanics have experienced an increasing popularity in real-world applications (MacKay, 2003; Zdeborová and Krzakala, 2016). Many of the practical challenges can be modeled by a graph and require the solution of fundamental probabilistic problems, such as the computation of the partition function or marginal probabilities. However, an exact solution to these problems is only available for restricted model classes; e.g., the one- and two-dimensional Ising model (Ising, 1925; Onsager, 1944) or small systems (Lauritzen and Spiegelhalter, 1988). Generally, one needs to apply approximation methods whose specific choice is often a compromise between efficiency and accuracy.

A large class of approximation algorithms relies on variational inference and the Gibbs variational principle (Mezard and Montanari, 2009; Wainwright et al., 2008). First, probabilistic inference is formulated in terms of an optimization problem with respect to the so-called variational Gibbs free energy; then, to relax the problem complexity, one optimizes a simpler objective that approximates the solutions to the inference problem. This framework has its origin in quantum mechanics and mean-field theory (Parisi, 1988), and has been successfully adopted to computer science (Jordan et al., 1999; Yedidia et al., 2005).

One important aspect is the choice of the auxilary objective to be optimized. On the one hand, it should be simple enough to entail a true relaxation of the NP-hard inference problem. On the other hand, a too simple objective might not capture the global behavior of the model well enough. Over time, different types of free energy approximations have been proposed, with the Bethe (or Bethe-Peierls) approximation being one popular representative that often proves to be superior to other constructions in terms of a tradeoff between efficiency and accuracy (Bethe, 1935; Peierls, 1936). It only considers effects between interacting variables, while ignoring long range correlations at the cost of an information loss; still, it often yields accurate results ¹ (Frey and MacKay, 1997; Murphy et al., 1999).

The quality of the Bethe approximation strongly varies between different models and particularly suffers from multiple and strong interactions in the graph. From a physisist's perspective this is due to a low model temperature; we may thus interpret a sudden decrease in its accuracy at some critical temperature as a phase transition in the model. This unwanted behavior of the Bethe approximation is well known and has often been observed in the literature (Meshi et al., 2009; Weller et al., 2014; Leisenberger et al., 2022); however, a precise quantification of its reliability (e.g., in terms of some critical temperature) is an open problem ². Another prohibitive factor is the practical minimization of the Bethe free energy which – despite being a relaxation to the Gibbs free energy – can be difficult.

In this work, we analyze the reliability of the Bethe approximation. We show when can expect its provided estimates of the partition function and marginals to be accurate. For that purpose, we distinguish between different 'stages' of the Bethe free energy: convexity, non-convexity but uniqueness of a minimum, and multiple minima. Based on this differentiation, we assess the quality of the Bethe approximation with respect to its stage.

The intuition for this split lies in the Gibbs variational principle: While the Gibbs free energy is convex on its domain, this is not guaranteed for the Bethe free energy. We aim to show that the Bethe approximation is accurate, whenever it is convex as well. Moreover, we examine if it is still accurate if the model temperature decreases, i.e., if the Bethe free energy changes its stage – from convex to non-convex (but uniqueness of a minimum), and later to multiple minima. To perform this analysis, we must determine the stage of the Bethe

^{1.} Often, the quality of the Bethe approximation is analyzed in terms of the loopy belief propagation (LBP) algorithm; a so-called message passing algorithm whose relationship to statistical mechanics and the Bethe free energy has been established by Yedidia et al. (2001).

^{2.} Sometimes the success of the Bethe approximation is attributed to the uniqueness of its minimum (Mooij and Kappen, 2004). However, we will show that this can be an inaccurate assumption.

free energy in a certain state of the model. While there exist methods to prove the uniqueness of a minimum (e.g., Mooij and Kappen (2007)), this is not the case for its convexity. We address this open issue by deriving two sufficient conditions for convexity of the Bethe free energy on an appropriately defined submanifold of its domain, the 'Bethe box'. Both results rely on a profound second-order analysis of the Bethe free energy, by characterizing the definiteness properties of its Hessian. They also provide estimates for a phase transition (i.e., the temperature at which the accuracy of the Bethe approximation begins to degrade).

Our first result includes conditions under which the Bethe Hessian is diagonally dominant and hence positive definite (Sec. 3.2). The starting point of this analysis is to reformulate diagonal dominance as a set of optimization problems, each defined on a local neighborhood of the graph. By analyzing these problems, we reduce the question of diagonal dominance of the Bethe Hessian to the positivity of a certain set of one-dimensional polynomials.

Our second result decomposes the Bethe Hessian into a sum of simpler matrices and characterizes the definiteness properties of the individual matrices in that sum (Sec. 3.3). We consider a natural decomposition into 'edge-specific Hessians' that represent the curvature of the Bethe free energy on individual edges and their end nodes. This specific choice induces a closed-form characterization of positive definiteness that is based on their determinant.

We conclude the theoretical part of this work by comparing our two conditions to similar results from the literature (Sec. 3.4). Specifically, we consider a complete graph with a perfectly symmetric potential configuration; a well understood model whose simplicity facilitates such a direct comparison. On this model, our second condition is exact in the sense that it correctly predicts the critical temperature at which a phase transition occurs.

After having established the theoretical framework, we perform an experimental analysis in which we evaluate the performance of the Bethe approximation on various graphical models. Specifically, we consider spin glasses (also known as general or mixed models) on graphs that either have a lattice or a random structure. For minimizing the Bethe free energy, we propose a 'projected quasi-Newton' algorithm (named BETHE-MIN, Sec. 4).

Our experiments show that the Bethe approximation is mostly accurate if it is convex. If the temperature decreases, the Bethe free energy changes its state while it also becomes much less accurate at some point. We demonstrate that the estimated temperature at which the Bethe free energy becomes non-convex often provides a good estimate of this phase transition. These experiments help to assess, whether the Bethe approximation is reliable or not.

This paper is structured as follows: Sec. 2 provides all relevant notations and background. Sec. 3 includes the theoretical part of this work in which introduce all details on the Bethe free energy and discuss its characteristics that are known from the literature. Afterwards, we derive our two sufficient conditions for convexity of the Bethe free energy, before we discuss their properties on the symmetric model. Sec. 4 includes the practical part of this work. We first explain our algorithm BETHE-MIN for minimizing the Bethe free energy,

which we then use in our experiments to analyze the quality of the Bethe approximation with respect to its stage. In Sec. 5 we conclude our work.

2 Background

In this section, we introduce the physical and mathematical concepts and notation that are relevant for this work. This includes matrix algebra and convex functions (Sec. 2.1), models on graphs and the Boltzmann distribution (Sec. 2.2), and the Gibbs and Bethe variational principle for probabilistic inference (Sec. 2.3). We also give an overview of the literature related to our specific research questions (Sec. 2.4).

2.1 Mathematical Preliminaries

A real matrix $\mathbf{M} = (m_{ij})_{i,j=1,...,n}$ of size $n \times n$ is positive definite if $\mathbf{y}^T \mathbf{M} \mathbf{y} > 0$ for all vectors \mathbf{y} in \mathbb{R}^n whenever $\mathbf{y} \neq \mathbf{0}$, and positive semidefinite if $\mathbf{y}^T \mathbf{M} \mathbf{y} \geq 0$ for all \mathbf{y} in \mathbb{R}^n . Equivalently, \mathbf{M} is positive definite if all its leading principal minors 3 are positive (Sylvester's Criterion). The sum of positive definite matrices is positive definite. Furthermore, \mathbf{M} is diagonally dominant if, for each row i, the magnitude of the corresponding diagonal entry is larger than the sum of the magnitudes of all other entries in that row, i.e.,

$$|m_{ii}| > \sum_{j \neq i} |m_{ij}|. \tag{1}$$

A diagonally dominant matrix with positive diagonal entries is positive definite (e.g., (Golub and Van Loan, 2013)).

Let f be a real-valued and twice continuously differentiable function defined on an open, convex set $\mathcal{D} \subseteq \mathbb{R}^n$. Let $\nabla f(\boldsymbol{p}) = \left(\frac{\partial f}{\partial p_1}(\boldsymbol{p}), \dots, \frac{\partial f}{\partial p_n}(\boldsymbol{p})\right)^T$ be the gradient of f and let $\mathbf{H}_f(\boldsymbol{p}) \coloneqq \nabla^2 f(\boldsymbol{p}) = \left(\frac{\partial^2 f}{\partial p_i p_j}(\boldsymbol{p})\right)_{i,j=1,\dots,n}$ be the Hessian matrix of f, each evaluated in some point \boldsymbol{p} of \mathcal{D} . If $\nabla f(\boldsymbol{p}) = \mathbf{0}$, then \boldsymbol{p} is a stationary point of f. A stationary point \boldsymbol{p} is a local minimum (resp., maximum) of f if $\mathbf{H}_f(\boldsymbol{p})$ (resp., $-\mathbf{H}_f(\boldsymbol{p})$) is positive definite, and it is a saddle point if neither $\mathbf{H}_f(\boldsymbol{p})$ nor $-\mathbf{H}_f(\boldsymbol{p})$ are positive definite. We define f to be strictly convex on \mathcal{D} if \mathbf{H}_f is positive definite f for all f in f. In that case, f has at most one local (and thus global) minimum in f (e.g., Rockafellar (1970)).

2.2 Model Specification

We consider a finite system of N variables X_1, \ldots, X_N with an identical configuration space $\mathcal{X}_i = \mathcal{X}$ describing the possible states of individual variables. A configuration $\boldsymbol{x} = (x_1, \ldots, x_N)$ in the product space $\mathcal{X}^N = \mathcal{X} \times \cdots \times \mathcal{X}$ thus represents one possible state of the

^{3.} A leading principal minor is the determinant of a $(k \times k)$ - submatrix of **M**, consisting of the first k rows and columns of **M** (for k in $\{1, \ldots, n\}$).

^{4.} This criterion is often easier to work with than the more common yet equivalent definition of strict convexity: f is strictly convex on \mathcal{D} if, for any pair of distinct points p_1, p_2 in \mathcal{D} , the straight line that connects $f(p_1)$ and $f(p_2)$ lies above the curve of f between p_1 and p_2 , i.e., $\gamma f(p_1) + (1 - \gamma)f(p_2) > f(\gamma f(p_1) + (1 - \gamma)f(p_2))$ for $0 < \gamma < 1$.

entire system. A real-valued energy function $E(\mathbf{x})$ characterizes the behavior of the system by assigning each system state to its energy. Then the Boltzmann distribution is defined as

$$p_{\beta}(\mathbf{x}) = \frac{1}{Z(\beta)} e^{-\beta E(\mathbf{x})},\tag{2}$$

where $\beta = \frac{1}{T}$ is the inverse temperature ⁵ of the system and $Z(\beta)$ is the (temperature dependent) normalization constant, known as partition function. Hence, $p_{\beta}(x)$ gives the probability that the system is found in state x. We focus on an important class of models, satisfying the following conditions:

- Variables are described in terms of their spin which takes one of two states (an *Ising spin*). The configuration space is thus $\mathcal{X} = \{+1, -1\}$.
- Variables interact in pairs only. Specifically, we distinguish between *ferromagnetic* (the spins are aligned) and *antiferromagnetic* (the spins are anti-aligned) interactions.
- An external (not necessarily uniform) magnetic field θ_i additionally influences the spin of variables.
- A graph $\mathbf{G} = (\mathbf{X}, \mathbf{E})$ models the structure of the system. Its node set ${}^{6}\mathbf{X} = \{X_{1}, \ldots, X_{N}\}$ represents the variables and its edge set \mathbf{E} represents all interacting pairs of variables. Depending on the kind of interaction, we call edges ferromagnetic or antiferromagnetic. Furthermore, let $\mathcal{N}(i)$ be the neighborhood of X_{i} in the graph (i.e., the set of all variables interacting with X_{i}) and $d_{i} = |\mathcal{N}(i)|$ be the degree of X_{i} .

Under these assumptions, the energy function E(x) decomposes into a sum of pairwise and single terms:

$$E(\mathbf{x}) = \sum_{(i,j)\in\mathbf{E}} E_{ij}(x_i, x_j) + \sum_{i\in\mathbf{X}} E_i(x_i) = -\sum_{(i,j)\in\mathbf{E}} J_{ij}x_ix_j - \sum_{i\in\mathbf{X}} \theta_i x_i.$$
(3)

The couplings J_{ij} are positive if X_i and X_j share a ferromagnetic edge, and negative if they share an antiferromagnetic edge. The field θ_i biases the spin of variable X_i towards +1 if $\theta_i > 0$, and towards -1 if $\theta_i < 0$. A model with purely positive (negative) couplings is ferromagnetic (antiferromagnetic); a model with both positive and negative couplings is a spin glass. A spin glass that is defined on a graph which contains cycles with an odd number of antiferromagnetic edges (implying that the local constraints on the involved spin pairs cannot be satisfied simultanously) is called frustrated.

Two fundamentally important problems of probabilistic inference 7 are:

^{5.} Usually the temperature is scaled by k_B , Boltzmann's constant. Without loss of generality we set $k_B = 1$, hence measure temperature in units of energy.

^{6.} With a slight abuse of notation, we usually identify a variable X_i with its representing node i in the graph instead of making an explicit distinction between them.

^{7.} Note that these problems are closely connected, since marginals can be written as a ratio between a 'partial' and the 'true' partition function (Weller and Jebara, 2014b).

(P1) The computation of the partition function:

$$Z(\beta) = \sum_{\boldsymbol{x} \in \mathcal{X}^N} e^{-\beta E(\boldsymbol{x})} \tag{4}$$

(P2) The computation of marginal probabilities of the Boltzmann distribution, primarily of single variables and pairs of variables:

$$p_i(x_i) = \sum_{\boldsymbol{x}' \in \mathcal{X}^N: \boldsymbol{x}' = x_i} p_{\beta}(\boldsymbol{x}') \tag{5}$$

$$p_{i}(x_{i}) = \sum_{\boldsymbol{x}' \in \mathcal{X}^{N}: x_{i}' = x_{i}} p_{\beta}(\boldsymbol{x}')$$

$$p_{ij}(x_{i}, x_{j}) = \sum_{\boldsymbol{x}' \in \mathcal{X}^{N}: x_{i}' = x_{i}, x_{j}' = x_{j}} p_{\beta}(\boldsymbol{x}')$$

$$(6)$$

These problems can be solved efficiently on tree-structured (i.e., acyclic) graphs by using dynamical programming (Gallager, 1962; Pearl, 1988), but are generally NP-hard on loopy (i.e., cyclic) graphs (Valiant, 1979; Cooper, 1990). In that case one needs to approximate the solution. One large class of approximation algorithms is based on variational inference. This approach converts the inference problem into an (also intractable) optimization problem, and afterwards optimizes an auxiliary objective that should be close to the original one. The solution to the auxiliary problem is then used as an estimate of the solution to the inference problem (Jordan et al., 1999; Wainwright et al., 2008). In Sec. 2.3 e present further details on the (Gibbs) variational principle.

2.3 Gibbs Variational Principle and Bethe Approximation

We can address the problems (P1) and (P2) stated in Sec. 2.2 by reformulating them in terms of the Gibbs variational principle (Mezard and Montanari, 2009; Wainwright et al., 2008). The idea is to interpret the partition function and marginals as minima of the variational Gibbs free energy, which is then – due to its intractability – approximated by an 'auxiliary free energy' that is easier to optimize. Examples are the Bethe free energy (Bethe, 1935; Peierls, 1936), the tree-reweighted free energies (Wainwright et al., 2005), and the Kikuchi free energies (Kikuchi, 1951; Pelizzola, 2005; Yedidia et al., 2005), each being defined over different clusters of variables. Their minima can be obtained by numerical optimization and serve as estimates of the solutions to (P1) and (P2).

Instead of directly minimizing an auxiliary free energy, one can alternatively use so-called message passing algorithms. These are iterative procedures on the graph whose fixed points are identical to minima of a certain kind of free energy approximation ⁸. The best-known such relationship is the duality between the Bethe approximation and the loopy belief propagation (LBP) algorithm (Yedidia et al., 2001). We do not primarily deal with LBP in this work, but draw conclusions about its behavior by analyzing the Bethe free energy (Sec. 3).

^{8.} More precisely, each class of message passing algorithm corresponds to a specific type of variational free energy approximation and vice versa.

Let us introduce the Gibbs variational principle and Bethe free energy approximation: Let q(x) be any probability distribution over the product space X^N . Then we define the variational Gibbs free energy as the functional

$$\mathfrak{F}(q) = \mathfrak{U}(q) - \frac{1}{\beta} \mathfrak{S}(q) \tag{7}$$

with the average energy (or expected energy)

$$U(q) = \mathbb{E}_q(E(\boldsymbol{x})) = \sum_{\boldsymbol{x} \in \mathcal{X}^N} q(\boldsymbol{x}) E(\boldsymbol{x})$$
(8)

and the entropy

$$S(q) = -\sum_{\boldsymbol{x} \in \Upsilon^N} q(\boldsymbol{x}) \log q(\boldsymbol{x}). \tag{9}$$

Splitting the Gibbs free energy into the Kullback-Leibler divergence 9 between q and the Boltzmann distribution p_{β} , and the partition function $Z(\beta)$ as

$$\mathcal{F}(q) = \frac{1}{\beta} D(q||p_{\beta}) - \frac{1}{\beta} \log Z(\beta)$$
 (10)

shows that $\mathcal{F}(q)$ is convex and has a unique minimum if q is chosen as p_{β} with the functional value $\mathcal{F}(p_{\beta}) = -\frac{1}{\beta} \log Z(\beta)$ (known as Helmholtz free energy).

While minimizing \mathcal{F} over all distributions q would leave us with an even increased complexity, the idea is to exploit the variational framework and replace \mathcal{F} by a simpler objective. One sophisticated approach is to introduce the Bethe free energy that makes two approximations: First, it relaxes the space of feasible distributions q to a larger space of 'pseudo-distributions' \tilde{p} that must only satisfy local instead of global probability constraints. More precisely, \tilde{p} induces pairwise pseudo-marginals \tilde{p}_{ij} and singleton pseudo-marginals \tilde{p}_i (all normalized) such that, for all pairs $(i, j) \in \mathbf{E}$, summing \tilde{p}_{ij} over all states of variable j (or i) yields \tilde{p}_i (or \tilde{p}_j); on the other hand, global constraints of the form $\sum_{\boldsymbol{x}' \in \mathcal{X}^N : x_i' = x_i, x_j' = x_j} \tilde{p}(x_1', \dots, x_N') = \tilde{p}_{ij}(x_i, x_j)$ and $\sum_{\boldsymbol{x} \in \mathcal{X}^N} \tilde{p}(\boldsymbol{x}) = 1 \text{ need not be satisfied. Formally, we describe the set } \mathbb{L} \text{ of all pseudo-}$

distributions – sometimes called the $local\ polytope\ ^{10}$ – as

$$\mathbb{L} = \{ \tilde{p} : \mathfrak{X}^N \to \mathbb{R}_{>0} \mid \sum_{x_j \in \mathfrak{X}} \tilde{p}_{ij}(x_i, x_j) = \tilde{p}_i(x_i),$$

$$\sum_{x_i, x_j \in \mathfrak{X}} \tilde{p}_{ij}(x_i, x_j) = 1, \sum_{x_i \in \mathfrak{X}} \tilde{p}_i(x_i) = 1,$$
for all $(i, j) \in \mathbf{E}$ and $i \in \mathbf{X} \}.$ (11)

^{9.} The Kullback-Leibler divergence (Cover and Thomas, 1991) measures the 'distance' between two probability distributions p_1 and p_2 over the same configuration space y and is – in the discrete case – defined as $D_{KL}(p_1||p_2) = -\sum_{\boldsymbol{y} \in \mathcal{Y}} p_1(\boldsymbol{y}) \log \left(\frac{p_2(\boldsymbol{y})}{p_1(\boldsymbol{y})}\right)$.

^{10.} Note that \mathbb{L} is a convex set that is bounded by $\mathcal{O}(|\mathbf{X}| + |\mathbf{E}|)$ linear constraints (Wainwright et al., 2008).

Second, the Bethe free energy approximates the entropy S(q) by a simpler expression, the Bethe entropy, that only takes pairwise and local statistics into account. For $\tilde{p} \in \mathbb{L}$, we define the variational Bethe free energy as

$$\mathcal{F}_B(\tilde{p}) = \mathcal{U}_B(\tilde{p}) - \frac{1}{\beta} \mathcal{S}_B(\tilde{p}) \tag{12}$$

with the Bethe average energy

$$\mathcal{U}_B(\tilde{p}) = \sum_{(i,j)\in\mathbf{E}} \sum_{x_i,x_j\in\mathcal{X}} \tilde{p}_{ij}(x_i,x_j) E_{ij}(x_i,x_j) + \sum_{i\in\mathbf{X}} \sum_{x_i\in\mathcal{X}} \tilde{p}_i(x_i) E_i(x_i)$$
(13)

and the Bethe entropy

$$S_{B}(\tilde{p}) = \sum_{(i,j)\in\mathbf{E}} \underbrace{\left(-\sum_{x_{i},x_{j}\in\mathcal{X}} \tilde{p}_{ij}(x_{i},x_{j})\log \tilde{p}_{ij}(x_{i},x_{j})\right)}_{S_{i}(\tilde{p})}$$

$$-\sum_{i\in\mathbf{X}} (d_{i}-1) \underbrace{\left(-\sum_{x_{i}\in\mathcal{X}} \tilde{p}_{i}(x_{i})\log \tilde{p}_{i}(x_{i})\right)}_{S_{i}(\tilde{p})}.$$

$$(14)$$

The Bethe entropy S_B uses the sum over all pairwise entropies S_{ij} to approximate S(q). This simplified computation results in an overcounting of entropy contributions from individual nodes, which is compensated by reducing the sum by a $(d_i - 1)$ -multiple of the local entropies S_i . Note that \mathcal{F}_B depends on \tilde{p} only via the singleton and pairwise pseudomarginals $\tilde{p}_i, \tilde{p}_{ij}$ (for each node and edge). This allows us, with a slight abuse of notation, to identify any element $\tilde{p} \in \mathbb{L}$ with the collection of all its associated pseudo-marginals $\{\tilde{p}_i, \tilde{p}_{ij}\}$.

By minimizing \mathcal{F}_B over \mathbb{L} , one usually tries to approximate the partition function $Z(\beta)$ and/or the marginals p_i, p_{ij} induced by p_{β} according to

$$\min_{\tilde{p}_i, \tilde{p}_{ij} \in \mathbb{L}} \mathcal{F}_B \approx -\frac{1}{\beta} \log Z(\beta)$$
 (15)

$$\underset{\tilde{p}_{i}, \tilde{p}_{ij} \in \mathbb{L}}{\operatorname{argmin}} \mathcal{F}_{B} \approx \{ p_{i}, p_{ij} \mid (i, j) \in \mathbf{E} \text{ and } i \in \mathbf{X} \}.$$

$$(16)$$

The expressions on the left-hand side are well-defined, because \mathcal{F}_B is bounded from below and its derivatives tend to infinity as \mathcal{F}_B approaches the boundary of \mathbb{L} ; i.e., \mathcal{F}_B attains its global minimum in an interior point of \mathbb{L} (Yedidia et al., 2005; Weller and Jebara, 2013).

The quality of the approximations made in (15) and (16) degrades with a high connectivity and strong correlations (or equivalently, a low temperature) in the graph (Meshi et al., 2009; Weller et al., 2014; Leisenberger et al., 2022). This can be explained by the shape of the Bethe free energy: Whenever the graph contains at least two cycles, \mathcal{F}_B is – in contrast to the Gibbs free energy – non-convex and may lose the favorable property of having a unique global minimum (Pakzad and Anantharam, 2005; Heskes, 2006; Watanabe and Fukumizu, 2009). However, this is not the complete story and we will argue in Sec. 3 that the Bethe approximation is still accurate if it is convex on a specific submanifold of \mathbb{L} .

2.4 Related Work

Statistical mechanics deals with infinite systems and their properties in thermodynamic equilibrium (Reif, 1965; Huang, 1987). On the basis of simplified mathematical models, it explains a system's macroscopic behavior in terms of its microscopic constitutents. The statistical properties of the system are fully described by the partition function and its derivatives; however, their analytical form is only known for a few models, e.g., the one-and two-dimensional Ising model, (Ising, 1925; Onsager, 1944). Of particular interest is the phenomenon of phase transitions, i.e., sudden changes in the qualitative behavior of the system (Yeomans, 1992). These are manifested as singularities of the thermodynamic potentials (or the partition function) with respect to the temperature.

The theory of Gibbs measures (Georgii, 1988) provides an elegant framework to study phase transitions directly in infinite systems, instead of computing the thermodynamic limit of finite systems. A Gibbs measure represents an equilibrium state of an infinite system and we may interpret a phase transition as the non-uniqueness of a Gibbs measure ¹¹. Conversely, the existence of a unique Gibbs measure predicts an absence of phase transitions in the system. As a consequence, researchers have made effort to derive conditions for uniqueness of Gibbs measures (Dobrushin, 1968; Simon, 1979).

In computer science, many applications use probabilistic graphical models (PGMs) to represent a probability distribution (Koller and Friedman, 2009). These are principally identical to models from statistical mechanics, with the major difference that the involved graphs are often relatively small and do not necessarily exhibit a lattice structure. In particular, finite systems do not exhibit phase transitions in the proper sense, because the thermodynamic potentials are always analytical functions. (Brezin and Zinn-Justin, 1985; Binder, 1987).

Researchers in this field strongly benefited from statistical mechanics and found a surprising connection between concepts that seem entirely unrelated: the loopy belief propagation (LBP) algorithm on the one hand, which is an iterative method to approximate marginal probabilities in PGMs; and the Bethe-Peierls approximation on the other hand, which has its origins in the theory of superlattices (Bethe, 1935; Peierls, 1936). More precisely, Yedidia et al. (2001) have proven that there exists a bijective mapping between fixed points ¹² of LBP and stationary points of the Bethe free energy. This was later complemented by the result that each stable fixed point of LBP corresponds to a local minimum of the Bethe free energy (Heskes, 2003). A successful application of the Bethe approximation (or loopy belief propagation) is defined in terms of its quality towards estimating marginal probabilities and the partition function. Due to the lack of general performance guarantees (Sec. 2.3), one requires alternative ways to assess the reliability of LBP and the Bethe approximation.

^{11.} Formally, a probability distribution μ on an infinite system S is a Gibbs measure if, for all finite subsystems $\Lambda \subset S$, the conditional probabilities induced by μ on Λ are consistent with the canonical ensemble in Λ , given that all degrees of freedom outside Λ are frozen.

^{12.} LBP iteratively exchanges statistical information in form of 'messages' between neighboring nodes in the graph. If this process converges, then we say that LBP has converged to a fixed point.

One line of research analyzes when LBP converges to a unique fixed point. This is often considered as an indicator that the LBP solution (and thus the Bethe approximation) is accurate. As is known, LBP always converges to a unique fixed point, if the graph is a tree or contains precisely one cycle (Pearl, 1988; Weiss, 2000); for other graphs, the number of fixed points and the convergence behavior depend on the potential configuration (or temperature). Results on this topic include the following: Tatikonda and Jordan (2002) have shown that LBP converges to a unique fixed point, if there exists a unique Gibbs measure on the computation tree ¹³; i.e., they established a direct connection to the theory of Gibbs measures. Heskes (2004) formulated a minimax problem on the Bethe free energy whose concavity is sufficient for the uniqueness of an LBP fixed point. Ihler et al. (2005); Mooij and Kappen (2007) consider LBP as a dynamical system and use contraction arguments to prove convergence to a unique fixed point. Further, Watanabe and Fukumizu (2009) use the Ihara zeta function from graph theory to prove uniqueness of an LBP fixed point. Figure 1 shows the relations between the different criteria that are described above.

Alternatively, one can try to quantify the approximation error induced by the Bethe free energy or LBP. Various results bound its approximation error with respect to the marginal probabilities, either in closed form (Tatikonda, 2003; Taga and Mase, 2006a) or recursively (Ihler, 2007; Mooij and Kappen, 2008; Weller and Jebara, 2013). Others use loop series (Chertkov and Chernyak, 2006) or graph covers (Vontobel, 2013) to establish a relationship between the Gibbs and the Bethe minimum, which induces bounds on the approximation error with respect to the partition function. In ferromagnetic models, the Bethe minimum bounds the Gibbs minimum from above (Willsky et al., 2007; Ruozzi, 2013) and can be approximated in polynomial time (Weller and Jebara, 2014a). Unfortunately, these bounds can be arbitrarily loose and are sometimes difficult to compute.

Intuitively, as the Bethe free energy is used to approximate a convex functional (the Gibbs free energy, Sec. 2.3), one would expect it to provide accurate estimates whenever it is convex as well. However, Watanabe and Fukumizu (2009) have proven that the Bethe free energy is convex, if and only if the graph is either a cycle or a tree. This might imply that the concept of convexity might not be appropriate for inferring about the quality of the Bethe approximation (because it cannot be convex except for these special graphs anyway).

In this work, we will have a closer look at the convexity of the Bethe free energy. We show how it can be made a useful concept for assessing the quality of the Bethe approximation.

3 Convexity of the Bethe Free Energy: Theory

This section includes our main theoretical contributions in this work. Particularly, we address the question under which conditions \mathcal{F}_B is convex and how this can be verified. Our theory is built on the results of previous work and exploits the current state of knowledge as a starting point. In detail, we proceed as follows: First, we summarize the most important

^{13.} The computation tree is an 'unwrapping' of the graph, starting from some node *i* and consisting of all non-backtracking paths. E.g., the Cayley tree is the computation tree of a complete graph. The concept of Gibbs measures is well defined on the computation tree, because it consists of infinitely many nodes.

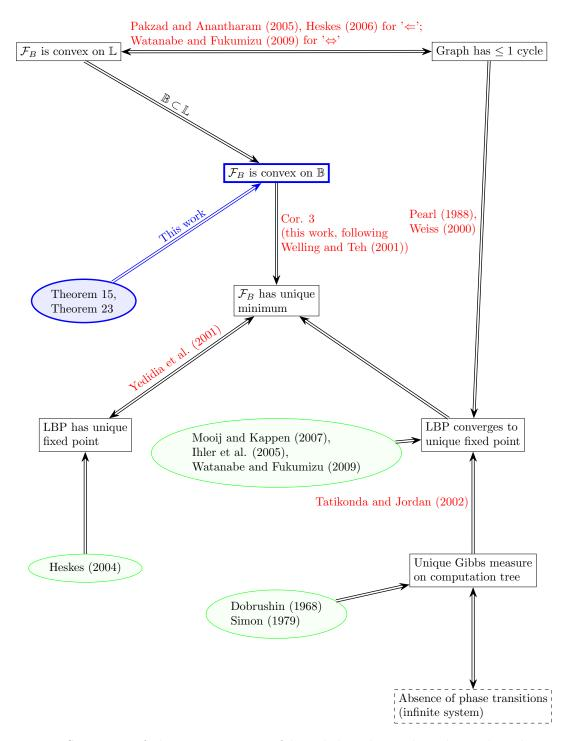


Figure 1: Summary of the current state of knowledge about the relationships between the Bethe free energy and loopy belief propagation. The white rectangles contain various properties of the Bethe free energy and LBP. The main results of this work are contained in the blue ellipse and serve as sufficient conditions for the convexity of the Bethe free energy. Sufficient conditions from previous research are included in the green ellipses. Other important results are shown as red label next to the logical arrows between properties.

properties of the Bethe free energy and specify the problem to be tackled (Sec. 3.1). Next, we perform a second-order analysis of the Bethe free energy and derive two sufficient conditions for its convexity, one of which is based on the criterion of diagonal dominance (Sec. 3.2), and the other on a sum decomposition of the Hessian matrix (Sec. 3.3). Finally, we compare our results to similar statements from the literature with respect to a perfectly symmetric model that facilitates a direct comparison (Sec. 3.4). Our notation in this section closely follows that of Welling and Teh (2001); Weller and Jebara (2013); Leisenberger et al. (2022).

3.1 Properties of the Bethe Free Energy

We first make a range of simplifications regarding the dimensionality of the local polytope (11) and the Bethe free energy (12) for binary variables. Let X_i, X_j be any pair of connected variables and let $\tilde{p}_i, \tilde{p}_j, \tilde{p}_{ij}$ be a set of associated pseudo-marginal vectors ¹⁴ from the local polytope \mathbb{L} (i.e., with all entries satisfying the constraints in the definition of \mathbb{L}). Let us denote the individual pseudo-marginal probabilities for X_i and X_j being in state +1 by $q_i := \tilde{p}_i(X_i = +1)$ and $q_j := \tilde{p}_j(X_j = +1)$ and let us further denote the joint pseudo-marginal probability for X_i, X_j being both in state +1 by $\xi_{ij} := \tilde{p}_{ij}(X_i = +1, X_j = +1)$. Then, as $\tilde{p}_i, \tilde{p}_j, \tilde{p}_{ij}$ must satisfy the constraints of \mathbb{L} , all five remaining entries of these vectors can already be expressed in terms of q_i, q_j, ξ_{ij} according to the following table:

Table 1: Joint probability table of two binary variables X_i and X_j .

$\tilde{p}_{ij}(X_i, X_j)$	$X_j = +1$	$X_j = -1$	
$X_i = +1$	ξ_{ij}	$q_i - \xi_{ij}$	q_i
$X_i = -1$	$q_j - \xi_{ij}$	$1 + \xi_{ij} - q_i - q_j$	$1-q_i$
	q_j	$1-q_j$	

Additionally, we have constraints on the independent parameters q_i, q_j, ξ_{ij} of the form

$$0 < q_i < 1, \tag{17}$$

$$0 < q_i < 1, \tag{18}$$

$$\max(0, q_i + q_j - 1) < \xi_{ij} < \min(q_i, q_j). \tag{19}$$

This step reparameterizes the local polytope by exploiting probabilistic dependencies between variables and removing a considerable number of redundant parameters. If we collect all node-specific variables q_i in a vector \boldsymbol{q} and all edge-specific parameters ξ_{ij} in a vector $\boldsymbol{\xi}$, we can compactly rewrite the local polytope (11) as the set

$$\mathbb{L} = \{ (\boldsymbol{q}; \boldsymbol{\xi}) \in \mathbb{R}^{|\mathbf{X}| + |\mathbf{E}|} : 0 < q_i < 1, i \in \mathbf{X};$$

$$\max(0, q_i + q_j - 1) < \xi_{ij} < \min(q_i, q_j), (i, j) \in \mathbf{E} \}.$$

$$(20)$$

14. More precisely,
$$\tilde{p}_i = \begin{pmatrix} \tilde{p}_i(X_i = +1) \\ \tilde{p}_i(X_i = -1) \end{pmatrix}$$
 and $\tilde{p}_{ij} = \begin{pmatrix} \tilde{p}_{ij}(X_i = +1, X_j = +1) \\ \tilde{p}_{ij}(X_i = +1, X_j = -1) \\ \tilde{p}_{ij}(X_i = -1, X_j = +1) \\ \tilde{p}_{ij}(X_i = -1, X_j = -1) \end{pmatrix}$.

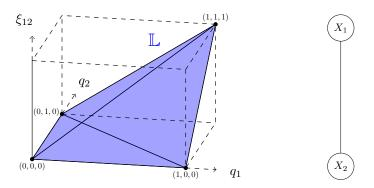


Figure 2: Local polytope L (left) on a single-edge graph (right).

Figure 2 shows the local polytope on a graph with two vertices and a single edge.

This reparameterization of the local polytope also reparameterizes the Bethe free energy: By substituting the expressions from Table 1 into the corresponding terms of (12) - (14), \mathcal{F}_B takes the simpler form

$$\mathcal{F}_{B}(\boldsymbol{q};\boldsymbol{\xi}) = \underbrace{-\sum_{(i,j)\in\mathbf{E}} (1+2(2\xi_{ij}-q_{i}-q_{j})) J_{ij} + \sum_{i\in\mathbf{X}} (1-2q_{i}) \theta_{i}}_{\mathcal{B}_{B}(\boldsymbol{q};\boldsymbol{\xi})}$$

$$-\frac{1}{\beta} \left(\sum_{(i,j)\in\mathbf{E}} \mathcal{S}_{ij} - \sum_{i\in\mathbf{X}} (d_{i}-1) \mathcal{S}_{i} \right), \tag{21}$$

with the pairwise entropies

$$S_{ij} = -\xi_{ij} \log \xi_{ij} - (1 + \xi_{ij} - q_i - q_j) \log(1 + \xi_{ij} - q_i - q_j) - (q_i - \xi_{ij}) \log(q_i - \xi_{ij}) - (q_j - \xi_{ij}) \log(q_j - \xi_{ij})$$
(22)

and the local entropies

$$S_i = -q_i \log q_i - (1 - q_i) \log(1 - q_i). \tag{23}$$

This and similar reparameterizations of \mathbb{L} and \mathcal{F}_B are not new and have been used for different purposes (Welling and Teh, 2001; Mooij and Kappen, 2005). One result from Watanabe and Fukumizu (2009) that is particularly relevant for our work is the following:

Proposition 1 (Corollary 2 in Watanabe and Fukumizu (2009))

 \mathfrak{F}_B is convex on \mathbb{L} , if and only if the graph G is either a tree or contains precisely one cycle.

In principle, this statement fully characterizes the convexity of \mathcal{F}_B . As it is only applicable for two types of graphs, convexity might not seem to be a suitable concept for explaining the success (or failure) of the Bethe approximation ¹⁵. However, we will show how we can refine Proposition 1 by defining an appropriate subset \mathbb{B} of \mathbb{L} , on which \mathcal{F}_B can preserve its convexity for general graphs. Moreover, we claim that \mathcal{F}_B provides accurate solutions if is convex on that specific subset \mathbb{B} of \mathbb{L} . From this, three questions arise:

- (i) How can we characterize \mathbb{B} such that \mathcal{F}_B can preserve its convexity for general graphs?
- (ii) How can we determine if \mathcal{F}_B is convex on \mathbb{B} ?
- (iii) Can we explain the reliability of the Bethe approximation through its convexity on \mathbb{B} ?

For the rest of this work, we focus on answering these three questions: (i) will be addressed in the remainder of the current subsection; (ii) will be subject of Sec. 3.2 and Sec. 3.3; and (iii) will be theoretically discussed in Sec. 3.4 and experimentally evaluated in Sec. 4.

First we identify a subset \mathbb{B} of \mathbb{L} on which \mathcal{F}_B can preserve its convexity for general graphs. For that purpose, recall that we are primarily interested in minimizing the Bethe free energy to approximate the minimum of the Gibbs free energy (Sec. 2.3). If we exclude regions of \mathbb{L} where no minimum of \mathcal{F}_B can lie, then we lose no relevant information on its accuracy. Or, in other words, we expect that \mathcal{F}_B should primarily be a convex approximation to the Gibbs free energy on a subset \mathbb{B} of \mathbb{L} , that includes all minima of \mathcal{F}_B . Following this idea, we adopt an approach made by Welling and Teh (2001); Shin (2012); Weller and Jebara (2013) – albeit in their work, to reduce the computational complexity of Bethe minimization:

Let $(q; \boldsymbol{\xi})$ be a point in \mathbb{L} where all partial derivatives of \mathcal{F}_B with respect to the edge-specific variables ξ_{ij} (not necessarily with respect to the node-specific variables q_i) are zero.; i.e., the gradient of \mathcal{F}_B evaluated in that point is $\nabla \mathcal{F}_B(q; \boldsymbol{\xi}) = \left(\frac{\partial \mathcal{F}_B}{\partial q_1}(q; \boldsymbol{\xi}), \dots, \frac{\partial \mathcal{F}_B}{\partial q_N}(q; \boldsymbol{\xi}); 0, \dots, 0\right)^T$. This imposes a necessary condition on any $(q; \boldsymbol{\xi}) \in \mathbb{L}$ for being a stationary point (and thus a minimum) of \mathcal{F}_B (Sec. 2.1). In Welling and Teh (2001) it has been shown that, if we choose an arbitrary (but fixed) q, there exists a unique $\boldsymbol{\xi}^*(q)$ – i.e., depending on the choice of q – such that $(q; \boldsymbol{\xi}^*(q))$ is a candidate for a stationary point of \mathcal{F}_B ; moreover, the explicit form of $\boldsymbol{\xi}^*(q)$ has been computed with its individual components given by

$$\xi_{ij}^{*}(q_{i}, q_{j}) = \frac{1}{2\alpha_{ij}} \left(Q_{ij} - \sqrt{Q_{ij}^{2} - 4\alpha_{ij}(1 + \alpha_{ij})q_{i}q_{j}} \right),$$
where $\alpha_{ij} = e^{4\beta J_{ij}} - 1$ and $Q_{ij} = 1 + \alpha_{ij}(q_{i} + q_{j}).$ (24)

In other words, for any \mathbf{q} there exists at most one $\boldsymbol{\xi}^*(\mathbf{q})$ (defined in (24)) such that $(\mathbf{q}; \boldsymbol{\xi}^*(\mathbf{q}))$ can be a minimum of \mathcal{F}_B . Consequently, we address question (i) according to our previously described requirements on \mathbb{B} , by defining a suitable subset \mathbb{B} of \mathbb{L} as follows:

^{15.} In particular, there are popular applications involving graphs with multiple cycles where the Bethe approximation (resp., LBP) is highly accurate (Frey and MacKay, 1997; Yanover and Weiss, 2002).

Theorem 2 (Adopted from Welling and Teh (2001))

Every minimum of \mathfrak{F}_B is located on an $|\mathbf{X}|$ - dimensional submanifold \mathbb{B} of \mathbb{L} , the **Bethe** box, which is defined as

$$\mathbb{B} := \{ (\boldsymbol{q}; \boldsymbol{\xi}^*(\boldsymbol{q})) \in \mathbb{L} : 0 < q_i < 1, i \in \mathbf{X}; \\ \boldsymbol{\xi}_{ij}^*(q_i, q_j) \text{ given by } (24), (i, j) \in \mathbf{E} \}.$$
 (25)

Note that \mathbb{B} is parameterized in terms of the q_i only, while the ξ_{ij} have lost their role as independent parameters but depend on the q_i through the bijective mapping (24). This implies that \mathbb{B} is isomorphic to the open unit cube $(0,1)^{|\mathbf{X}|}$ of dimension $|\mathbf{X}|$, which explains the naming of \mathbb{B} . Figure 3 shows the Bethe box with respect to a graph on two vertices and a single edge for different values of the associated coupling J_{ij} and inverse temperature β .

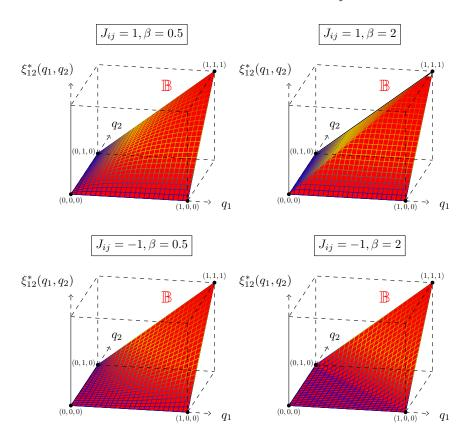


Figure 3: Bethe box $\mathbb{B} \subset \mathbb{L}$ for different values of coupling J_{ij} and inverse temperature β on a single-edge graph. For a ferromagnetic edge $(J_{ij} > 0$; first row), \mathbb{B} approaches the upper boundary of \mathbb{L} as β increases; for an antiferromagnetic edge $(J_{ij} < 0$; second row), \mathbb{B} approaches the lower boundary of \mathbb{L} as β increases.

The Bethe box \mathbb{B} satisfies our intuitive requirements on a subset of \mathbb{L} , on which \mathcal{F}_B can preserve its convexity for general graphs (in fact, we prove this in Sec. 3.2 and Sec. 3.3). Also, the definition (25) of \mathbb{B} once again reduces the number of independent variables \mathcal{F}_B , as we can define \mathcal{F}_B directly on the space of its potential minima, by substituting $\xi_{ij}^*(q_i, q_j)$ from (24) into ξ_{ij} in (21). An immediate implication of Theorem 2 is:

Corollary 3

If \mathcal{F}_B is strictly convex on \mathbb{B} , then it has a unique global minimum in \mathbb{L} .

In Sec. 3.4, we will have a closer look at the connection between convexity of \mathcal{F}_B uniqueness of a minimum. Finally, we require the first-order and second-order derivatives of \mathcal{F}_B on \mathbb{B} :

Lemma 4 ((a): Welling and Teh (2001); (b): Lemma 9 in Weller and Jebara (2013))

(a) The first-order partial derivatives of \mathfrak{F}_B on \mathbb{B} are

$$\frac{\partial \mathcal{F}_B}{\partial q_i} = -2 \,\theta_i + 2 \sum_{j \in \mathcal{N}(i)} J_{ij} + \frac{1}{\beta} \log \left(\frac{(1 - q_i)^{d_i - 1}}{q_i^{d_i - 1}} \prod_{j \in \mathcal{N}(i)} \frac{q_i - \xi_{ij}^*}{1 + \xi_{ij}^* - q_i - q_j} \right). \tag{26}$$

(b) The second-order partial derivatives of \mathfrak{F}_B on \mathbb{B} are

$$\frac{\partial^{2} \mathcal{F}_{B}}{\partial q_{i} \partial q_{j}} = \begin{cases}
\frac{1}{\beta} \left(-\frac{d_{i} - 1}{q_{i}(1 - q_{i})} + \sum_{j \in \mathcal{N}(i)} \frac{q_{j}(1 - q_{j})}{T_{ij}} \right) & i = j \\
\frac{1}{\beta} \left(\frac{q_{i}q_{j} - \xi_{ij}^{*}}{T_{ij}} \right) & j \in \mathcal{N}(i) \\
0 & otherwise,
\end{cases}$$
(27)

where
$$T_{ij}(q_i, q_j) := q_i q_j (1 - q_i) (1 - q_j) - (\xi_{ij}^*(q_i, q_j) - q_i q_j)^2 > 0.$$
 (28)

Also, we have that $\frac{\partial^2 \mathcal{F}_B}{\partial q_i^2}$ is always > 0.

A simple, but remarkable consequence from Lemma 4 is:

Corollary 5

The Hessian matrix of \mathfrak{F}_B is independent from θ_i . In other words, the curvature of the Bethe free energy is not influenced by the local potentials.

Next, we deal with question (ii): How can we determine, if \mathcal{F}_B is convex on the Bethe box \mathbb{B} ? To address this problem, we propose two different methodologies – the first one in Sec. 3.2, the second one in Sec. 3.3 – that both rely on a profound analysis of the Hessian matrix, i.e., the curvature of the Bethe free energy. The basic idea of both approaches is the same: to apply the formal definition of strict convexity (Sec. 2.1) to the Bethe free energy: Let $\mathbf{H}_B(q) : \mathbb{B} \to \mathbb{R}^{|\mathbf{X}| \times |\mathbf{X}|}$ be the Hessian matrix of \mathcal{F}_B (the Bethe Hessian), considered as a matrix-valued function on the Bethe box ¹⁶. Then \mathcal{F}_B is strictly convex on \mathbb{B} , if $\mathbf{H}_B(q)$ is positive definite for all $q \in \mathbb{B}$. Unfortunately, the complex analytical form of \mathbf{H}_B (Lemma 4, (b)) prevents a direct application of this definition and requires relaxations to the problem.

^{16.} To simplify the notation, we denote the Bethe Hessian by \mathbf{H}_B instead of $\mathbf{H}_{\mathcal{F}_B}$, as formally defined in Sec. 2.1. Also, we mostly omit the dependency of \mathbf{H}_B on \mathbf{q} , since this is usually clear from the context.

3.2 Node-Specific Convexity Criterion: Diagonal Dominance of Bethe Hessian

Our first approach to relax the convexity of \mathcal{F}_B uses the concept of diagonal dominance, a sufficient condition for positive definiteness of a matrix (Sec. 2.1). The main result is Theorem 15, which reduces diagonal dominance of the Bethe Hessian to the positivity of a set of one-dimensional polynomials. All proofs for this section are collected in Appendix A.

Let us compactly write the (i, j)-th entry of \mathbf{H}_B (i.e., $\frac{\partial^2 \mathfrak{F}_B}{\partial q_i \partial q_j}$) as h_{ij} . Then the diagonal dominance criterion (equation (1)) says that \mathbf{H}_B is positive definite in $\mathbf{q} \in \mathbb{B}$, if

$$h_{ii} - \sum_{j \in \mathcal{N}(i)} |h_{ij}| > 0 \tag{29}$$

for each row of \mathbf{H}_B , i.e., for all $i \in \mathbf{X}$. Note that $h_{ii} > 0$, and $h_{ij} = 0$ if neither i = j nor $j \in \mathcal{N}(i)$. If we insert the expressions from (27) into (29), this is equivalent to

$$\frac{1}{\beta} \left(-\frac{d_i - 1}{q_i(1 - q_i)} + \sum_{j \in \mathcal{N}(i)} \frac{q_j(1 - q_j)}{T_{ij}} - \sum_{j \in \mathcal{N}(i)} \frac{|q_i q_j - \xi_{ij}^*|}{T_{ij}} \right) > 0, \tag{30}$$

because $T_{ij} > 0$ (Lemma 4, (b)). To compute the absolute values, we can use the following result:

Lemma 6 (Lemma 2 in Weller and Jebara (2013))

If (i,j) is a ferromagnetic edge $(J_{ij} > 0)$, then $\xi_{ij}^* > q_i q_j$. If (i,j) is an antiferromagnetic edge $(J_{ij} < 0)$, then $\xi_{ij}^* < q_i q_j$.

If we distinguish between the two types of edges, inequality (30) becomes

$$-\frac{d_{i}-1}{q_{i}(1-q_{i})} + \sum_{\substack{j \in \mathcal{N}(i) \\ J_{ij} > 0}} \frac{q_{j}(1-q_{j}) - \xi_{ij}^{*} + q_{i}q_{j}}{T_{ij}} + \sum_{\substack{j \in \mathcal{N}(i) \\ J_{ij} < 0}} \frac{q_{j}(1-q_{j}) - q_{i}q_{j} + \xi_{ij}^{*}}{T_{ij}} > 0.$$
 (31)

So far, we have only considered one specific point $q \in \mathbb{B}$; however, to guarantee the convexity of \mathcal{F}_B on the entire Bethe box \mathbb{B} , inequality (31) must be valid for all $q \in \mathbb{B}$ or, equivalently, for the infimum ¹⁷ over all $q \in \mathbb{B}$. In summary, we arrive at the following problem:

Proposition 7

Let us denote the expression on the left-hand side of inequality (31) by $R_i(\mathbf{q})$. Then \mathfrak{F}_B is convex on the Bethe box \mathbb{B} if, for all nodes $i \in \mathbf{X}$,

$$\inf_{\boldsymbol{q} \in \mathbb{R}} R_i(\boldsymbol{q}) > 0. \tag{32}$$

In Proposition 7 we have reformulated diagonal dominance of the Bethe Hessian in terms of an optimization problem. The infimum of $R_i(q)$ measures to what extent the diagonal

^{17.} Strictly speaking, the infimum could also be equal to zero, while positivity holds for all interior points of B. However, we will ignore this subtlety as it is does not affect our later results.

dominance criterion is satisfied (or violated) in node i. As R_i is a nonlinear function of potentially many variables ¹⁸, its solution (i.e., the verification of inequality (32)) is not trivial.

In the remainder of this section, we analyze the left-hand side of the inequality (32) and finally present a condition that is equivalent to (32) but much easier to verify (Theorem 15). Our first observation is that $R_i(\mathbf{q})$ has the special form

$$R_{i}(\mathbf{q}) = r_{i}(q_{i}) + \sum_{\substack{j \in \mathcal{N}(i) \\ J_{ij} > 0}} r_{ij}^{+}(q_{i}, q_{j}) + \sum_{\substack{j \in \mathcal{N}(i) \\ J_{ij} < 0}} r_{ij}^{-}(q_{i}, q_{j}), \quad \text{where}$$
(33)

$$r_i(q_i) := -\frac{d_i - 1}{q_i(1 - q_i)}$$
 depends only on q_i , (34)

$$r_{ij}^{+}(q_i, q_j) := \frac{q_j(1 - q_j) - \xi_{ij}^* + q_i q_j}{T_{ij}} \quad \text{depends on } q_i \text{ and } q_j, \text{ and}$$
 (35)

$$r_{ij}^-(q_i, q_j) := \frac{q_j(1 - q_j) - q_i q_j + \xi_{ij}^*}{T_{ij}} \quad \text{depends on } q_i \text{ and } q_j.$$
 (36)

Note that, for each ferromagnetic edge we have one term of the form (35), and for each antiferromagnetic edge we have one term of the form (36) (with q_i and q_j being the variables associated to the end nodes of a specific edge (i, j)). In particular, q_i (associated to node i) is the only variable that appears in each individual sum term, while any other variable q_j (for $j \in \mathcal{N}(i)$) appears in precisely one of the pairwise terms $r_{ij}^+(q_i, q_j)$ or $r_{ij}^-(q_i, q_j)$ (depending on the type of the edge that connects i and j). Figure 4 illustrates this situation.

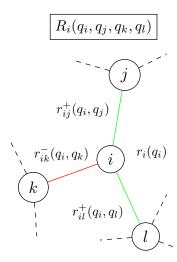


Figure 4: Dependencies and components of the function $R_i(\mathbf{q})$ associated to some node *i*. Ferromagnetic edges are drawn in green and antiferromagnetic edges are drawn in red.

We can exploit the specific structure (33) of $R_i(\mathbf{q})$ and decompose the computation of $\inf_{\mathbf{q} \in \mathbb{B}} R_i(\mathbf{q})$ into a collection of simpler sub-problems, each involving only a single variable.

^{18.} More precisely, R_i depends on $(d_i + 1)$ variables: on q_i that is associated to node i, and additionally on all q_i that are associated to neighboring nodes $j \in \mathcal{N}(i)$.

Concretely, we apply a two-step procedure: In the first step, we fix q_i and determine

$$\inf_{q_j \in (0,1)} r_{ij}^+(q_i, q_j) \quad \text{and} \quad \inf_{q_j \in (0,1)} r_{ij}^-(q_i, q_j)$$
 (37)

for each of the pairwise terms $r_{ij}^+(q_i, q_j), r_{ij}^-(q_i, q_j)$ separately (with respect to q_j as a function of q_i). In the second step, we fix the solutions to these sub-problems and compute the infimum of the overall function $R_i(q)$ with respect to q_i . Altogether, we determine

$$\tilde{R}_{i} := \inf_{\substack{q_{i} \in (0,1) \\ J_{ij} > 0}} \left[r_{i}(q_{i}) + \sum_{\substack{j \in \mathcal{N}(i): \\ J_{ij} > 0}} \left(\inf_{\substack{q_{j} \in (0,1) \\ q_{j} \in (0,1)}} r_{ij}^{+}(q_{i}, q_{j}) \right) + \sum_{\substack{j \in \mathcal{N}(i): \\ J_{ij} < 0}} \left(\inf_{\substack{q_{j} \in (0,1) \\ q_{j} \in (0,1)}} r_{ij}^{-}(q_{i}, q_{j}) \right) \right]$$
(38)

which is equal to the infimum of $R_i(q)$ as the following Lemma shows:

Lemma 8

Let $R_i(\mathbf{q})$ be the expression ¹⁹ in (33) and let \tilde{R}_i be the expression in (38). Then

$$\inf_{\boldsymbol{q}\in\mathbb{B}} R_i(\boldsymbol{q}) = \tilde{R}_i. \tag{39}$$

Lemma 8 justifies the described two-step procedure for evaluating $\inf_{q \in \mathbb{B}} R_i(q)$ from 'inside' (fix $q_i \in (0,1)$ and compute the infima of $r_{ij}^+(q_i,q_j)$ and $r_{ij}^-(q_i,q_j)$ with respect to q_j as a function of q_i) to 'outside' (given the solutions to these sub-problems, compute the infimum of $R_i(q)$ with respect to q_i). Hence, we must first solve the 'inner' sub-problems (37) whose solutions are required in the 'outer' problem (38). We have two types of sub-problems to be solved: one for ferromagnetic edges and one for antiferromagnetic edges. Instead of treating them separately, we show that they can be transformed into each other:

Lemma 9

Let $J_{ij} > 0$, and let $r_{ij}^+(q_i, q_j)$ and $r_{ij}^-(q_i, q_j)$ be the two types of pairwise functions in the sum decomposition (33) of $R_i(\mathbf{q})$, with $r_{ij}^+(q_i, q_j)$ implicitly depending on J_{ij} (corresponding to a ferromagnetic edge) and $r_{ij}^-(q_i, q_j)$ implicitly depending on $-J_{ij}$ (corresponding to an antiferromagnetic edge). Then we have

$$r_{ij}^{-}(q_i, q_j) = r_{ij}^{+}(q_i, 1 - q_j) = r_{ij}^{+}(1 - q_i, q_j).$$
(40)

In other words, if we reflect $r_{ij}^+(q_i, q_j)$ in its domain $(0,1) \times (0,1)$ either across the line $q_i = 0.5$ or the line $q_j = 0.5$, we obtain $r_{ij}^-(q_i, q_j)$ (and vice versa).

Lemma 9 establishes a direct relationship between $r_{ij}^-(q_i, q_j)$ and $r_{ij}^+(q_i, q_j)$. It therefore facilitates the determination of \tilde{R}_i in (38) by focusing on a single edge type, instead of distinguishing between two types of edges. Without loss of generality, we may replace each

^{19.} We remark that our proof of Lemma 8 does not require the specific definition of the functions r_i, r_{ij}^+, r_{ij}^- , but only relies on the structure of the decomposition (33) of $R_i(q)$.

pairwise term $r_{ij}^-(q_i, q_j)$ (which implicitly depends on $J_{ij} < 0$) in (38) with $r_{ij}^+(1 - q_i, q_j)$ and the sign-inverted coupling $|J_{ij}| > 0$. Under this assumption, (38) becomes

$$\tilde{R}_{i} := \inf_{q_{i} \in (0,1)} \left[r_{i}(q_{i}) + \sum_{\substack{j \in \mathcal{N}(i):\\J_{ij} > 0}} \left(\inf_{q_{j} \in (0,1)} r_{ij}^{+}(q_{i}, q_{j}) \right) + \sum_{\substack{j \in \mathcal{N}(i):\\J_{ij} < 0}} \left(\inf_{q_{j} \in (0,1)} r_{ij}^{+}(1 - q_{i}, q_{j}) \right) \right].$$

$$(41)$$

We now return to the 'inner' sub-problems stated in (37) with our focus on the first problem type: the determination of $\inf_{q_j \in (0,1)} r_{ij}^+(q_i, q_j)$ with $q_i \in (0,1)$ arbitrary but fixed ²⁰. In partic-

ular, we consider $r_{ij}^+(q_i, q_j)$ as a one-dimensional function of q_j defined on the interval (0, 1) (representing the line segment that connects $(q_i, 0)$ and $(q_i, 1)$ in the domain $(0, 1) \times (0, 1)$). To find the greatest lower bound on r_{ij}^+ in that interval, we first show that r_{ij}^+ has a unique stationary point in (0, 1) (Theorem 11) which, however, is a maximum (Theorem 13). This implies that the infimum is not taken by r_{ij}^+ but exists as a limit value at the boundary of (0, 1). In Lemma 12 and Corollary 14, we derive the explicit formula for the infimum, in dependence of the chosen q_i . Figure 5 shows sketches of $r_{ij}^+(q_i, q_j)$ for different values of q_i .

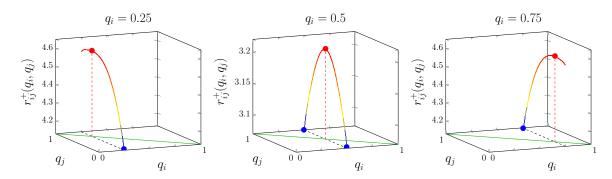


Figure 5: $r_{ij}^+(q_i, q_j)$ as a function of $q_j \in (0, 1)$ and for different fixed values of q_i . The green line $q_j = 1 - q_i$ represents the space of all stationary points of $r_{ij}^+(q_i, q_j)$ (exactly one for each $q_i \in (0, 1)$, Theorem 11), which are always maxima (drawn as red points, Theorem 13). The blue points at the boundary represent the infima of $r_{ij}^+(q_i, q_j)$ with respect to q_j , which are never taken by $r_{ij}^+(q_i, q_j)$ (Lemma 12 and Corollary 14). Note that $q_i = 0.5$ represents the only scenario where the infimum exists at both boundary points 0 and 1.

For proving Theorem 11, we require the first-order partial derivatives of the functions ξ_{ij}^* , T_{ij} , and r_{ij}^+ with respect to q_i and q_j . Moreover, we prepare the second-order partial derivatives of ξ_{ij}^* and T_{ij} , that we will require in the proof of Theorem 21 (Sec. 3.3).

^{20.} By Lemma 9, the determination of $\inf_{q_j \in (0,1)} r_{ij}^-(q_i,q_j)$ can be reduced to the ferromagnetic case.

Lemma 10

(a) The first-order partial derivatives of $\xi_{ij}^*(q_i, q_j), T_{ij}(q_i, q_j), r_{ij}^+(q_i, q_j)$ are

$$\frac{\partial \xi_{ij}^*}{\partial q_i} = \frac{\alpha_{ij}(q_j - \xi_{ij}^*) + q_j}{1 + \alpha_{ij}(q_i + q_j - 2\xi_{ij}^*)},\tag{42}$$

$$\frac{\partial \xi_{ij}^*}{\partial q_j} = \frac{\alpha_{ij} (q_i - \xi_{ij}^*) + q_i}{1 + \alpha_{ij} (q_i + q_j - 2\xi_{ij}^*)},\tag{43}$$

$$\frac{\partial T_{ij}}{\partial q_i} = (1 - 2q_i)q_j(1 - q_j) - 2(\xi_{ij}^* - q_i q_j)(\frac{\partial \xi_{ij}^*}{\partial q_i} - q_j),\tag{44}$$

$$\frac{\partial T_{ij}}{\partial q_j} = (1 - 2q_j)q_i(1 - q_i) - 2(\xi_{ij}^* - q_i q_j)(\frac{\partial \xi_{ij}^*}{\partial q_j} - q_i),\tag{45}$$

$$\frac{\partial r_{ij}^+}{\partial q_i} = \frac{\left(-\frac{\partial \xi_{ij}^*}{\partial q_i} + q_j\right) T_{ij} - \left(q_j(1 - q_j) - \xi_{ij}^* + q_i q_j\right) \frac{\partial T_{ij}}{\partial q_i}}{T_{ij}^2},\tag{46}$$

$$\frac{\partial r_{ij}^{+}}{\partial q_{j}} = \frac{(1 - 2q_{j} - \frac{\partial \xi_{ij}^{*}}{\partial q_{j}} + q_{i})T_{ij} - (q_{j}(1 - q_{j}) - \xi_{ij}^{*} + q_{i}q_{j})\frac{\partial T_{ij}}{\partial q_{j}}}{T_{ij}^{2}}.$$
 (47)

(b) The second-order partial derivatives of $\xi_{ij}^*(q_i,q_j)$ and $T_{ij}(q_i,q_j)$ are

$$\frac{\partial^2 \xi_{ij}^*}{\partial q_i^2} = \alpha_{ij} \frac{\left(-\frac{\partial \xi_{ij}^*}{\partial q_i}\right) \cdot A_{ij} - \left(\alpha_{ij}(q_j - \xi_{ij}^*) + q_j\right) \left(1 - 2\frac{\partial \xi_{ij}^*}{\partial q_i}\right)}{A_{ij}^2},\tag{48}$$

$$\frac{\partial^2 \xi_{ij}^*}{\partial q_i \partial q_j} = \frac{\alpha_{ij} \left[\left(1 - \frac{\partial \xi_{ij}^*}{\partial q_j} + \frac{1}{\alpha_{ij}} \right) \cdot A_{ij} - \left(\alpha_{ij} (q_j - \xi_{ij}^*) + q_j \right) \left(1 - 2 \frac{\partial \xi_{ij}^*}{\partial q_j} \right) \right]}{A_{ij}^2},\tag{49}$$

$$\frac{\partial^2 \xi_{ij}^*}{\partial q_j^2} = \alpha_{ij} \frac{\left(-\frac{\partial \xi_{ij}^*}{\partial q_j}\right) \cdot A_{ij} - \left(\alpha_{ij}(q_i - \xi_{ij}^*) + q_i\right) \left(1 - 2\frac{\partial \xi_{ij}^*}{\partial q_j}\right)}{A_{ij}^2},\tag{50}$$

$$\frac{\partial^2 T_{ij}}{\partial q_i^2} = -2q_j(1 - q_j) - 2\left(\left(\frac{\partial \xi_{ij}^*}{\partial q_i} - q_j\right)^2 + (\xi_{ij}^* - q_i q_j)\left(\frac{\partial^2 \xi_{ij}^*}{\partial q_i^2}\right)\right),\tag{51}$$

$$\frac{\partial^2 T_{ij}}{\partial q_i \partial q_j} = (1 - 2q_j)(1 - 2q_i) - 2\left(\left(\frac{\partial \xi_{ij}^*}{\partial q_i} - q_j\right)\left(\frac{\partial \xi_{ij}^*}{\partial q_j} - q_i\right) + (\xi_{ij}^* - q_iq_j)\left(\frac{\partial^2 \xi_{ij}^*}{\partial q_i \partial q_j} - 1\right)\right),\tag{52}$$

$$\frac{\partial^2 T_{ij}}{\partial q_j^2} = -2q_i(1 - q_i) - 2\left(\left(\frac{\partial \xi_{ij}^*}{\partial q_j} - q_i\right)^2 + (\xi_{ij}^* - q_i q_j)\left(\frac{\partial^2 \xi_{ij}^*}{\partial q_j^2}\right)\right),\tag{53}$$

where we have defined $A_{ij} := (1 + \alpha_{ij}(q_i + q_j - 2\xi_{ij}^*)).$

Theorem 11

Let q_i be an arbitrary (but fixed) value in (0,1) and consider $r_{ij}^+(q_i,q_j)$ as a function of q_j in the interval (0,1). The only stationary point of $r_{ij}^+(q_i,q_j)$ in that interval is $q_j^* = 1 - q_i$. In other words, the nonlinear equation

$$\frac{\partial r_{ij}^+}{\partial q_i} = 0 \tag{54}$$

has the unique solution $q_i^* = 1 - q_i$.

Next, we analyze what kind of stationary point $r_{ij}^+(q_i, q_j)$ has in $q_j^* = 1 - q_i$ and if this depends on the choice of q_i . We answer this in Theorem 13, by comparing the value of r_{ij}^+ in q_j^* to its limit values at the boundary points. These are computed in the next Lemma:

Lemma 12

Let $q_i \in (0,1)$ be arbitrary (but fixed)- and consider $r_{ij}^+(q_i,q_j)$ as a function of q_j in (0,1).

(a) In its unique stationary point $q_j^* = 1 - q_i$, r_{ij}^+ takes the value

$$r_{ij}^{+}(q_i, 1 - q_i) = \frac{1}{\xi_{ij}^{*}(q_i, 1 - q_i)}.$$
 (55)

(b) If r_{ij}^+ approaches the boundary points of (0,1), its limit values are

$$\lim_{q_j \to 0} r_{ij}^+(q_i, q_j) = \frac{1 + \alpha_{ij} q_i^2}{(1 + \alpha_{ij} q_i) q_i (1 - q_i)}, \quad and$$
 (56)

$$\lim_{q_j \to 1} r_{ij}^+(q_i, q_j) = \frac{1 + \alpha_{ij} (1 - q_i)^2}{\left(1 + \alpha_{ij} (1 - q_i)\right) q_i (1 - q_i)}.$$
 (57)

This further implies the relation

$$\lim_{q_i \to 1} r_{ij}^+(q_i, q_j) = \lim_{q_i \to 0} r_{ij}^+(1 - q_i, q_j). \tag{58}$$

For a more compact notation, let us define

$$r_{ij}^{(+,0)}(q_i) := \lim_{q_i \to 0} r_{ij}^+(q_i, q_j), \quad \text{and}$$
 (59)

$$r_{ij}^{(+,1)}(q_i) := \lim_{q_j \to 1} r_{ij}^+(q_i, q_j).$$
 (60)

Note that $r_{ij}^{(+,0)}$ and $r_{ij}^{(+,1)}$ are not functions of q_j any longer but only depend on q_i .

The next Theorem shows that $q_j^* = 1 - q_i$ is always a maximum of $r_{ij}^+(q_i, q_j)$ (still considered as a function of q_i).

Theorem 13

We have the following relations between the values of $r_{ij}^+(q_i, q_j)$ in its stationary point $q_j^* = 1 - q_i$ and its limit values at the boundary:

- If $0 < q_i < 0.5$, then $r_{ij}^{(+,0)}(q_i) < r_{ij}^{(+,1)}(q_i) < r_{ij}^{+}(q_i, 1 q_i)$.
- If $0.5 < q_i < 1$, then $r_{ij}^{(+,1)}(q_i) < r_{ij}^{(+,0)}(q_i) < r_{ij}^{+}(q_i, 1 q_i)$.
- If $q_i = 0.5$, then $r_{ij}^{(+,0)}(q_i) = r_{ij}^{(+,1)}(q_i) < r_{ij}^+(q_i, 1 q_i)$.

In particular, for any choice of $q_i \in (0,1)$, the unique stationary point $q_j^* = 1 - q_i$ is a maximum of $r_{ij}^+(q_i,q_j)$.

Let us recap the insights from the previous statements: To find the infimum of $r_{ij}^+(q_i, q_j)$ with respect to $q_j \in (0,1)$ as the variable and $q_i \in (0,1)$ arbitrary but fixed, we have first shown that this function has the unique stationary point $q_j^* = 1 - q_i$ (Theorem 11). We argued that this must be a maximum (Theorem 13), which implies that the infimum is not taken by $r_{ij}^+(q_i, q_j)$ in the interior of (0,1), but approached at one of the boundary points (i.e, for $q_j \to 0$ or for $q_j \to 1$). We have derived an analytical formula for the limit values of $r_{ij}^+(q_i, q_j)$ at these boundary points as a function of q_i (Lemma 12), and determined which of the two limit values is less than the other, depending on the choice of $q_i \in (0,1)$. Together with the other observations, we conclude that this must then be the infimum.

Corollary 14

For $q_i \in (0,1)$ arbitrary (but fixed), we have

$$\inf_{q_j \in (0,1)} r_{ij}^+(q_i,q_j) = \begin{cases} \frac{1 + \alpha_{ij}q_i^2}{(1 + \alpha_{ij}q_i)q_i(1 - q_i)}, & \text{if } 0 < q_i \le 0.5, \quad \text{and} \\ \frac{1 + \alpha_{ij}(1 - q_i)^2}{\left(1 + \alpha_{ij}(1 - q_i)\right)q_i(1 - q_i)}, & \text{if } 0.5 < q_i < 1. \end{cases}$$

Figure 6 illustrates $\inf_{q_j \in (0,1)} r_{ij}^+(q_i, q_j)$ as a function of q_i (drawn in solid blue curves).

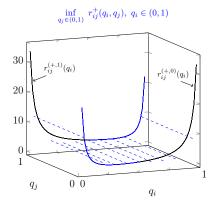


Figure 6: Visualization of the limit values of $r_{ij}^+(q_i, q_j)$ at the boundary points $q_j = 0$ and $q_j = 1$ as a function of q_i . The solid blue curves indicate the position of the infimum, which is approached for $q_j \to 0$ if $q_i \le 0.5$, and for $q_j \to 1$ if $q_i \ge 0.5$ (Corollary 14). The dashed blue lines represent the level of the infimum for different fixed values of q_i .

Corollary 14 provides the solution to the 'inner' sub-problems stated in (37). Hence, we return to the 'outer' problem (41) which is the evaluation of \tilde{R}_i . Before we substitute the formulas derived in Corollary 14 and the expression for $r_i(q_i)$ from (34) into (41), we observe that, for all $q_i \in (0,1)$,

$$\inf_{q_i \in (0,1)} r_{ij}^+(q_i, q_j) = \inf_{q_i \in (0,1)} r_{ij}^+(1 - q_i, q_j). \tag{61}$$

This follows directly from the relation (58) from Lemma 12. Consequently, $\inf_{q_j \in (0,1)} r_{ij}^+(q_i, q_j)$

(as a function of q_i) is symmetric across $q_i = 0.5$, which makes it sufficient to evaluate R_i for $q_i \in (0, 0.5]$. If we assume that, for each edge, we only take the coupling strength $|J_{ij}|$ but not the sign of J_{ij} into account (which is justified by Lemma 9), equation (41) becomes

$$\tilde{R}_{i} = \inf_{q_{i} \in (0,0.5)} \left[\frac{-(d_{i} - 1)}{q_{i}(1 - q_{i})} + \sum_{j \in \mathcal{N}(i)} \frac{1 + \alpha_{ij}q_{i}^{2}}{(1 + \alpha_{ij}q_{i})q_{i}(1 - q_{i})} \right]$$
(62)

$$= \inf_{q_i \in (0,0.5)} \left[\frac{-(d_i - 1) \prod_{j \in \mathcal{N}(i)} (1 + \alpha_{ij} q_i) + \sum_{j \in \mathcal{N}(i)} \left((1 + \alpha_{ij} q_i^2) \prod_{k \in \mathcal{N}(i) \setminus j} (1 + \alpha_{ik} q_i) \right)}{q_i (1 - q_i) \prod_{j \in \mathcal{N}(i)} (1 + \alpha_{ij} q_i)} \right].$$
(63)

To check the diagonal dominance criterion (32) stated in Proposition 7, we do not need to compute the exact value of this infimum (which, by Lemma 8, is identical to $\inf_{\boldsymbol{q} \in \mathbb{B}} R_i(\boldsymbol{q})$), but only have to determine if it is positive. One simple observation further facilitate this task: All terms in the denominator of (63) are positive; i.e., positivity of the infimum depends only on the numerator, which is a polynomial in a single variable q_i and of degree $d_i + 1$. Altogether, we present the final Theorem of this subsection:

Theorem 15

The convexity criterion stated in Proposition 7 is equivalent to the following condition: The Bethe free energy \mathcal{F}_B is convex on the Bethe box \mathbb{B} if, for all nodes $i \in \mathbf{X}$, the one-dimensional polynomial

$$\Psi_i(q_i) := -(d_i - 1) \prod_{j \in \mathcal{N}(i)} (1 + \alpha_{ij} q_i) + \sum_{j \in \mathcal{N}(i)} \left((1 + \alpha_{ij} q_i^2) \prod_{k \in \mathcal{N}(i) \setminus j} (1 + \alpha_{ik} q_i) \right)$$
(64)

is strictly positive on the interval (0,0.5].

Theorem 15 is the central result of this subsection. It provides a sufficient condition for the convexity of the Bethe free energy \mathcal{F}_B on the Bethe box \mathbb{B} . Figure 7 shows the behavior of the polynomial $\Psi_i(q_i)$ in dependence of the inverse temperature β .

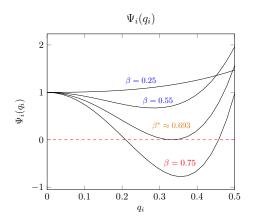


Figure 7: Development of the polynomial $\Psi_i(q_i)$ for increasing values of the inverse temperature β , associated to a node i with three neighbors $(d_i = 3)$, and a coupling $J_{ij} = J = 0.5$ that is shared by all three incident edges. For $\beta = 0.25$ and $\beta = 0.55$, condition (64) from Theorem 15 is satisfied with respect to node i (blue). $\beta^* \approx 0.693$ is the critical threshold at which (64) is violated for the first time, as $\Psi_i(q_i)$ touches the horizontal axis and takes root in the interval (0,0.5) (orange); for higher values of the inverse temperature (e.g., $\beta = 0.75$), $\Psi_i(q_i)$ has multiple roots in (0,0.5) which causes (64) to be violated (red).

3.3 Edge-Specific Convexity Criterion: Sum Decomposition of Bethe Hessian

Our second approach to relax the convexity of \mathcal{F}_B decomposes the Bethe Hessian into a sum of sparse matrices, and derives a sufficient condition for the positive definiteness of the individual matrices in that sum. The main result is Theorem 23, a closed formula for the critical threshold of the inverse temperature, at which convexity of the Bethe free energy is not guaranteed any longer. All proofs for this section are collected in Appendix B.

The starting point is the same as in Sec. 3.2, namely to ask under which conditions the Bethe Hessian $\mathbf{H}_B(q)$ is positive definite for all q in the Bethe box \mathbb{B} (the definition of convexity, Sec. 2.1). However, we use an alternative approach to relax this problem: While, in Sec. 3.2, we have applied the diagonal dominance criterion to the entire Bethe Hessian, we now decompose \mathbf{H}_B into a sum of sparse matrices \mathbf{H}'_B (i.e., by writing $\mathbf{H}_B = \sum \mathbf{H}'_B$) and then characterize the positive definiteness of the individual matrices in that sum. In case that all \mathbf{H}'_B are positive definite over \mathbb{B} , their sum \mathbf{H}_B is positive definite over \mathbb{B} as well. This induces a sufficient (but not necessary 21) condition for the convexity of \mathcal{F}_B on the Bethe box \mathbb{B} . Further differences between the our approaches will be discussed in Sec. 3.4.

The first problem we are facing is how to define the matrices \mathbf{H}'_B in a sum decomposition of \mathbf{H}_B . On the one hand, they should be simple enough to allow for an exact characterization of their definiteness properties. On the other hand, too many (simple) matrices in the

^{21.} Note that \mathbf{H}_B might still be positive definite if some (or even all) matrices \mathbf{H}_B' in the sum decomposition are not. This explains why our approach is merely a relaxation to the problem of characterizing the positive definiteness of \mathbf{H}_B .

sum may induce a relatively high gap between the 'true' and the predicted convexity (as a sufficient criterion for convexity requires positive definiteness of each individual matrix in the sum). Instead of trying to minimize this gap, we propose an edge-specific class of sum decompositions, in which the individual matrices are naturally related to the edges in the graph (i.e., for each edge (i,j) we have one associated matrix $\mathbf{H}_B^{(i,j)}$ in the sum). This particular choice can be motivated by the properties of the Bethe free energy, which is itself a sum of edge- and node-specific statistics (21). While it might be tempting to write the Bethe Hessian as a sum of Hessians corresponding to these statistics (i.e., computing the Hessians of the individual terms in (21) and summing them up), we must consider one aspect: the local entropies \mathcal{S}_i are always concave and their Hessians can never be positive definite (i.e., considering them as separate matrices in the sum can never result in a sufficient criterion for convexity). Also, these are the only node-specific statistics contributing to the Bethe Hessian, because \mathbf{H}_B is independent from the fields θ_i (Corollary 5). Thus, instead of defining separate 'node-specific Hessians' \mathbf{H}_B^i for each node i, it is preferable to absorb the node-specific statistics from \mathbf{H}_B into the 'edge-specific Hessians' $\mathbf{H}_B^{(i,j)}$.

We consider the following class of sum decompositions: Let us write the Bethe Hessian as

$$\mathbf{H}_B = \sum_{(i,j) \in \mathbf{E}} \mathbf{H}_B^{(i,j)},\tag{65}$$

with the entries of $\mathbf{H}_{B}^{(i,j)}$ – for an arbitrary edge (i,j) and indices $k,l \in \{1,\ldots,|\mathbf{X}|\}$ – being defined as

$$(\mathbf{H}_{B}^{(i,j)})_{k,l} = \begin{cases} \frac{1}{\beta} \left(-s_{ij} \frac{(d_{i}-1)}{q_{i}(1-q_{i})} + \frac{q_{j}(1-q_{j})}{T_{ij}} \right) & k = l = i \\ \frac{1}{\beta} \left(-s_{ji} \frac{(d_{j}-1)}{q_{j}(1-q_{j})} + \frac{q_{i}(1-q_{i})}{T_{ij}} \right) & k = l = j \\ \frac{1}{\beta} \left(\frac{q_{i}q_{j} - \xi_{ij}^{*}}{T_{ij}} \right) & k, j \in \{i, j\}, k \neq l \\ 0 & \text{otherwise.} \end{cases}$$
 (66)

This definition requires some explanation. First, note that we have introduced parameters s_{ij} and s_{ji} (i.e., two parameters per edge) whose purpose is to 'distribute' the second-order local entropy contributions from \mathbf{H}_B (using the equations from (27), (b)) over the edge-specific Hessians $\mathbf{H}_B^{(i,j)}$. More precisely, s_{ij} represents the relative proportion of the second-order local entropy contribution related to node i (i.e., of $\frac{\partial^2}{\partial q_i^2} \left(-\frac{1}{\beta}(d_i-1)\mathcal{S}_i\right) = -\frac{1}{\beta}\frac{(d_i-1)}{q_i(1-q_i)}$) that we absorb from \mathbf{H}_B into the edge-specific Hessian $\mathbf{H}_B^{(i,j)}$. Analogously, s_{ji} does the same with the second-order local entropy contribution related to node j (i.e., with $-\frac{1}{\beta}\frac{(d_j-1)}{q_j(1-q_j)}$)). In other words, for each node i, we distribute its second-order local entropy contributions from \mathbf{H}_B over all edge-specific Hessians $\mathbf{H}_B^{(i,j)}$ with $j \in \mathcal{N}(i)$. To make this a reasonable approach, where each s_{ij} represents a certain proportion of the corresponding second-order local entropy contribution, we assume that all parameters satisfy

$$0 \le s_{ij}, s_{ji} \le 1. \tag{67}$$

Then, to guarantee that the sum decomposition (65) holds, we introduce linear constraints

$$\sum_{j \in \mathcal{N}(i)} s_{ij} = 1 \tag{68}$$

for all nodes. By this, the second-order local entropy contributions are exactly distributed over the edge-specific Hessians. The other terms in the definition (66) of $\mathbf{H}_{B}^{(i,j)}$ (i.e., the main diagonal entries $\frac{1}{\beta} \left(\frac{q_{i}(1-q_{j})}{T_{ij}} \right)$ resp. $\frac{1}{\beta} \left(\frac{q_{i}(1-q_{i})}{T_{ij}} \right)$, and the off-diagonal entries $\frac{1}{\beta} \left(\frac{q_{i}q_{j}-\xi_{ij}^{*}}{T_{ij}} \right)$ stem from the second-order pairwise entropy contributions $\frac{\partial^{2}}{\partial q_{i}^{2}} \left(-\frac{1}{\beta} \left(\mathbf{S}_{ij} \right) \right)$ in \mathbf{H}_{B} .

One favorable property of this specific class of sum decompositions is the sparseness of its involved matrices. From (66), we observe that each edge-specific Hessian $\mathbf{H}_{B}^{(i,j)}$ has precisely four non-zero entries at the index positions [i,i],[i,j],[j,i], and [j,j], with identical entries at [i,j] and [j,i]. More generally, we deal with a sum of quadratic matrices of the form

$$\mathbf{M}^{(i,j)} := \begin{pmatrix} 0 & \cdots & 0 & \cdots & 0 \\ \vdots & \ddots & \vdots & & \vdots \\ & a^{(i,j)} & \cdots & c^{(i,j)} & \\ 0 & \cdots & \vdots & \vdots & \cdots & 0 \\ \vdots & c^{(i,j)} & \cdots & b^{(i,j)} & & \vdots \\ & & \vdots & & \ddots & \\ 0 & \cdots & 0 & \cdots & 0 \end{pmatrix}$$
(69)

where at most one matrix in the sum can have non-zero entries at a specific pair of offdiagonal positions [i,j] and [j,i] (which is precisely the case if (i,j) is an edge in the graph). Here is another subtlety to be addressed: Strictly speaking, this kind of matrix can never be positive definite – but only positive semidefinite – as one can always find vectors $\mathbf{y} \neq \mathbf{0}$ such that $\mathbf{y}^T \mathbf{M}^{(i,j)} \mathbf{y} = \mathbf{0}$. However, one can show that a sum of positive semidefinite matrices of the form (69) is positive definite, if only the (2×2) - submatrices

$$\mathbf{M}_{2\times 2}^{(i,j)} := \begin{pmatrix} a^{(i,j)} & c^{(i,j)} \\ c^{(i,j)} & b^{(i,j)} \end{pmatrix}$$
 (70)

are positive definite for each individual matrix $\mathbf{M}^{(i,j)}$ in the sum 22 . This facilitates our analysis, as we can focus on studying the definiteness properties of (2×2) - submatrices of the edge-specific Hessians $\mathbf{H}_B^{(i,j)}$ defined as

$$\mathbf{H}_{2\times2}^{(i,j)} := \frac{1}{\beta} \begin{pmatrix} -s_{ij} \frac{(d_i-1)}{q_i(1-q_i)} + \frac{q_j(1-q_j)}{T_{ij}} & \frac{q_iq_j - \xi_{ij}^*}{T_{ij}} \\ \frac{q_iq_j - \xi_{ij}^*}{T_{ij}} & -s_{ji} \frac{(d_j-1)}{q_j(1-q_j)} + \frac{q_i(1-q_i)}{T_{ij}} \end{pmatrix}.$$
(71)

^{22.} To prove this, write $\mathbf{y}^T \left(\sum \mathbf{M}^{(i,j)}\right) \mathbf{y}$ equivalently as a sum of quadratic forms $\sum \left(y_i \quad y_j\right) \mathbf{M}_{2\times 2}^{(i,j)} \left(\begin{matrix} y_i \\ y_j \end{matrix}\right)$ (by exploiting the structure (69) of $\mathbf{M}^{(i,j)}$) and use the positive definiteness of all submatrices $\mathbf{M}_{2\times 2}^{(i,j)}$.

So far, we have explained our approach to deriving a sufficient criterion for convexity of the Bethe free energy \mathcal{F}_B on the Bethe box \mathbb{B} by writing its Hessian \mathbf{H}_B (Lemma 4, (b)) as a sum of matrices and proving positive definiteness of the individual matrices in that sum. Moreover, we have introduced a class of edge-specific sum decompositions (65) and shown that an edge-specific Hessian (66) is positive semidefinite, if and only if a (2×2) - submatrix $\mathbf{H}_{2\times 2}^{(i,j)}$ of $\mathbf{H}_B^{(i,j)}$, defined by (71), is positive definite. We have also argued that positive semidefiniteness of all edge-specific Hessians $\mathbf{H}_B^{(i,j)}$ is sufficient for positive definiteness of the Bethe Hessian \mathbf{H}_B . In the remainder of this section, we analyze when the submatrices $\mathbf{H}_{2\times 2}^{(i,j)}$ are positive definite 23 ; i.e., in dependence of its involved parameters (which are the independent variables q_i, q_j ; the model-specific parameters d_i, d_j, J_{ij} ; the constrained parameters s_{ij}, s_{ji} ; and the inverse temperature β).

According to Sylvester's criterion (Sec. 2.1), a quadratic real matrix is positive definite if and only if all its leading principle minors are positive. In the case of a (2×2) - matrix, these are the upper left element of the matrix and the determinant of the entire matrix. This implies that a submatrix $\mathbf{H}_{2\times 2}^{(i,j)}$ of $\mathbf{H}_{B}^{(i,j)}$ is positive definite in an arbitrary point (q_i,q_j) in $(0,1)\times(0,1)$, if and only if the inequalities

$$-s_{ij}\frac{(d_i-1)}{q_i(1-q_i)} + \frac{q_j(1-q_j)}{T_{ij}} > 0 \quad \text{and}$$
 (72)

$$\left(-s_{ij}\frac{(d_{i}-1)}{q_{i}(1-q_{i})} + \frac{q_{j}(1-q_{j})}{T_{ij}}\right) \cdot \left(-s_{ji}\frac{(d_{j}-1)}{q_{j}(1-q_{j})} + \frac{q_{i}(1-q_{i})}{T_{ij}}\right) - \left(\frac{q_{i}q_{j} - \xi_{ij}^{*}}{T_{ij}}\right)^{2} > 0$$
(73)

are satisfied (for some prespecified parameters s_{ij}, s_{ji}). The left-hand side of (73) is the determinant of $\mathbf{H}_{2\times 2}^{(i,j)}$, where we have omitted the positive scale factor $\frac{1}{\beta^2}$ as it does not influence the sign of the determinant (still, we have implicit dependence on the inverse temperature β via ξ_{ij} and T_{ij}). These formulas are analytically complex, as ξ_{ij} and T_{ij} are themselves functions of q_i, q_j (defined in (24) and (28)). Also, both inequalites must be satisfied for all (q_i, q_j) in $(0, 1) \times (0, 1)$ (or, equivalently, for the infimum over all such pairs) which complicates their verification. To simplify the analysis, we further specify our definition of edge-specific Hessians. Recall that there is some freedom in selecting the constrained parameters s_{ij}, s_{ji} , as long as they satisfy the constraints (67) and (68). A particularly natural choice arises if we distribute the second-order local entropy contributions related to node i uniformly over the edge-specific Hessians $\mathbf{H}_B^{(i,j)}$ (for j in $\mathcal{N}(i)$); i.e., if we take $s_{ij} = \frac{1}{d_i}$ and $s_{ji} = \frac{1}{d_j}$. Clearly, this is a valid choice since $0 < \frac{1}{d_i} < 1$ and $\sum_{j \in \mathcal{N}(i)} \frac{1}{d_i} = d_i \cdot \frac{1}{d_i} = 1$.

Note that other choices of s_{ij} , s_{ji} might induce more powerful criteria for convexity ²⁴ (as

^{23.} Note that \mathbf{H}_B and the matrices in its sum decomposition are functions defined over the Bethe box, i.e., depend on $\mathbf{q} \in \mathbb{B}$. This implies that the edge-specific Hessians and their submatrices must be positive (semi-)definite for all pairs (q_i, q_j) in $(0, 1) \times (0, 1)$ (as $\mathbf{H}_B^{(i,j)}$ depends only on the associated variables q_i and q_j) to guarantee convexity of \mathcal{F}_B .

^{24.} One possible alternative would be to distribute the second-order local entropy contribution according to the strength of couplings related to the edges between neighboring nodes; i.e., take $s_{ij} = \frac{|J_{ij}|}{\sum\limits_{k \in \mathbb{N}(i)} |J_{ik}|}$.

this might be the case for different kind of sum decompositions than the edge-specific one); however, our choice entails the positive aspect that inequality (72) is always satisfied:

$$-s_{ij} \frac{(d_i - 1)}{q_i(1 - q_i)} + \frac{q_j(1 - q_j)}{T_{ij}}$$

$$= -\frac{1}{d_i} \frac{(d_i - 1)}{q_i(1 - q_i)} + \frac{q_j(1 - q_j)}{T_{ij}}$$

$$\stackrel{(28)}{=} -\frac{1}{d_i} \frac{(d_i - 1)}{q_i(1 - q_i)} + \frac{q_j(1 - q_j)}{q_iq_j(1 - q_i)(1 - q_j) - (\xi_{ij}^* - q_iq_j)^2}$$

$$> -\frac{1}{d_i} \frac{(d_i - 1)}{q_i(1 - q_i)} + \frac{q_j(1 - q_j)}{q_iq_j(1 - q_i)(1 - q_j)}$$

$$= \frac{-(d_i - 1) + d_i}{d_iq_i(1 - q_i)} = \frac{1}{d_iq_i(1 - q_i)} > 0$$

Using this 'uniform' choice of s_{ij} , s_{ji} , we can thus focus on inequality (73) whose left-hand side is the determinant of $\mathbf{H}_{2\times 2}^{(i,j)}$, defined as

$$\det \mathbf{H}_{2\times2}^{(i,j)}(q_i, q_j) \\ := \left(\frac{-(d_i - 1)}{d_i q_i (1 - q_i)} + \frac{q_j (1 - q_j)}{T_{ij}}\right) \cdot \left(\frac{-(d_j - 1)}{d_j q_j (1 - q_j)} + \frac{q_i (1 - q_i)}{T_{ij}}\right) - \left(\frac{q_i q_j - \xi_{ij}^*}{T_{ij}}\right)^2.$$
(74)

Before we proceed, we simplify the expression in (74) and work with a more compact formula of det $\mathbf{H}_{2\times 2}^{(i,j)}$. Namely, (74) is the same as

$$\frac{d_{i}-1}{d_{i}} \cdot \frac{d_{j}-1}{d_{j}} \cdot \frac{1}{q_{i}q_{j}(1-q_{i})(1-q_{j})} - \frac{1}{T_{ij}} \cdot \left(\frac{d_{i}-1}{d_{i}} + \frac{d_{j}-1}{d_{j}}\right) \\
= \frac{T_{ij}}{q_{i}q_{j}(1-q_{i})(1-q_{j}) - (q_{i}q_{j}-\xi_{ij}^{*})^{2}}{T_{ij}^{2}} \\
= \frac{d_{i}-1}{d_{i}} \cdot \frac{d_{j}-1}{d_{j}} \cdot \frac{1}{q_{i}q_{j}(1-q_{i})(1-q_{j})} + \frac{1}{T_{ij}}\left(1 - \frac{d_{i}-1}{d_{i}} - \frac{d_{j}-1}{d_{j}}\right). \tag{75}$$

Let us summarize the essentials of our present analysis:

Proposition 16

Let $\mathbf{H}_{2\times2}^{(i,j)}(q_i,q_j)$ be the submatrices of the edge-specific Hessians $\mathbf{H}_B^{(i,j)}(q_i,q_j)$ defined in (71) resp. (66) together with a set of parameters $\{s_{ij},s_{ji}\}$ for each edge (i,j) satisfying the constraints (67) and (68). Then the Bethe free energy \mathfrak{F}_B is convex on the Bethe box \mathbb{B} , if all submatrices $\mathbf{H}_{2\times2}^{(i,j)}(q_i,q_j)$ are positive definite for all (q_i,q_j) in $(0,1)\times(0,1)$, i.e., if the inequalities (72) and (73) are satisfied. If we set $s_{ij}=\frac{1}{d_i}$, then $\mathbf{H}_{2\times2}^{(i,j)}(q_i,q_j)$ is positive definite if and only if the determinant of $\mathbf{H}_{2\times2}^{(i,j)}(q_i,q_j)$ defined in (75) is positive.

Also, it remains an open problem if we can 'optimize' the choice of s_{ij} , s_{ji} to minimize the gap between the convexity induced by a certain criterion and the true convexity.

To use these qualitative statements for proving the convexity of \mathcal{F}_B , we need to characterize the behavior of $\det \mathbf{H}_{2\times 2}^{(i,j)}(q_i,q_j)$ (as a function of q_i and q_j) in dependence of its parameters. In particular, we must determine whether $\det \mathbf{H}_{2\times 2}^{(i,j)}(q_i,q_j)$ is positive for all points (q_i,q_j) in $(0,1)\times(0,1)$, or if there exists a point where it is non-positive (in which case positive definiteness of $\mathbf{H}_{2\times 2}^{(i,j)}$ would be violated). In principle, we could once again formulate an optimization problem in which we try to compute the infimum of $\det \mathbf{H}_{2\times 2}^{(i,j)}$ and determine whether it is positive or not (analogously to problem (32) in Sec. 3.2); however, we follow a slightly different path in this analysis. Let us consider an edge (i,j) in the graph with fixed degrees d_i , d_j of its end nodes and with an associated coupling J_{ij} , and let us assume that we vary the inverse temperature β . First of all, we observe that $\det \mathbf{H}_{2\times 2}^{(i,j)}$ is positive on its domain if β approaches zero (or in other words, in the infinite temperature limit $T \to \infty$):

Lemma 17

In the infinite temperature limit, we have for all (q_i, q_i) in $(0, 1) \times (0, 1)$:

$$\lim_{\beta \to 0} \left[\det \mathbf{H}_{2 \times 2}^{(i,j)}(q_i, q_j) \right] = \frac{1}{d_i d_j} \cdot \frac{1}{q_i q_j (1 - q_i) (1 - q_j)} > 0$$
 (76)

Lemma 17 characterizes the behavior of $\det \mathbf{H}_{2\times 2}^{(i,j)}$ in the infinite temperature limit. It also states that the determinant is positive on its domain, if the inverse temperature β is sufficiently small (because $\det \mathbf{H}_{2\times 2}^{(i,j)}$ is a continuous function of q_i and q_j). This proves the existence 25 of some critical threshold $\beta^* > 0$ such that, for all values $0 < \beta < \beta^*$, Proposition 16 is satisfied 26 , and therefore justifies our approach in this section. Moverover, Proposition 16 and Lemma 17 prove a fundamental result:

Corollary 18

For a sufficiently high temperature, the Bethe free energy \mathfrak{F}_B is convex on the Bethe box \mathbb{B} .

Regarding our previous analysis, this statement is not surprising; however, to the best of our knowledge, this is the first time that this result has been proven in the literature.

The next question is how det $\mathbf{H}_{2\times 2}^{(i,j)}$ behaves, if we make an infinitesimal change in the (inverse) temperature. Intuitively, we expect the determinant to decrease if we reduce the temperature, as the Bethe approximation often deteriorates with stronger interactions in the model (thus, the conditions in Proposition 16 would be expected to be violated at some point, Meshi et al. (2009); Weller et al. (2014); Knoll and Pernkopf (2020)). This is confirmed by the following Lemma, in which we prove an even stronger result, namely that $\det \mathbf{H}_{2\times 2}^{(i,j)}$ is a monotonically decreasing function of β :

^{25.} We remark that β^* might take the value ∞ , i.e., \mathcal{F}_B might be convex for any temperature. Also, if we additionally require that β^* is the greatest positive number (including ∞) satisfying the described property, then it is even unique.

^{26.} More precisely, Lemma 17 is only an edge-specific result, where we have considered the submatrix $\mathbf{H}_{2\times 2}^{(i,j)}$ associated to some arbitrary edge (i,j) in the graph. However, the statement in the text follows immediately, if we have one such 'edge-specific' threshold $(\beta^*)^{(i,j)}$ for each edge (i,j) and then identify their minimum as the critical threshold β^* .

Lemma 19

For all (q_i, q_j) in $(0, 1) \times (0, 1)$, the determinant of $\mathbf{H}_{2 \times 2}^{(i,j)}(q_i, q_j)$ is monotonically decreasing, as β increases, i.e.,

$$\frac{\partial}{\partial \beta} \left[\det \mathbf{H}_{2 \times 2}^{(i,j)}(q_i, q_j) \right] < 0. \tag{77}$$

Lemma 19 makes an important statement as it says the following: If the determinant of $\mathbf{H}_{2\times2}^{(i,j)}$ is negative for some value of the inverse temperature β (by which positive definiteness of $\mathbf{H}_{2\times2}^{(i,j)}$ and thus the condition in Proposition 16 would be violated), then it is also negative for all larger values of β . On the other hand, we know by Lemma 17 that $\det \mathbf{H}_{2\times2}^{(i,j)}$ is always positive if β is sufficiently small. To complete the image, we will next show that there exists a real (and unique) value β^* , for which $\det \mathbf{H}_{2\times2}^{(i,j)}$ equals zero in some point (q_i,q_j) in $(0,1)\times(0,1)$, and which is consequently the smallest β for which the determinant is not positive. Moreover, we show that the point where this scenario occurs is precisely the 'center' of the domain, i.e., the point (0.5,0.5). Figure 8 illustrates this behavior of the determinant. Regarding our analysis, this implies that we can explicitly compute a critical value β^* such that Proposition 16 is either satisfied or violated.

Before we address the global properties of the determinant, we focus on the center point (0.5, 0.5). The following result provides the critical value β^* of the inverse temperature, at which the determinant is zero in that point:

Lemma 20

Let $d_i, d_j > 2$ and let

$$\beta^* := \frac{1}{2|J_{ij}|}\operatorname{arccosh}\left(1 + \frac{2}{d_i d_j - d_i - d_j}\right) \tag{78}$$

be the 'critical' value of the inverse temperature. Then

$$\det \mathbf{H}_{2\times2}^{(i,j)}(0.5,0.5) \begin{cases} > 0 & for \quad \beta < \beta^*, \\ = 0 & if \quad \beta = \beta^*, \quad and \\ < 0 & for \quad \beta > \beta^*. \end{cases}$$
(79)

Lemma 20 provides the critical threshold β^* of the inverse temperature at which det $\mathbf{H}_{2\times 2}^{(i,j)}$, evaluated in the center point (0.5,0.5), changes its sign from positive to negative (i.e., at which det $\mathbf{H}_{2\times 2}^{(i,j)}(0.5,0.5)$ becomes indefinite). This may not seem especially important as there might exist other points (q_i,q_j) in the domain, in which the determinant is already negative for smaller values of β than β^* (while we are searching for the greatest value of β at which the determinant is positive on its entire domain). However, as already indicated ahead of Lemma 20, the center point is precisely the point where det $\mathbf{H}_{2\times 2}^{(i,j)}$ first changes its sign if the inverse temperature steadily increases (when starting from close to zero).

^{27.} Due to numerical reasons, an exact visualization of the situation for $\beta = \beta^*$ was not possible.

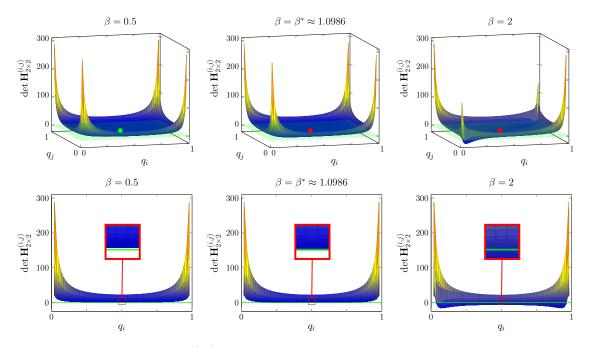


Figure 8: Behavior of det $\mathbf{H}_{2\times 2}^{(i,j)}$ on its domain $(0,1)\times(0,1)$ for $d_i=d_j=3$ and $J_{ij}=0.5$ (corresponding to a ferromagnetic edge whose end nodes have both three neighbors), and for varying values of the inverse temperature β .

Top row: 3D plots of $\det \mathbf{H}_{2\times 2}^{(i,j)}$ for increasing values of β . The green planes represent the q_iq_j - plane (i.e, the zero level of the determinant). If the graph of $\det \mathbf{H}_{2\times 2}^{(i,j)}$ lies above this plane, then $\mathbf{H}_{2\times 2}^{(i,j)}$ is positive definite for the associated value of β ; if the graph cuts (or touches) the plane, it is not. According to Theorem 23, $\det \mathbf{H}_{2\times 2}^{(i,j)}$ is positive on its domain if and only if it is positive in the center point (0.5,0.5). This is, e.g., the case for $\beta=0.5$, as is indicated by the green circle in the left-hand figure. In the middle figure, the graph of $\det \mathbf{H}_{2\times 2}^{(i,j)}$ touches the green plane in the center point. This occurs precisely for the critical value β^* , which is the smallest β such that $\det \mathbf{H}_{2\times 2}^{(i,j)}$ is not longer positive on its domain. This is because $\det \mathbf{H}_{2\times 2}^{(i,j)}$ takes the value zero in the center point (Lemma 20), as is indicated by a red circle. Since $\det \mathbf{H}_{2\times 2}^{(i,j)}$ is monotonically decreasing as β increases (Lemma 19), it is negative in (0.5,0.5) for all larger values of β . In the right-hand figure $(\beta=2)$, the graph of $\det \mathbf{H}_{2\times 2}^{(i,j)}$ cuts the green plane in multiple points.

Bottom row: The same graphs as in the top row, but from a side perspective at the level of the q_iq_j - plane (with the q_i - axis located in front of the viewpoint and the q_j - axis hidden behind). The area around the center point has been magnified, so that the described behavior is better visible²⁷.

Theorem 21

Let $d_i, d_j > 2$, let β^* be the critical threshold of the inverse temperature derived in Lemma 20, and let $\det \mathbf{H}_{2\times 2}^{(i,j)}$ (considered as a function of (q_i,q_j)) implicitly depend on β^* . Then $\det \mathbf{H}_{2\times 2}^{(i,j)}$ has a unique root in the center point (0.5,0.5) and is positive for all other points (q_i,q_j) in $(0,1)\times (0,1)$.

Theorem 21 is a strong result that fully characterizes the global behavior of det $\mathbf{H}_{2\times 2}^{(i,j)}$ on its domain. It says that, if the inverse temperature of the model takes the critical value β^* (derived in Lemma 20), there exists precisely one point in the domain – the center point – where the determinant is non-positive (while it is positive for all other points). As a consequence, the conditions for convexity of the Bethe free energy from Proposition 16 are not satisfied if $\beta = \beta^*$. If we combine this knowledge with the insights gained in Lemma 19 (the determinant monotonically decreases as β increases), we can conclude as follows: On the one hand, $\det \mathbf{H}_{2\times 2}^{(i,j)}$ must be positive on the entire domain whenever the inverse temperature β is below that critical threshold β^* ; on the other hand, det $\mathbf{H}_{2\times 2}^{(i,j)}$ is negative in (0.5, 0.5) whenever the inverse temperature β is beyond that critical threshold β^* . Hence, the complete information about the global definiteness properties of $\mathbf{H}_{2\times 2}^{(i,j)}$ lies already in the center point: If $\mathbf{H}_{2\times 2}^{(i,j)}$ is positive definite in (0.5,0.5), then it is positive definite on its entire domain. This induces a particularly simple criterion for checking the positive definiteness of $\mathbf{H}_{2\times 2}^{(i,j)}$ on its domain, as one simply needs to compute the critical value of the inverse temperature β^* derived in Lemma 20. If $\beta < \beta^*$, then $\mathbf{H}_{2\times 2}^{(i,j)}$ is positive definite; otherwise it is indefinite (because at least the main diagonal entries are always positive). Lemma 19, Lemma 20, and Theorem 21 therefore imply the following corollary:

Corollary 22

If det $\mathbf{H}_{2\times2}^{(i,j)}$ is positive in the center point (0.5,0.5), then it is positive for all (q_i,q_j) in $(0,1)\times(0,1)$. This is precisely the case, if the inverse temperature of the model lies below the critical threshold β^* . Equivalently, if $\mathbf{H}_{2\times2}^{(i,j)}$ is positive definite in the center point (0.5,0.5), then it is positive definite 28 for all (q_i,q_j) in $(0,1)\times(0,1)$.

Up to this point, we have analyzed the properties of a single edge-specific Hessian $\mathbf{H}_{B}^{(i,j)}$ in the sum decomposition (65) of the Bethe Hessian \mathbf{H}_{B} . However, there might of course be values of the critical temperature for which certain matrices in the sum are positive definite, while others are not. Our sufficient criterion for positive definiteness of \mathbf{H}_{B} (and thus convexity of \mathcal{F}_{B}) requires positive definiteness of each individual matrix in that sum. We finally arrive at the central result of this section, which is a reformulation of Proposition 16, based on the insights that we have gained from our analysis:

^{28.} More precisely, the second statement is true if we have defined the constrained parameters s_{ij}, s_{ji} in the definition of the edge-specific Hessians (66) as $s_{ij} = \frac{1}{d_i}, s_{ji} = \frac{1}{d_j}$; not necessarily, however, for all parameters s_{ij}, s_{ji} satisfying the constraints (67), (68).

Theorem 23

Let β be the inverse model temperature. The Bethe free energy \mathcal{F}_B is convex on the Bethe box \mathbb{B} if, for all edges (i,j) in the graph with degrees $d_i,d_j>2$ of their end nodes, the following inequality is satisfied:

$$\beta < \frac{1}{2|J_{ij}|} \operatorname{arccosh} \left(1 + \frac{2}{d_i d_j - d_i - d_j} \right) \tag{80}$$

In Sec. 3.2 and Sec. 3.3 we have derived conditions for the convexity of \mathcal{F}_B on \mathbb{B} , and thus provided answers to the second of our three questions (i) - (iii) formulated in Sec. 3.1 that were the starting point of our analysis. In the remaining part of this work, we address question (iii): Can we explain the reliability of the Bethe approximation through its convexity on the Bethe box \mathbb{B} ? Or in other words, is convexity of \mathcal{F}_B on \mathbb{B} a property that is necessary and/or sufficient for guaranteeing a high quality of the marginal and partition function estimates provided by the Bethe approximation (according to the approximations made in (15) and (16), Sec. 2.3)? In Sec. 3.4 we specify this query and discuss a few of its theoretical aspects. In Sec. 4 we present our experimental results.

3.4 Theoretical Discussion

The purpose of this section is to recap a few characteristics and differences of our main results from Sec. 3.2 (Theorem 15) and Sec. 3.3 (Theorem 23). Furthermore, we put them into the context of similar results from the literature (Sec. 2.4), by comparing them on a perfectly symmetric model (a complete graph with homogenous potentials) whose simplicity allows for an analytical specification of its phase transition boundaries ²⁹ (Georgii, 1988; Taga and Mase, 2006b). Then, to discuss theoretical aspects of question (iii), we analyze the behavior of the Bethe free energy in dependence of the inverse temperature, by distinguishing between its three different 'stages': convexity, non-convexity but uniqueness of a Bethe minimum, and the coexistence of multiple Bethe minima. This specification refines the conceptual view on the Bethe approximation and motivates our experimental analysis in Sec. 4.

Let us once again summarize the main results from the two previous sections, both being sufficient conditions for the convexity of the Bethe free energy \mathcal{F}_B on the Bethe box \mathbb{B} . According to Theorem 15 (derived from diagonal dominance of the Bethe Hessian), \mathcal{F}_B is convex on \mathbb{B} if, for all nodes i in the graph, the one-dimensional polynomial

$$\Psi_{i}(q_{i}) = -(d_{i} - 1) \prod_{j \in \mathcal{N}(i)} (1 + \alpha_{ij}q_{i}) + \sum_{j \in \mathcal{N}(i)} \left((1 + \alpha_{ij}q_{i}^{2}) \prod_{k \in \mathcal{N}(i) \setminus j} (1 + \alpha_{ik}q_{i}) \right)$$

is strictly positive on the interval (0,0.5]. To apply this result in practice, we need to verify for all polynomials $\Psi_i(q_i)$ (for $i \in \mathbf{X}$) if none of them has a root in the interval (0,0.5]. This can be done efficiently by computational methods from numerical optimization ³⁰. The

^{29.} More precisely, this characterization is valid for the infinite version of a complete graph, which is the Cayley tree. However, we argue that at least for the case of vanishing fields (i.e., $\theta = 0$) these boundaries are sharp for the finite versions as well.

^{30.} If an exact statement is desired, one can apply Sturm's theorem which calculates the total number of real roots of any one-dimensional polynomial in an arbitrary interval (Thomas, 1941).

degree of $\Psi_i(q_i)$ is $d_i + 1$ and thus increases with the number of neighbors of node i. This can make a numerical search for potential roots of $\Psi_i(q_i)$ more challenging (still, it remains a polynomial in one variable). The overall computational effort increases at least linearly with the number of nodes in the graph (since positivity must be verified for $|\mathbf{X}|$ polynomials).

Other than the above result, Theorem 23 (derived from a sum decomposition of the Bethe Hessian) provides a condition in closed-form. It says that \mathcal{F}_B is convex on \mathbb{B} if, for all edges (i,j) in \mathbf{E} whose end nodes i and j have at least three neighbors, the inverse temperature of the model satisfied the inequality

$$\beta < \frac{1}{2|J_{ij}|}\operatorname{arccosh}\Big(1 + \frac{2}{d_id_j - d_i - d_j}\Big).$$

This condition is particularly easy to verify and additionally provides an explicit estimate of the temperature at which the Bethe free energy might become non-convex (by taking the greatest β that simultanously satisfies all inequalities – i.e., for all edges (i, j) – of the above form). Note that Theorem 15 induces such an estimate only in implicit form, given as the greatest β such that none of the polynomials $\Psi_i(q_i)$ has a root in (0, 0.5]. To compute it, one can steadily increase β and stop when the first polynomial $\Psi_i(q_i)$ has a root in (0, 0.5]. The computational effort for checking Theorem 23 increases linearly with the number of edges in the graph (whereby for each edge only an elementary calculation needs to be performed).

In summary, Theorem 23 has computational advantages over Theorem 15 and appears to be better interpretable. However, this does not imply that it is more powerful in the sense of inducing more accurate estimates of the critical temperature at which \mathcal{F}_B changes its stage from convex to non-convex.

In the sequel, we put our results in a broader context by comparing them to similar results from the literature. An overview of all important statements and their connections has been given in Fig. 1 (Sec. 2.4). First, it seems convenient to categorize them according to their purposes and properties. Subsequently, we discuss them on complete graphs with homogenous potentials. For further details, we refer to Mooij and Kappen (2007).

- In infinite systems, the theory of Gibbs measures interprets a phase transition as the existence of a unique Gibbs measure. The result of Dobrushin (1968) is sufficient for uniqueness of a Gibbs measure and takes the influence of the fields θ_i into account; however, its evaluation time increases exponentially with the number of nodes in the graph. The condition of Simon (1979) is sufficient for Dobrushin's condition and simpler to evaluate, but it is only based on the couplings J_{ij} and thus weaker for models that are strongly influenced by the fields θ_i .
- The relationship between Gibbs measure theory and approximate inference in (finite) probabilistic graphical models has been established by Tatikonda and Jordan (2002). Namely, loopy belief propagation converges to a unique fixed point if there exists a unique Gibbs measure on the computation tree (which is an infinite unwrapping of the graph; in particular, Gibbs measures are well-defined on such a tree). To the best of our knowledge, nothing is known about the reverse direction of this statement.

- The results of Ihler et al. (2005); Mooij and Kappen (2007); Watanabe and Fukumizu (2009) are sufficient for the convergence of LBP to a unique fixed point, and thus for the uniqueness of a Bethe minimum. Their evaluation is based on closed-form expressions or eigenvalue problems, and can be done efficiently. Moreover, Mooij's criterion also takes the influence of fields θ_i into account. Experimental results indicate that Mooij's criterion is the most powerful condition ³¹ for predicting uniqueness of an LBP fixed point (or Bethe minimum). Another sufficient condition for the uniqueness of an LBP fixed point (but not convergence to it) is that of Heskes (2004). It appears to be less powerful than other criteria, but is of theoretical importance. Its evaluation requires the solution of a linear program and only takes the couplings J_{ij} into account.
- The results in this work (Theorem 15 and Theorem 23) are sufficient for the convexity of the Bethe free energy \mathcal{F}_B on a submanifold \mathbb{B} (the Bethe box) of its actual domain \mathbb{L} (the local polytope). As Proposition 1 shows, \mathcal{F}_B can never be convex on the entire local polytope, unless the graph contains at most one cycle. However, convexity of \mathcal{F}_B on \mathbb{B} implies the uniqueness of a Bethe minimum (Cor. 3, Sec. 3.1). Our results are based on the couplings J_{ij} only, because convexity of \mathcal{F}_B is a property that is not influenced by the fields θ_i (Cor. 5). Both conditions can be evaluated efficiently.

These results fulfill different purposes, being sufficient for convergence of LBP to a unique fixed point, uniqueness of a Gibbs measure on the computation tree, or convexity of the Bethe free energy. Still, all of them estimate a critical temperature β^* – either implicitly (e.g., Theorem 15) or explicitly (e.g., Theorem 23) – at which the Bethe free energy changes its stage (from convex to non-convex, or from uniqueness of a minimum to multiple minima).

Ultimately, we aim to better understand the impact of the current stage of the Bethe free energy on its approximation accuracy (i.e., with respect to the marginals and partition function). For many models, the quality of the Bethe approximation significantly degrades at some critical temperature, and thus loses its reliability. This effect can be interpreted as a finite version of a 'phase transition' in the model ³². In our analysis, we aim to understand if this reliability loss can be attributed to a specific stage change of the Bethe free energy.

As we do not have an oracle to tell us in which stage \mathcal{F}_B is at a certain temperature, we must rely on the results from the literature and our work. To get a notion about their individual power, we perform an analysis on a particularly simple model whose behavior can be exactly characterized: a complete graph with homogenous potentials (i.e., each node is connected to each other with a uniform node degree $d = d_i$, and we have $J_{ij} = J$ for all edges and $\theta_i = \theta$ for all nodes). We discuss how powerful the above discussed results are on that simple model towards predicting a state change of the Bethe free enegry (of course, this does not imply that they are equally powerful for more complex models).

^{31.} By most powerful we mean that it correctly predicts the uniqueness of an LBP fixed point for the largest variety of models, when compared to other conditions. This usually implies more accurate estimates of the temperature, at which multiple LBP fixed points (or Bethe minima) arise.

^{32.} These are not phase transitions in the sense of infinite models, because the partition function in finite models is always a continuous function of the temperature (Sec. 2.4).

We first consider our condition based on diagonal dominance of the Bethe Hessian. For this model, Theorem 15 says that \mathcal{F}_B is convex on \mathbb{B} if the polynomial

$$\Psi_i(q_i) = -(d-1)(1 + \alpha_{ij}q_i)^d + d(1 + \alpha_{ij}q_i^2)(1 + \alpha_{ij}q_i)^{d-1}$$

is positive in the interval (0,0.5]. Note that, due to symmetries, this polynomial is the same for all nodes. Positivity of $\Psi_i(q_i)$ is equivalent to the positivity of

$$-(d-1)(1 + \alpha_{ij}q_i) + d(1 + \alpha_{ij}q_i^2),$$

which is a quadratic polynomial and has the roots $\frac{d-1}{2d} \pm \frac{1}{2d} \sqrt{(d-1)^2 - \frac{4d}{\alpha_{ij}}}$. If the discriminant is negative, there are only complex roots and $\Psi_i(q_i)$ is positive in (0,0.5]. This is precisely the case if $\alpha_{ij} < \frac{4d}{(d-1)^2}$ or, with $\alpha_{ij} = e^{4\beta|J|} - 1$ from (24) substituted, if

$$\beta < \frac{1}{4|J|} \log \left(\frac{(d+1)^2}{(d-1)^2} \right). \tag{81}$$

If the discriminant is zero, $\Psi_i(q_i)$ has the unique root $\frac{d-1}{2d}$ which (for $d \geq 2$) is a number in (0,0.5] (i.e., $\Psi_i(q_i)$ is not longer positive in (0,0.5]). If the discriminant is positive, we have two real roots. We claim that the lower root is always in (0,0.5] and thus the diagonal dominance criterion is violated for all values of β that are greater or equal to the right-hand side of (81). This follows from the observation that the value of the lower root monotonically decreases, if β (and thus α_{ij} and the square root term) increases. In the limit $\beta \to \infty$, the lower root approaches zero and is consequently always in $(0, \frac{d-1}{2d})$, which is a subset of (0,0.5]. We conclude that the diagonal dominance criterion is satisfied, if and only if β satisfies the inequality (81).

Further, we consider our second result based on the sum decomposition of the Bethe Hessian on the symmetric model. For all edges the inequalities in Theorem 23 are identical and \mathcal{F}_B is convex on \mathbb{B} if

$$\beta < \frac{1}{2|J|}\operatorname{arccosh}\left(1 + \frac{2}{d(d-2)}\right)$$

is satisfied (for $d \geq 3$). We can use the trigonometric identity

$$\operatorname{arccosh}(x) = \log (x + \sqrt{x-1}\sqrt{x+1})$$

and perform a few simplifications to show that this is equivalent to

$$\beta < \frac{1}{2|J|} \log \left(\frac{d}{d-2} \right). \tag{82}$$

As already mentioned, the exact behavior for the symmetric model can be characterized. More precisely, for $\theta=0$, it has been shown that Gibbs measures become non-unique (Georgii, 1988; Taga and Mase, 2006b) and LBP stops converging to a unique fixed point (Mooij and Kappen, 2005), if the inverse temperature passes the critical threshold of

$$\frac{1}{|J|}\operatorname{arctanh}\left(\frac{1}{d-1}\right). \tag{83}$$

For $d \geq 3$, this expression is the same as the critical threshold in inequality (82). This follows directly from the trigonometric identity

$$\operatorname{arctanh}(x) = \frac{1}{2} (\log(1+x) - \log(1-x)).$$

Thus, our result in Theorem 23 is sharp in the sense, that it correctly predicts the value of β at which a modified behavior occurs ³³. Other results that are sharp on the symmetric model without fields are those of Ihler et al. (2005), Mooij and Kappen (2007), and Watanabe and Fukumizu (2009). Table 2 and Fig. 9 show a comparison between the critical thresholds that are predicted by the various criteria from the literature on the symmetric model without fields. If $\theta \neq 0$, none of these conditions are sharp any longer (with the results of Dobrushin and Mooij tending to more accurate predictions, as they consider the influence of the fields).

Table 2: Estimates of a critical inverse temperature, predicted by various results from the literature on a complete graph with homogenous potentials and vanishing fields (i.e., $J_{ij} = J$ for all edges, $\theta_i = 0$ and $d_i = d$ for all nodes). The conditions in the first row are sharp on this model (i.e., they correctly predict β^* at which the model changes its behavior).

Description	Reference	β^*
Exact characterization	Georgii (1988),Ihler et al. (2005)	$\frac{1}{ J }\operatorname{arctanh}\left(\frac{1}{d-1}\right)$
	Mooij and Kappen (2007),	
	Theorem 23 (this work)	
Dobrushin	Dobrushin (1968)	$d \text{ odd: } \frac{1}{ J } \operatorname{arctanh} \left(\frac{1}{d}\right)$
		d even: $\frac{1}{2 J } \operatorname{arctanh} \left(\frac{2}{d}\right)$
Simon	Simon (1979)	$\frac{1}{ J } \frac{1}{d}$
Diagonal Dominance	Theorem 15 (this work)	$\frac{1}{4 J }\log\left(\frac{(d+1)^2}{(d-1)^2}\right)$
Heskes	Heskes (2004)	$\frac{1}{4 J }\log\left(\frac{d-1}{d-2}\right)$

After having compared various results and their power with respect to predicting properties of a model, we briefly discuss a few aspects of these properties themselves; specifically, we focus on the different stages of the Bethe free energy. As convexity of \mathcal{F}_B on the Bethe box \mathbb{B} implies uniqueness of a Bethe minimum (but not vice versa), there is generally a certain 'temperature gap' between these two properties. Any condition that predicts the convexity of \mathcal{F}_B cannot explain this gap, as it is caused by the presence of fields θ_i and increases with stronger fields. The fields can affect the location (and number) of Bethe minima, but not the curvature of \mathcal{F}_B . If there are no fields, convexity of \mathcal{F}_B and uniqueness of a Bethe minimum are supposed to be equivalent. Although we do not have a formal proof of this statement, we would like to formulate it as a conjecture:

^{33.} More precisely, Gibbs measures become non-unique and LBP stops converging to a unique fixed point. However, \mathcal{F}_B might still be convex and have a unique minimum if the inverse temperature increases beyond the predicted thresholds. This can be observed in an antiferromagnetic model (J < 0, Fig. 10).

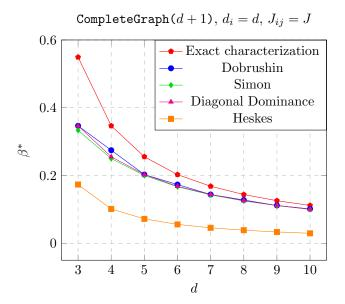


Figure 9: Comparison of critical values of the inverse temperature predicted by different criteria from the literature on a complete graph with homogenous potentials and vanishing fields ($J_{ij} = J$ for all edges, $\theta_i = 0$ and $d_i = d$ for all nodes), in dependence of the degree.

Conjecture 24

Assume we have no external fields in our model (i.e., $\theta_i = 0$ for all nodes i). Then \mathfrak{F}_B is convex on \mathbb{B} , if and only if it has a unique minimum.

Figure 10 schematically illustrates the state change behavior of the Bethe free energy in dependence of the inverse temperature and the presence (or absence) of fields on a perfectly symmetric model. A detailed interpretation is given in the figure caption. Interestingly, \mathcal{F}_B preserves its convexity (and thus its unique minimum) in the antiferromagnetic model for any inverse temperature. We believe that this phenomenon is due to frustrations in the model, which are cycles in the graph with an odd number of antiferromagnetic edges (Toulouse, 1977). While frustrations can induce multiple Gibbs measures and prevent loopy belief propagation from converging (Georgii, 1988; Knoll and Pernkopf, 2017; Mooij and Kappen, 2005), they may have 'stabilizing' effects on the convexity (and reliability) of the Bethe free energy. Without providing further details on this problem, we would like to formulate another conjecture:

Conjecture 25

Frustrations help the Bethe free energy to preserve its convexity.

The considerations made in this section are instructive and aim to explain the behavior of the Bethe free energy in dependence of the inverse temperature. We primarily analyzed special kind of models to understand its different 'stages', and discussed several criteria to predict changes between them. In the next and final step of our analysis, we put our focus on the quality of the Bethe approximation during these stages, regarding the accuracy of the estimates for the marginals and partition function. We will address these topics in Sec. 4 and present our experimental results on a broad variety of models.

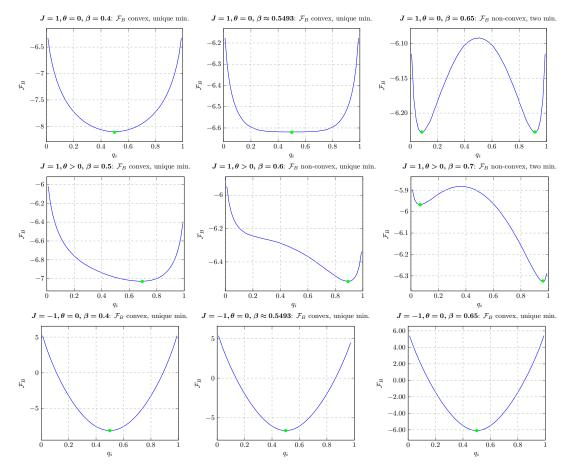


Figure 10: Stage change behavior of the Bethe free energy in dependence of the inverse temperature β and fields θ on a complete graph with 4 nodes and homogenous potentials (i.e., $J_{ij} = J$ for all edges and $\theta_i = \theta$ for all nodes). These plots represent a projection of \mathcal{F}_B onto the main diagonal of \mathbb{B} , i.e, points $\mathbf{q} = (q_1, q_2, q_3, q_4)$ with $q_1 = \cdots = q_4$.

First row: For $\theta = 0$ and J > 0 (a ferromagnetic model without fields), \mathcal{F}_B is convex and has a unique minimum in $q_i = 0.5$ if β is below a critical threshold of $\beta^* \approx 0.5493$. If β increases beyond that threshold, \mathcal{F}_B becomes non-convex and at the same time two new minima arise (while the 'old' minimum disappears).

Second row: For $\theta > 0$ and J > 0 (a ferromagnetic model with fields), \mathcal{F}_B is convex and has a unique minimum if β is sufficiently small. The location of the minimum is biased by the fields and thus not in $q_i = 0.5$. If β increases, \mathcal{F}_B reaches a point where it becomes non-convex but still has a unique minimum. If β further increases, there arises a second Bethe minimum (with the up-to-then minimum still existing). This shows that the fields can induce a gap between convexity of \mathcal{F}_B and uniqueness of a Bethe minimum.

Third row: For $\theta = 0$ and J < 0 (an antiferromagnetic model without fields), \mathcal{F}_B preserves its convexity (and its unique minimum) at any temperature.

4 Convexity of the Bethe Free Energy: Experiments

In Sec. 3.4, we have exposed how the Bethe free energy passes through different stages if the inverse model temperature increases, and discussed possibilities to predict in which stage it currently is. We now focus on analyzing the reliability of the Bethe approximation, i.e., the accuracy of the marginal and partition function estimates that it provides.

The quality of the Bethe approximation has been analyzed, e.g., by Meshi et al. (2009); Weller et al. (2014); Knoll and Pernkopf (2020), but rather at a qualitative level and without specifying its different stages. We extend this analysis by a quantitative component (i.e., concrete estimates for critical phase transition temperatures or, in other words, reliability thresholds), and the concept of convexity on the Bethe box \mathbb{B} that we have introduced in this work. Specifically, we analyze if the Bethe approximation is always reliable if \mathcal{F}_B is convex on \mathbb{B} ; if it is still reliable if it is non-convex but has a unique minimum; or if its current stage has no significant influence on the quality of the Bethe approximation.

In Sec. 4.1, we show how we measure the quality of the Bethe free energy approximation and introduce our algorithm BETHE-MIN that we use for its minimization. In Sec. 4.2, we explain our experimental setup and present all experimental results in detail.

4.1 Minimization of the Bethe Free Energy

Let us recap the essential ideas of the Bethe approximation (introduced in Sec. 2.3) to clarify the concept of the subsequent experiments. In a finite graphical model, we intend to find approximations to the (generally non-accessible) partition function (4), and/or marginal distributions (5), (6). Arising from the Gibbs variational principle, the Bethe approximation provides estimates for these unknown quantities by making the approximations (15) and (16), i.e., by using its minimum on the set \mathbb{L} of local probability constraints, the local polytope (20). As we have shown in Sec. 3.1, we can reduce the dimension of this domain and instead minimize the Bethe free energy \mathcal{F}_B on a submanifold \mathbb{B} of \mathbb{L} , the Bethe box (25). In other words, to approximate the partition function and singleton marginals 34 we use

$$-\frac{1}{\beta}\log Z_B := \min_{\tilde{\mathbf{q}} \in \mathbb{B}} \mathcal{F}_B \approx -\frac{1}{\beta}\log Z(\beta), \qquad (84)$$

$$\{q_i : \mathbf{q} = \operatorname*{argmin}_{\tilde{\mathbf{q}} \in \mathbb{B}} \mathcal{F}_B \mid i \in \mathbf{X}\} \approx \{p_i \mid i \in \mathbf{X}\}. \tag{85}$$

The approximations to the pairwise marginals $\{p_{ij} \mid (i,j) \in \mathbf{E}\}$ can directly be computed from the elements in the set on the left-hand side of (85), according to the probability table in Sec. 3.1 (Table 1), where $\xi_{ij}^*(q_i, q_j)$ is computed from (24) as a direct function of q_i and q_j .

To analyze the quality of the Bethe approximation, we compare the exact partition function $Z(\beta)$, singleton marginals $p_i(X_i = \pm 1)$, and pairwise marginals $p_{ij}(X_i = \pm 1, X_j = \pm 1)$ to the estimated quantities Z_B , $(q_i, 1 - q_i)$, and $(\xi_{ij}^*, q_i - \xi_{ij}^*, q_j - \xi_{ij}^*, 1 + \xi_{ij}^* - q_i - q_j)$, for all nodes i and all edges (i, j). For that purpose, we use the following error measures:

^{34.} More precisely, q_i (the i-th component of q) approximates the first entry of the marginal p_i , i.e., the probability that variable X_i takes the value +1. The second entry (the probability that X_i takes the value -1) can be estimated with $1 - q_i$ (Table 1).

• For the partition function, we evaluate the absolute error between the negative logarithms of $Z(\beta)$ and Z_B , i.e.,

$$|-\log Z(\beta) + \log Z_B|. \tag{86}$$

• For the singleton marginals, we evaluate the average (with respect to all nodes) l^1 -error between the exact and estimated quantities, i.e.,

$$\frac{1}{|\mathbf{X}|} \sum_{i \in \mathbf{X}} \left(|p_i(X_i = +1) - q_i| + |\underbrace{p_i(X_i = +1)}_{=1 - p_i(X_i = +1)} - (1 - q_i)| \right)
= \frac{2}{|\mathbf{X}|} \sum_{i \in \mathbf{X}} \left(|p_i(X_i = +1) - q_i| \right).$$
(87)

• For the pairwise marginals, we evaluate the average (with respect to all edges) l^1 -error between the exact and estimated quantities, i.e.,

$$\frac{1}{|\mathbf{E}|} \sum_{(i,j)\in\mathbf{E}} \left(|p_{ij}(X_i = +1, X_j = +1) - \xi_{ij}^*| + |p_{ij}(X_i = +1, X_j = -1) - (q_i - \xi_{ij}^*)| + |p_{ij}(X_i = -1, X_j = +1) - (q_j - \xi_{ij}^*)| + |p_{ij}(X_i = -1, X_j = -1) - (1 + \xi_{ij}^* - q_i - q_j)| \right).$$
(88)

As we do generally not have access to the partition function and marginals (that we are actually trying to approximate), we evaluate the above error measures by performing our experiments in Sec. 4.2 on graphs that are small enough to allow for an exact computation of these quantities. For that purpose, we use the so-called junction tree algorithm (Lauritzen and Spiegelhalter, 1988) that returns the correct solution, but whose computational complexity increases exponentially with the size of the largest clique ³⁵ in the graph.

As discussed in previous sections, the errors induced by the Bethe approximation strongly depend on the model parameters (in particular the graph connectivity, potentials, and inverse temperature). We leave this problem to the experimental analysis in Sec. 4.2 as, we first need to address another important issue: the practical minimization of the Bethe free energy. Following the approximations (84) and (85), we need to compute its global minimum in the constrained set \mathbb{B} . This can be a challenging task in practice, especially if we deal with large systems and numerical difficulties. Another prohibitive aspect is the potential existence of multiple local minima. In that case, there is no general technique that efficiently returns the global minimum, and we must usually rely on the quality of a (possibly sub-optimal) local minimum 36 . Besides, there is no guarantee that the global minimum, if we manage to find it, induces a low error on the partition function or marginals. Finally,

^{35.} A clique is a subgraph where each node is connected to each other.

^{36.} For ferromagnetic models, Weller and Jebara (2014a) have proposed an – at least, in theory – efficient approximation scheme to compute the partition function up to some ϵ in polynomial time (an FPTAS).

 \mathcal{F}_B may exhibit particularly flat or steep regimes, implying extremely small or exploding gradients and slow convergence to a minimum (even if \mathcal{F}_B is convex on \mathbb{B}).

For an efficient minimization of the Bethe free energy, various methods 37 have been proposed: gradient-based algorithms combined with projection steps (Welling and Teh, 2001; Shin, 2012); a double-loop algorithm that decomposes \mathcal{F}_B into a convex and a concave part and iterates between these two components (Yuille, 2002); combinatorial optimization (Weller and Jebara, 2014a); and convex optimization (Weller et al., 2014). A drawback of these methods is that they do not exploit second-order properties of the Bethe free energy.

We propose BETHE-MIN, a projected quasi-Newton method that not only uses the information of the gradient but also of the Bethe Hessian. While parameter updates in the 'ordinary' Newton method require a costly inversion of the Hessian matrix, a quasi-Newton method uses an approximation to the inverse Hessian that is updated in each iteration as well. More precisely, if $\mathbf{H}_B(\boldsymbol{q}^{(t)})$ is the Bethe Hessian evaluated in the current parameter vector $\boldsymbol{q}^{(t)}$ at time t and $\mathbf{B}^{(t)}$ is an approximation to its inverse, then we perform the update

$$\boldsymbol{q}^{(t+1)} = \boldsymbol{q}^{(t)} - \rho^{(t)} \cdot (\mathbf{B}^{(t)})^T \nabla \mathcal{F}_B(\boldsymbol{q}^{(t)}), \tag{89}$$

where $\rho^{(t)} > 0$ is the step size of the current iteration. To ensure that the next parameter vector $\boldsymbol{q}^{(t+1)}$ remains feasible (i.e., a point in the Bethe box \mathbb{B}), we project it back into \mathbb{B} if $\rho^{(t)}$ is too large. More precisely, we reduce 38 $\rho^{(t)}$ until any component $q_i^{(t+1)}$ is a number in (0,1) so that $\boldsymbol{q}^{(t+1)}$ lies in \mathbb{B} . For faster convergence, we then optimize the choice of $\rho^{(t)}$ by applying a line search technique with respect to the so-called Wolfe conditions (Wolfe, 1969). After each update of $\boldsymbol{q}^{(t)}$, we also need to update $\boldsymbol{B}^{(t)}$. For that purpose, we use the relatively robust BFGS update rules for approximating the inverse Hessian (Nocedal and Wright, 2006). The described steps are iterated, until we arrive at a stationary point \boldsymbol{q}^* of \mathcal{F}_B . All details on BETHE-MIN including pseudocode are provided in Appendix C.

4.2 Experimental Results

Through our experiments, we aim to evaluate the quality of the Bethe approximation in dependence of its stage (i.e.: convexity; non-convexity but uniqueness of a minimum; and multiple minima). The Bethe free energy is convex on the Bethe box \mathbb{B} , if the inverse temperature is sufficiently small (Lemma 17, Sec. 3.3). Often \mathcal{F}_B first becomes non-convex and later develops multiple minima if β increases; however, sometimes \mathcal{F}_B does not change its stage and remains convex at any temperature (e.g., in the antiferromagnetic model, Sec. 3.4). To predict in which stage \mathcal{F}_B currently is, we use some of the results discussed in Sec. 2.4 and Sec. 3.4. In particular, to predict convexity, we use our result derived from diagonal dominance ³⁹ of the Bethe Hessian (Sec. 3.2, Theorem 15), and to predict unique-

^{37.} Note that LBP can be seen as a minimization of \mathcal{F}_B too (Heskes, 2003). However, its convergence rate is often not satisfying – still, several works have improved on it over time (Aksenov et al., 2020; Knoll et al., 2015; Sutton and McCallum, 2007).

^{38.} Alternatively, one could use an orthogonal projection of $q_i^{(t+1)}$ into $\mathbb B$ as, e.g., in Kim et al. (2010). However, this might entail a significant change of the search direction.

^{39.} We observed in our experiments that the diagonal dominance criterion often provides slightly more accurate estimates of the critical β at which \mathcal{F}_B becomes non-convex, than the sum decomposition

ness of a minimum, we use the result of Mooij and Kappen (2007) ⁴⁰. Since all of these conditions are only sufficient (but not necessary), we expect that the true thresholds of β at which \mathcal{F}_B changes its stage are somewhat underestimated by the predicted values.

Our experimental setup is as follows: We consider four different types of graphs: two lattice graphs (or square grid graphs) of size 5×5 and 8×8 ; a complete graph on 10 nodes; and random graphs on 25 nodes and an edge probability of 0.2 for each pair of nodes (Erdos and Renyi, 1959). For each graph, we consider ferromagnetic models (i.e., with all interactions being ferromagnetic) and spin glasses (i.e., in which ferromagnetic and antiferromagnetic edges occur). For ferromagnetic models we uniformly sample the couplings J_{ij} from the range (0,1), for spin glasses we uniformly sample them from the range (-1,1). Also, we assume that there exist fields θ_i , that we uniformly sample from the range $\left(-\frac{1}{8},\frac{1}{8}\right)$. For each type of graphical model (i.e., with a specific graph structure and either purely ferromagnetic or mixed – i.e., both ferromagnetic and antiferromagnetic – couplings), we create 200 different instances; that is, altogether we create $4 \times (200+200) = 1600$ different graphical models. For each individual model we increase the inverse temperature β from 0 to 2 (in steps of 0.1), and for each value of β we use our algorithm BETHE-MIN (Algorithm 1, Appendix C) with 100 random initializations of the parameter vector $\mathbf{q}^{(0)}$ to minimize the Bethe free energy and estimate the marginals and partition function associated to the specific model and current value of β . We compare the obtained estimates to the exact marginals and partition function – computed by the junction tree algorithm (Lauritzen and Spiegelhalter, 1988) – and evaluate the errors with respect to the error measures defined in Sec. 4.1. We average these errors over the 100 runs of BETHE-MIN and afterwards over the 200 different models corresponding to a specific graph type and potential configuration (with β still fixed to some value between 0 and 2). The errors together with standard deviations are plotted in Fig. 11 (ferromagnetic models) and Fig. 12 (spin glasses) against the inverse temperature. These figures also show the estimated values of β at which \mathcal{F}_B becomes non-convex – in green, Theorem 15 – and develops multiple minima – in blue, Mooij and Kappen (2007)). These values were first estimated for each model invividually and then averaged over the 200 different models (together with standard deviations). Furthermore, Fig. 13 shows the percentages of models, for which \mathcal{F}_B is predicted to be convex or to have a unique minimum at a specific value of β . It illustrates the 'gap' between convexity and uniqueness of a minimum (with respect to β), which becomes smaller with a higher connectivity in the graph. Fig. 14 shows the number of required iterations until BETHE-MIN converges to a stationary point. The iteration number increases as the inverse temperature increases, which is most likely due to a changed stage of the Bethe free energy (in particular, multiple minima) and the numerical difficulties that arise for regimes of high inverse temperature; however, this appears to be less distinct in spin glasses (right-hand side) than in ferromagnetic models (left-hand side). The general convergence rate of BETHE-MIN is higher than 99% (with respect to all 1600 sampled models) which is an astonishingly convincing result.

criterion (Sec. 3.3, Theorem 23). This is somewhat surprising, as Theorem 23 is exact on the perfectly symmetric model without fields, while Theorem 23 is not (Sec. 3.4).

^{40.} More precisely, we use Corollary 4 from Mooij and Kappen (2007) with the specific choice of m=5.

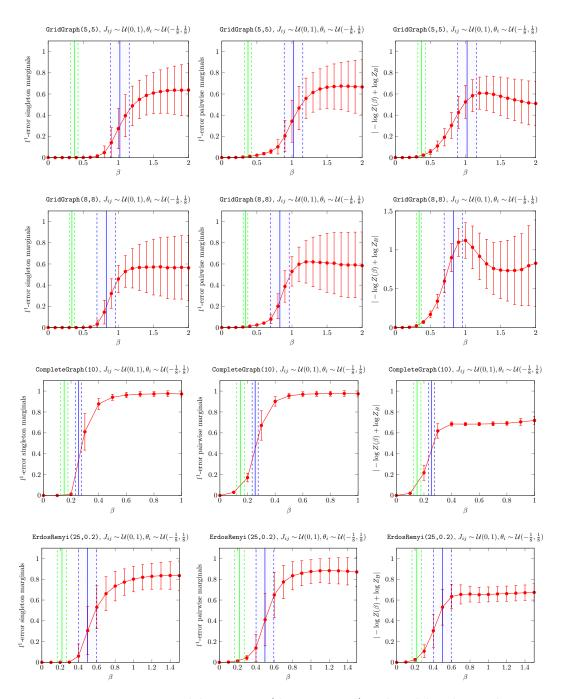


Figure 11: Ferromagnetic models. Errors (drawn in red) induced by the Bethe approximation on four different graph types, in dependence on the inverse temperature β . The critical point at which an increasing error becomes significant can be interpreted as a phase transition in the model. The green solid lines estimate the stage changes of \mathcal{F}_B from convex to non-convex; the blue solid lines estimate the stage changes of \mathcal{F}_B from a unique minimum to multiple minima. The dashed lines and error bars represent the corresponding standard deviations with respect to 200 models, respectively. First column: singleton marginal error; second column: pairwise marginal error; third column: partition function error.

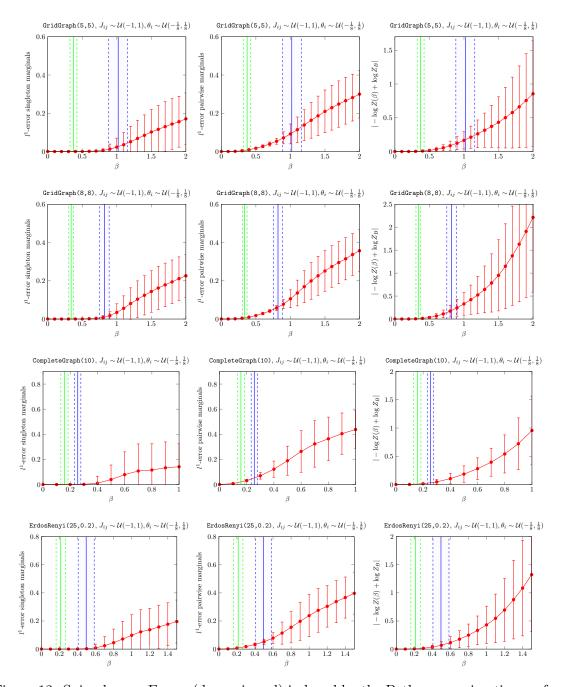


Figure 12: Spin glasses. Errors (drawn in red) induced by the Bethe approximation on four different graph types, in dependence on the inverse temperature β . The critical point at which an increasing error becomes significant can be interpreted as a phase transition in the model. The green solid lines estimate the stage changes of \mathcal{F}_B from convex to non-convex; the blue solid lines estimate the stage changes of \mathcal{F}_B from a unique minimum to multiple minima. The dashed lines and error bars represent the corresponding standard deviations with respect to 200 models, respectively. First column: singleton marginal error; second column: pairwise marginal error; third column: partition function error.

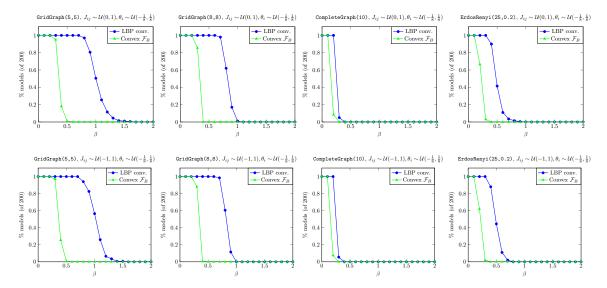


Figure 13: Percentage of models on which \mathcal{F}_B is predicted to be convex – according to Theorem 15 – and to have a unique minimum (or, more precisely, convergence of LBP to a unique minimum) – according to Corollary 4 in Mooij and Kappen (2007). On graphs with a higher connectivity \mathcal{F}_B induces a smaller gap between these two properties. In the top row we consider ferromagnetic models, in the bottom row we consider spin glasses.

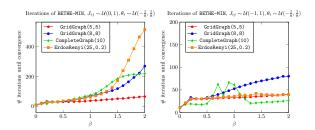


Figure 14: Required iteration number until BETHE-MIN (Algorithm 1) converges to a stationary point of \mathcal{F}_B . For ferromagnetic models (left-hand side), the iteration number increases as β increases, with the steepest decrease for the Erdos-Renyi model. For spin glasses (right-hand side), the iteration number keeps at a lower level than for ferromagnetic models.

Generally, we observe in Fig. 11 and Fig. 12 that the quality of the Bethe approximation degrades (and later stabilizes at a high level), if β passes a certain critical threshold (which is – due to a steeper increase of the errors – more distinct for ferromagnetic models, but also observable for spin glasses). We define this phenomenon to be a phase transition in the model, i.e., the point at which the Bethe approximation begins to lose its reliability. Following this interpretation, different error measures are associated to different phase transitions. Ideally, we would like to predict the critical β at which a phase transition occurs (though some errors might still be tolerable after a phase transition has occurred). The main focus of our analysis is to show how the predicted Bethe stage changes can be used to estimate a phase transition and thus to quantify a reliability threshold for the Bethe approximation.

We first discuss our results on ferromagnetic models in more detail. As can be seen in Fig. 11, phase transitions not only differ between the considered error measures but also depend on the graph structure. If the connectivity among nodes is high (such as in the complete graph), phase transitions already occur for smaller values of β ; if the graphs are sparse (such as the grid graphs), they occur somewhat later and the subsequent degradation of the Bethe approximation accuracy happens more slowly. Also, the phase transition with respect to the partition function happens earlier, than the phase transition with respect to the marginal errors (with the singleton marginal phase transition happening as latest).

If we use the Bethe stage change temperature that is predicted by Theorem 15 (i.e., from convex to non-convex, drawn by the green solid line) to estimate singleton marginal phase transitions, we observe that these seem to be slightly underestimate. Whether the reason for this is the gap between the predicted and the 'true' convexity of \mathcal{F}_B , or that convexity is less relevant for explaining this error, is not clear. In any case, the Bethe approximation is accurate for the predicted β . The Bethe stage change temperature that is predicted by Mooij and Kappen (2007) (i.e., from a unique minimum to multiple minima, drawn by the solid blue line) overestimates the sigleton marginal phase transition. In particular, it predicts some β at which the singleton marginal error is already considerable; i.e., the Bethe approximation is not any longer reliable at this point. The actual phase transition lies between the values predicted by these two results. For the pairwise marginals, Theorem 15 predicts the phase transition quite accurately (with a slight overestimation on the complete graph, where the associated error already increases very early). Mooij and Kappen (2007) again overestimate the value of the phase transition and predict a value of β at which the associated error is already significant. For the partition function, the situation is roughly similar as for the pairwise marginals; generally, however, the absolute error on the partition function seems always to remain in an acceptable regime for ferromagnetic models.

Second, we discuss our results on spin glasses (Fig. 12). The general development of all three types of errors behaves differently compared to ferromagnetic models. In particular, the increase of errors at a phase transition happens less abrupt and subsequently lasts over a longer period. Also, the errors on the marginals keep at a lower level as in the ferromagnetic case (however, the error on the partition function grows even stronger, the higher β increases). As for ferromagnetic models, singleton marginal phase transitions occur later than those with respect to the pairwise marginals and partition function. For the singleton marginals, Theorem 15 clearly underestimates phase transitions, while Mooij and Kappen (2007) provide accurate estimates (with a slight over-/ or underestimation depending on the graph type). The pairwise marginal phase transitions are quite accurately predicted by Theorem 15, while the value predicted Mooij and Kappen (2007) tend to an overestimation. For the partition function, the phase transition lies somewhere between the thresholds that are predicted by the two results.

Our experiments show that both convexity and uniqueness of a Bethe minimum (resp., the results to predict these stages) are useful concepts to infer about the reliability of the Bethe approximation. We summarize our experimental observations in the following statements:

- The Bethe stage change from convexity to non-convexity (as predicted by Theorem 15) accurately predicts a phase transition with respect to the pairwise marginals and partition function in ferromagnetic models, and with respect to the pairwise marginals in spin glasses.
- The Bethe stage change from a unique minimum to multiple minima (as predicted by Mooij and Kappen (2007)) accurately predicts a phase transition with respect to the singleton marginals in and spin glasses.
- A phase transition with respect to the partition function in spin glasses lies between the two Bethe stage changes described above.

5 CONCLUSION

In this work, we have considered the Bethe approximation in the context of probabilistic models on finite graphs. We have refined the concept of a convex Bethe free energy by studying its behavior on a specific submanifold of its domain, the Bethe box. In an extent theoretical part, we have derived two sufficient conditions for convexity of the Bethe free energy that are easily applicable in practice. In the experimental part, we have specified different stages of the Bethe free energy (one of them its convexity) and analyzed its reliability with respect to its stage. We have demonstrated with help of our theoretical results that convexity is a strong concept for verifying the reliability of the Bethe approximation in important problems of probabilistic inference. We have further proposed an effective algorithm for minimizing the Bethe free energy that uses the information of its Hessian. To the best of our knowledge, the analyzes and experiments in this work are novel and fundamentally improve the understanding and accessibility of the Bethe approximation.

Appendix A. Proofs of Sec. 3.2

Proof [Proof of Lemma 8]

Without loss of generality, we may assume that we have only one pairwise term $r_{ij}^+(q_i, q_j)$ in the definition of $R_i(\mathbf{q})$ (i.e., one single ferromagnetic edge that is incident to node i). The statement involving multiple edges follows by induction over the number of edges; furthermore, Lemma 9 shows ⁴¹ that $r_{ij}^-(q_i, q_j)$ (corresponding to an antiferromagnetic edge) is identical to $r_{ij}^+(q_i, q_j)$ (only with shifted symmetries.) Hence, we must prove that

$$\inf_{(q_i,q_j)\in(0,1)\times(0,1)} \left[r_i(q_i) + r_{ij}^+(q_i,q_j) \right] = \inf_{q_i\in(0,1)} \left[r_i(q_i) + \left(\inf_{q_j\in(0,1)} r_{ij}^+(q_i,q_j) \right) \right]. \tag{90}$$

To prove this, we show that the left-hand side in (90) is as most as large as the right-hand side, and vice versa.

First, let \hat{q}_i and \hat{q}_j be fixed values in (0,1). Then, by definition of the infimum,

$$\inf_{q_j \in (0,1)} \left[r_i(\hat{q}_i) + r_{ij}^+(\hat{q}_i, q_j) \right] \le r_i(\hat{q}_i) + r_{ij}^+(\hat{q}_i, \hat{q}_j)$$

^{41.} Note that Lemma 9 follows independently from Lemma 8, although it appears chronologically later in this work. Thus we can utilize its statements at this point.

or, equivalently,

$$\inf_{q_i \in (0,1)} \left[r_i(\hat{q}_i) + r_{ij}^+(\hat{q}_i, q_j) \right] - r_i(\hat{q}_i) \le r_{ij}^+(\hat{q}_i, \hat{q}_j).$$

Since this holds for all $\hat{q}_j \in (0,1)$, we can also take the infimum with respect to q_j of the expression on the right-hand side and obtain

$$\inf_{q_j \in (0,1)} \left[r_i(\hat{q}_i) + r_{ij}^+(\hat{q}_i, q_j) \right] - r_i(\hat{q}_i) \le \inf_{q_j \in (0,1)} r_{ij}^+(\hat{q}_i, q_j).$$

Now add $r_i(\hat{q}_i)$ again and take the infimum with respect to q_i on both sides of the inequality, which results in

$$\inf_{(q_i,q_j)\in(0,1)\times(0,1)} \left[r_i(q_i) + r_{ij}^+(q_i,q_j) \right] \le \inf_{q_i\in(0,1)} \left[r_i(q_i) + \left(\inf_{q_j\in(0,1)} r_{ij}^+(q_i,q_j) \right) \right]$$

and proves the first of the two inequalities.

To prove the reverse inequality, let once again \hat{q}_i and \hat{q}_j be fixed in (0,1) and observe that

$$r_i(\hat{q}_i) + r_{ij}^+(\hat{q}_i, \hat{q}_j) \ge r_i(\hat{q}_i) + \inf_{q_j \in (0,1)} r_{ij}^+(\hat{q}_i, q_j).$$

This is valid for all $\hat{q}_i \in (0,1)$ and we can take the infimum with respect to q_i of both sides of this inequality:

$$\inf_{q_i \in (0,1)} \left[r_i(q_i) + r_{ij}^+(q_i, \hat{q_j}) \right] \ge \inf_{q_i \in (0,1)} \left[r_i(q_i) + \inf_{q_j \in (0,1)} r_{ij}^+(q_i, q_j) \right]$$

Finally, we recall that this inequality holds for all $\hat{q}_j \in (0,1)$ and we can once again take the infimum with respect to q_j of the expression on the left-hand side, resulting in the reverse inequality

$$\inf_{(q_i,q_j)\in(0,1)\times(0,1)} \left[r_i(q_i) + r_{ij}^+(q_i,q_j) \right] \ge \inf_{q_i\in(0,1)} \left[r_i(q_i) + \inf_{q_i\in(0,1)} r_{ij}^+(q_i,q_j) \right].$$

Proof [Proof of Lemma 9]

For this proof we require some additional notation: Recall from (35) and (36) that $r_{ij}^+(q_i, q_j)$ and $r_{ij}^-(q_i, q_j)$ implicitly depend on $\xi_{ij}^*(q_i, q_j)$ – defined in (24) – and $T_{ij}(q_i, q_j)$ – defined in (28) – which are functions of q_i and q_j (with $T_{ij}(q_i, q_j)$ itself depending on $\xi_{ij}^*(q_i, q_j)$). Here we refine the definition of these two sub-functions according to the type of edge they represent: If $\xi_{ij}^*(q_i, q_j)$ and thus $T_{ij}(q_i, q_j)$ are associated to a ferromagnetic edge (i.e., implicitly depend on $J_{ij} > 0$), we denote them by $\xi_{ij}^+(q_i, q_j)$ and $T_{ij}^+(q_i, q_j)$; if they are associated to an antiferromagnetic edge (i.e., implicitly depend on $-J_{ij} < 0$), we denote them by $\xi_{ij}^-(q_i, q_j)$ and $T_{ij}^-(q_i, q_j)$. In terms of this refined notation, we can also adapt the definition of $r_{ij}^+(q_i, q_j)$ and $r_{ij}^-(q_i, q_j)$ according to

$$r_{ij}^{+}(q_i, q_j) = \frac{q_j(1 - q_j) - \xi_{ij}^{+}(q_i, q_j) + q_i q_j}{T_{ij}^{+}(q_i, q_j)} \quad \text{and}$$
 (91)

$$r_{ij}^{-}(q_i, q_j) = \frac{q_j(1 - q_j) - q_i q_j + \xi_{ij}^{-}(q_i, q_j)}{T_{ij}^{-}(q_i, q_j)}.$$
(92)

To prove (40), we first show the following symmetry properties:

$$\xi_{ij}^{+}(q_i, q_j) = \xi_{ij}^{+}(q_j, q_i)
\xi_{ij}^{-}(q_i, q_j) = \xi_{ij}^{-}(q_j, q_i)$$
(93)

$$\xi_{ij}^{-}(q_i, q_j) - q_i q_j = -\xi_{ij}^{+}(q_i, 1 - q_j) + q_i (1 - q_j)$$

$$= -\xi_{ij}^{+}(1 - q_i, q_j) + (1 - q_i)q_j$$
(94)

$$T_{ij}^{-}(q_i, q_j) = T_{ij}^{+}(1 - q_j, q_i)$$

$$= T_{ij}^{+}(q_j, 1 - q_i)$$

$$= T_{ij}^{+}(q_i, 1 - q_j)$$

$$= T_{ij}^{+}(1 - q_i, q_j)$$
(95)

The two equalities in (93) are clear from definition (24), where we have commutativity with respect to q_i and q_j . We thus begin with the first equality in (94). Let us define $\alpha_{ij}^+ := e^{4\beta J_{ij}} - 1$ and $\alpha_{ij}^- := e^{4\beta (-J_{ij})} - 1$. Then, using (24) for an antiferromagnetic edge, we have

$$\xi_{ij}^{-}(q_i, q_j) = \frac{1}{2\alpha_{ij}^{-}} \left(1 + \alpha_{ij}^{-}(q_i + q_j) - \sqrt{\left(1 + \alpha_{ij}^{-}(q_i + q_j)\right)^2 - 4\alpha_{ij}^{-}(1 + \alpha_{ij}^{-})q_iq_j} \right). \tag{96}$$

If we express α_{ij}^- in terms of α_{ij}^+ , we observe that

$$\alpha_{ij}^{-} = \frac{\alpha_{ij}^{+}}{-e^{4\beta J_{ij}}} = \frac{-\alpha_{ij}^{+}}{\alpha_{ij}^{+} + 1}, \quad \text{which implies} \quad \frac{1}{2\alpha_{ij}^{-}} = \frac{-(\alpha_{ij}^{+} + 1)}{2\alpha_{ij}^{+}}, \tag{97}$$

$$1 + \alpha_{ij}^{-}(q_i + q_j) = 1 - \frac{\alpha_{ij}^{+}}{\alpha_{ij}^{+} + 1}(q_i + q_j), \quad \text{and}$$
 (98)

$$\sqrt{\left(1 + \alpha_{ij}^{-}(q_i + q_j)\right)^2 - 4\alpha_{ij}^{-}(1 + \alpha_{ij}^{-})q_iq_j}
= \sqrt{\left(1 - \frac{\alpha_{ij}^{+}}{\alpha_{ij}^{+} + 1}(q_i + q_j)\right)^2 + 4\frac{\alpha_{ij}^{+}}{\alpha_{ij}^{+} + 1}\left(1 - \frac{\alpha_{ij}^{+}}{\alpha_{ij}^{+} + 1}\right)q_iq_j}
= \sqrt{1 - 2\frac{\alpha_{ij}^{+}}{\alpha_{ij}^{+} + 1}(q_i + q_j) + \frac{(\alpha_{ij}^{+})^2}{(\alpha_{ij}^{+} + 1)^2}(q_i + q_j)^2 + 4\frac{\alpha_{ij}^{+}}{(\alpha_{ij}^{+} + 1)^2}q_iq_j}
= \frac{1}{\alpha_{ij}^{+} + 1}\sqrt{(\alpha_{ij}^{+} + 1)^2 - 2\alpha_{ij}^{+}(\alpha_{ij}^{+} + 1)(q_i + q_j) + (\alpha_{ij}^{+})^2(q_i + q_j)^2 + 4\alpha_{ij}^{+}q_iq_j}
= \frac{1}{\alpha_{ij}^{+} + 1}\sqrt{\left(1 + \alpha_{ij}^{+}(q_i + (1 - q_j)\right)^2 - 4\alpha_{ij}^{+}(1 + \alpha_{ij}^{+})q_i(1 - q_j)}.$$
(99)

Now substitute (97) - (99) into (96) and subtract $q_i q_i$:

$$\xi_{ij}^{-}(q_i, q_j) - q_i q_j
= \frac{-1}{2\alpha_{ij}^{+}} \left((\alpha_{ij}^{+} + 1) - \alpha_{ij}^{+}(q_i + q_j) \right)
- \sqrt{\left(1 + \alpha_{ij}^{+}(q_i + (1 - q_j))^2 - 4\alpha_{ij}^{+}(1 + \alpha_{ij}^{+})q_i(1 - q_j) \right)} - q_i q_j
= \frac{-1}{2\alpha_{ij}^{+}} \left(1 + \alpha_{ij}^{+}((q_i + (1 - q_j))) \right)
- \sqrt{\left(1 + \alpha_{ij}^{+}(q_i + (1 - q_j))^2 - 4\alpha_{ij}^{+}(1 + \alpha_{ij}^{+})q_i(1 - q_j) \right)} + q_i - q_i q_j
= -\xi_{ij}^{+}(q_i, 1 - q_j) + q_i(1 - q_j),$$

where we have inserted ξ_{ij}^+ according to its definition (24) for a ferromagnetic edge. For the second equality in (94), we can perform the same computation as above but with reversed role of q_i and q_j . Next, we use the symmetry properties of ξ_{ij}^+ and ξ_{ij}^- to prove (95), where we only show the first equality (the others follow analogously):

$$T_{ij}^{-}(q_i, q_j) \stackrel{(28)}{=} q_i q_j (1 - q_i) (1 - q_j) - (\xi_{ij}^{-}(q_i, q_j) - q_i q_j)^2$$

$$\stackrel{(94)}{=} q_i q_j (1 - q_i) (1 - q_j) - (-\xi_{ij}^{+}(q_i, 1 - q_j) + q_i (1 - q_j))^2$$

$$\stackrel{(93)}{=} (1 - q_j) q_i q_j (1 - q_i) - (\xi_{ij}^{+}(1 - q_j, q_i) - (1 - q_j) q_i)^2$$

$$\stackrel{(28)}{=} T_{ij}^{+} (1 - q_j, q_i)$$

Finally, we use the derived properties to prove (40):

$$\begin{split} r_{ij}^-(q_i,q_j) &\overset{(92)}{=} \frac{q_j(1-q_j) - q_iq_j + \xi_{ij}^-(q_i,q_j)}{T_{ij}^-(q_i,q_j)} \\ &\overset{(94)}{=} \frac{q_j(1-q_j) + q_i(1-q_j) - \xi_{ij}^+(q_i,1-q_j)}{T_{ij}^-(q_i,q_j)} \\ &\overset{(95)}{=} \frac{q_j(1-q_j) - \xi_{ij}^+(q_i,1-q_j) + q_i(1-q_j)}{T_{ij}^+(q_i,1-q_j)} \\ &\overset{(91)}{=} r_{ij}^+(q_i,1-q_j) \end{split}$$

An analogous computation shows the second equality in (40).

Proof [Proof of Lemma 10]

The formulas (42), (43) for the partial derivatives of ξ_{ij}^* are derived in Lemma 13 in (Weller and Jebara, 2013). All other formulas (44) - (53) follow from the elementary rules of differentiation, applied to the definitions (24), (28), (35) of ξ_{ij}^* , T_{ij} , r_{ij}^+ .

Proof [Proof of Theorem 11]

First, we multiply both sides in (54) (using formula (47)) by T_{ij}^2 to remove the denominator. The resulting equation is

$$(1 - 2q_j - \frac{\partial \xi_{ij}^*}{\partial q_j} + q_i)T_{ij} = (q_j(1 - q_j) - \xi_{ij}^* + q_i q_j)\frac{\partial T_{ij}}{\partial q_i}.$$
 (100)

Let us consider both sides of this equation separately. We substitute the formulas for T_{ij} from (28) and $\frac{\partial \xi_{ij}^*}{\partial q_j}$ from (43) into the left-hand side of (100):

$$((1 - 2q_{j} - \frac{\partial \xi_{ij}^{*}}{\partial q_{j}} + q_{i})T_{ij}$$

$$= (1 - 2q_{j} - \frac{\alpha_{ij}(q_{i} - \xi_{ij}^{*}) + q_{i}}{1 + \alpha_{ij}(q_{i} + q_{j} - 2\xi_{ij}^{*})} + q_{i})(q_{i}q_{j}(1 - q_{i})(1 - q_{j}) - (\xi_{ij}^{*} - q_{i}q_{j})^{2})$$

$$= \left[(1 + \alpha_{ij}(q_{i} + q_{j} - 2\xi_{ij}^{*}))(1 - 2q_{j} + q_{i})(q_{i}q_{j}(1 - q_{i})(1 - q_{j}) - (\xi_{ij}^{*} - q_{i}q_{j})^{2}) - (\alpha_{ij}(q_{i} - \xi_{ij}^{*}) + q_{i})(q_{i}q_{j}(1 - q_{i})(1 - q_{j}) - (\xi_{ij}^{*} - q_{i}q_{j})^{2}) \right]$$

$$\cdot \frac{1}{1 + \alpha_{ij}(q_{i} + q_{j} - 2\xi_{ij}^{*})}$$

$$= (2q_{j} - 1 + \alpha_{ij}(\xi_{ij}^{*} - q_{j} - q_{i}^{2} + 2q_{j}^{2} + q_{i}q_{j} + 2q_{i}\xi_{ij}^{*} - 4q_{j}\xi_{ij}^{*}))$$

$$\cdot (q_{i}^{2}q_{j} + q_{i}q_{j}^{2} - 2q_{i}q_{j}\xi_{ij}^{*} - q_{i}q_{j} + (\xi_{ij}^{*})^{2}) \frac{1}{1 + \alpha_{ij}(q_{i} + q_{j} - 2\xi_{ij}^{*})}$$

We also substitute the analytical expression for $\frac{\partial T_{ij}}{\partial q_j}$ from (45) (with $\frac{\partial \xi_{ij}^*}{\partial q_j}$ already substituted into $\frac{\partial T_{ij}}{\partial q_j}$) into the right-hand side of (100):

$$(q_{j}(1-q_{j})-\xi_{ij}^{*}+q_{i}q_{j})\frac{\partial T_{ij}}{\partial q_{j}}$$

$$=(q_{j}(1-q_{j})-\xi_{ij}^{*}+q_{i}q_{j})$$

$$\cdot ((1-2q_{j})q_{i}(1-q_{i})-2(\xi_{ij}^{*}-q_{i}q_{j})(\frac{\alpha_{ij}(q_{i}-\xi_{ij}^{*})+q_{i}}{1+\alpha_{ij}(q_{i}+q_{j}-2\xi_{ij}^{*})}-q_{i}))$$

$$=\left[(1+\alpha_{ij}(q_{i}+q_{j}-2\xi_{ij}^{*}))((q_{j}(1-q_{j})-\xi_{ij}^{*}+q_{i}q_{j})(1-2q_{j})q_{i}(1-q_{i})+2q_{i}(\xi_{ij}^{*}-q_{i}q_{j})(q_{j}(1-q_{j})-(\xi_{ij}^{*}-q_{i}q_{j})))\right]$$

$$-2(\xi_{ij}^{*}-q_{i}q_{j})(\alpha_{ij}(q_{i}-\xi_{ij}^{*})+q_{i})(q_{j}(1-q_{j})-\xi_{ij}^{*}+q_{i}q_{j})$$

$$\cdot \frac{1}{1+\alpha_{ij}(q_{i}+q_{j}-2\xi_{ij}^{*})}$$

If we multiply the obtained expressions for both sides by $1 + \alpha_{ij}(q_i + q_j - 2\xi_{ij}^*)$ and simplify some terms, equation (100) becomes

$$(2q_{j} - 1 + \alpha_{ij}(\xi_{ij}^{*} - q_{j} - q_{i}^{2} + 2q_{j}^{2} + q_{i}q_{j} + 2q_{i}\xi_{ij}^{*} - 4q_{j}\xi_{ij}^{*}))$$

$$\cdot (q_{i}^{2}q_{j} + q_{i}q_{j}^{2} - 2q_{i}q_{j}\xi_{ij}^{*} - q_{i}q_{j} + (\xi_{ij}^{*})^{2})$$

$$- (1 + \alpha_{ij}(q_{i} + q_{j} - 2\xi_{ij}^{*}))q_{i}(q_{j}(1 - q_{j}) - \xi_{ij}^{*} + q_{i}q_{j})(1 - q_{i} + 2(\xi_{ij}^{*} - q_{j}))$$

$$+ 2(\xi_{ij}^{*} - q_{i}q_{j})(\alpha_{ij}(q_{i} - \xi_{ij}^{*}) + q_{i})(q_{j}(1 - q_{j}) - \xi_{ij}^{*} + q_{i}q_{j}) = 0$$

or, after expanding and grouping terms with the same power of ξ_{ij}^* together,

$$(q_i^2 q_j^2 + 2q_i^2 q_j^3 - 2q_i^3 q_j^2 - q_i^2 q_j + q_i^3 q_j - \alpha_{ij} q_i^2 q_j + \alpha_{ij} q_i^3 q_j - \alpha_{ij} q_i^2 q_j^2 + 4\alpha_{ij} q_i^2 q_j^3)$$

$$+ (q_i - q_i^2 + \alpha_{ij} q_i^2 - \alpha_{ij} q_i^3 - 4q_i q_j^2 + 2q_i^2 q_j + 4\alpha_{ij} q_i q_j - 3\alpha_{ij} q_i q_j^2 - 2\alpha_{ij} q_i^2 q_j$$

$$- 4\alpha_{ij} q_i q_j^3 - 4\alpha_{ij} q_i^2 q_j^2) \xi_{ij}^*$$

$$+ (2q_j - 1 - 4\alpha_{ij} q_i - 3\alpha_{ij} q_j + 3\alpha_{ij} q_i^2 + 4\alpha_{ij} q_j^2 + 5\alpha_{ij} q_i q_j + 4\alpha_{ij} q_i q_j^2) (\xi_{ij}^*)^2$$

$$+ (3\alpha_{ij} - 2\alpha_{ij} q_i - 4\alpha_{ij} q_j) (\xi_{ij}^*)^3 = 0.$$

Now recall from (24) that $\xi_{ij}^*(q_i, q_j)$ is a function of q_i and q_j , having the form $\xi_{ij}^*(q_i, q_j) = \frac{1}{2\alpha_{ij}} \left(Q_{ij} - \sqrt{Q_{ij}^2 - 4\alpha_{ij}(1 + \alpha_{ij})q_iq_j} \right)$ with $Q_{ij} = 1 + \alpha_{ij}(q_i + q_j)$. For a shorter notation, let us denote the square root term in ξ_{ij}^* by $\sqrt{\cdots}$. By inserting the analytical form of ξ_{ij}^* in the previous equation, we then get

$$\tilde{A} + \tilde{B} \left(Q_{ij} - \sqrt{\cdots} \right) + \tilde{C} \left(Q_{ij} - \sqrt{\cdots} \right)^2 + \tilde{D} \left(Q_{ij} - \sqrt{\cdots} \right)^3 = 0 \tag{101}$$

with the coefficients

$$\begin{split} \tilde{A} &:= (q_i^2 q_j^2 + 2 q_i^2 q_j^3 - 2 q_i^3 q_j^2 - q_i^2 q_j + q_i^3 q_j - \alpha_{ij} q_i^2 q_j + \alpha_{ij} q_i^3 q_j - \alpha_{ij} q_i^2 q_j^2 + 4 \alpha_{ij} q_i^2 q_j^3), \\ \tilde{B} &:= \frac{1}{2\alpha_{ij}} (q_i - q_i^2 + \alpha_{ij} q_i^2 - \alpha_{ij} q_i^3 - 4 q_i q_j^2 + 2 q_i^2 q_j + 4 \alpha_{ij} q_i q_j - 3 \alpha_{ij} q_i q_j^2 - 2 \alpha_{ij} q_i^2 q_j \\ &- 4 \alpha_{ij} q_i q_j^3 - 4 \alpha_{ij} q_i^2 q_j^2), \\ \tilde{C} &:= \frac{1}{4\alpha_{ij}^2} (2 q_j - 1 - 4 \alpha_{ij} q_i - 3 \alpha_{ij} q_j + 3 \alpha_{ij} q_i^2 + 4 \alpha_{ij} q_j^2 + 5 \alpha_{ij} q_i q_j + 4 \alpha_{ij} q_i q_j^2), \quad \text{and} \\ \tilde{D} &:= \frac{1}{8\alpha_{ij}^3} (3 \alpha_{ij} - 2 \alpha_{ij} q_i - 4 \alpha_{ij} q_j). \end{split}$$

Also, the power terms can be expanded according to

$$(Q_{ij} - \sqrt{\cdots})^2 = 2Q_{ij}^2 - 2Q_{ij}\sqrt{\cdots} - 4\alpha_{ij}(1 + \alpha_{ij})q_iq_j$$
 and (102)

$$(Q_{ij} - \sqrt{\cdots})^3 = 4\left(Q_{ij}^3 + \left(\alpha_{ij}(1 + \alpha_{ij})q_iq_j - Q_{ij}^2\right)\sqrt{\cdots} - 3Q_{ij}\alpha_{ij}(1 + \alpha_{ij})q_iq_j\right).$$
(103)

Next, we substitute (102) and (103) into (101), which we subsequently write as a radical equation:

$$\tilde{A} + Q_{ij}\tilde{B} + 2(Q_{ij}^2 - 2\alpha_{ij}(1 + \alpha_{ij})q_iq_j)\tilde{C} + 4(Q_{ij}^3 - 3Q_{ij}\alpha_{ij}(1 + \alpha_{ij})q_iq_j)\tilde{D}$$

$$= \left[\tilde{B} + 2Q_{ij}\tilde{C} + 4(Q_{ij}^2 - \alpha_{ij}(1 + \alpha_{ij})q_iq_j)\right]\sqrt{\cdots}$$
(104)

To find all $q_j \in (0,1)$ that solve (104), we distinguish between two cases regarding the coefficient $\tilde{B} + 2Q_{ij}\tilde{C} + 4(Q_{ij}^2 - \alpha_{ij}(1 + \alpha_{ij})q_iq_j)$ of the root term:

Case 1:
$$\tilde{B} + 2Q_{ij}\tilde{C} + 4(Q_{ij}^2 - \alpha_{ij}(1 + \alpha_{ij})q_iq_j) = 0$$

We treat this case by first computing the set of all $q_j \in (0,1)$ that satisfy this equation. For this purpose, we substitute the algebraic expressions for $\tilde{B}, \tilde{C}, \tilde{D}$ from above, and $Q_{ij} = 1 + \alpha_{ij}(q_i + q_j)$ into this equation and, after a few simplifications, obtain

$$((2\alpha_{ij}q_i - \alpha_{ij})q_i^2 + (2\alpha_{ij}q_i^2 - 4\alpha_{ij}q_i + \alpha_{ij} - 1)q_j + \alpha_{ij}q_i(1 - q_i) - q_i + 1) = 0.$$

We recognize this as a quadratic equation in q_j , whose solutions are

$$q_j^{(1)} = 1 - q_i$$
 and $q_j^{(2)} = \frac{1 + \alpha_{ij}q_i}{\alpha_{ij}(2q_i - 1)}$.

While $q_j^{(1)}=1-q_i$ is of course a feasible solution (i.e., lies in the interval (0,1) whenever $q_j \in (0,1)$), we show that this is not the case for $q_j^{(2)}$: If $q_i < 0.5$, then $(2q_i-1) < 1$, and hence $q_j^{(2)} < 0$; if $q_i = 0.5$, then $q_j^{(2)}$ is not even well-defined; if $q_i > 0.5$, then $q_j^{(2)}$ is lower bounded by $\frac{1+\alpha_{ij}}{\alpha_{ij}}$, which is > 1. In summary, $q_j^{(1)}=1-q_i$ is the only candidate for being a feasible solution to equation (104), under the assumption that we are in Case 1. It remains to check, if $q_j^{(1)}$ indeed solves equation (104) or if Case 1 does not admit a feasible solution of (104). We thus insert $(1-q_i)$ for q_j in all terms (including $\tilde{A}, \tilde{B}, \tilde{C}, \tilde{D}, Q_{ij}$) of (104) and, considering that the right-hand side equals to zero, arrive at the equation

$$(q_i^2(1-q_i)^2+2q_i^2(1-q_i)^3-2q_i^3(1-q_i)^2-q_i^2(1-q_i)+q_i^3(1-q_i)$$

$$-\alpha_{ij}q_i^2(1-q_i)+\alpha_{ij}q_i^3(1-q_i)-\alpha_{ij}q_i^2(1-q_i)^2+4\alpha_{ij}q_i^2(1-q_i)^3)$$

$$+(1+\alpha_{ij})\frac{1}{2\alpha_{ij}}(q_i-q_i^2+\alpha_{ij}q_i^2-\alpha_{ij}q_i^3-4q_i(1-q_i)^2+2q_i^2(1-q_i)$$

$$+4\alpha_{ij}q_i(1-q_i)-3\alpha_{ij}q_i(1-q_i)^2-2\alpha_{ij}q_i^2(1-q_i)-4\alpha_{ij}q_i(1-q_i)^3$$

$$-4\alpha_{ij}q_i^2(1-q_i)^2)$$

$$+2((1+\alpha_{ij})^2-2\alpha_{ij}(1+\alpha_{ij})q_i(1-q_i))$$

$$\cdot\frac{1}{4\alpha_{ij}^2}(2(1-q_i)-1-4\alpha_{ij}q_i-3\alpha_{ij}(1-q_i)+3\alpha_{ij}q_i^2+4\alpha_{ij}(1-q_i)^2$$

$$+5\alpha_{ij}q_i(1-q_i)+4\alpha_{ij}q_i(1-q_i)^2)$$

$$+4((1+\alpha_{ij})^3-3(1+\alpha_{ij})\alpha_{ij}(1+\alpha_{ij})q_i(1-q_i))$$

$$\cdot\frac{1}{8\alpha_{ij}^3}(3\alpha_{ij}-2\alpha_{ij}q_i-4\alpha_{ij}(1-q_i))=0.$$

After a series of elementary algebraic manipulations, all terms on the left-hand side of this equation cancel. This finally proves that $q_j = 1 - q_i$ is the unique solution of equation (104), assuming that we are in Case 1.

Case 2:
$$\tilde{B} + 2Q_{ij}\tilde{C} + 4(Q_{ij}^2 - \alpha_{ij}(1 + \alpha_{ij})q_iq_j) \neq 0$$

Using the assumption of Case 2, we can isolate the radical in equation (104), by dividing both sides by $\tilde{B} + 2Q_{ij}\tilde{C} + 4(Q_{ij}^2 - \alpha_{ij}(1 + \alpha_{ij})q_iq_j)$. If we then, to remove the root term, square both sides of the resulting equation and simplify the involved terms, we obtain the purely polynomial equation

$$\frac{1}{\alpha_{ij}^{4}} \Big[(q_i + q_j - 1)^2 (2\alpha_{ij}^2 q_i^2 q_j^2 - 2\alpha_{ij}^2 q_i^2 q_j + \alpha_{ij}^2 q_i^2 - 2\alpha_{ij}^2 q_i q_j^2
+ \alpha_{ij}^2 q_j^2 - 4\alpha_{ij} q_i q_j + 2\alpha_{ij} (q_i + q_j) + 1)^2 \Big]
= \frac{1}{\alpha_{ij}^{4}} \Big[\Big((1 + \alpha_{ij} (q_i + q_j))^2 - 4\alpha_{ij} (1 + \alpha_{ij}) q_i q_j \Big)
\cdot (q_i + q_j - 1)^2 \Big(1 + \alpha_{ij} (q_i + q_j - 2q_i q_j)^2 \Big]$$

or, equivalently,

$$4\alpha_{ij}^4 q_i^2 q_j^2 (1 - q_i)^2 (1 - q_j)^2 = 0.$$

Since the solutions to this equation, $q_j^{(3)} = 0$ and $q_j^{(4)} = 1$, are boundary points of the open interval (0,1) and thus not feasible, equation (104) does not admit any feasible solution in Case 2.

We conclude that $q_j^* := q_j^{(1)} = 1 - q_i$ is the unique solution to equation (104) and thus to equation $\frac{\partial r_{ij}^+}{\partial q_j} = 0$, which finally proves the Theorem.

Proof [Proof of Lemma 12]

(a) We evaluate r_{ij}^+ in $(q_i, 1 - q_i)$ and get

$$r_{ij}^{+}(q_{i}, 1 - q_{i}) \stackrel{\text{(35)}}{=} \frac{(1 - q_{i})q_{i} - \xi_{ij}^{*}(q_{i}, 1 - q_{i}) + q_{i}(1 - q_{i})}{T_{ij}(q_{i}, 1 - q_{i})}$$

$$\stackrel{\text{(28)}}{=} \frac{2q_{i}(1 - q_{i}) - \xi_{ij}^{*}(q_{i}, 1 - q_{i})}{q_{i}(1 - q_{i})(1 - q_{i})q_{i} - (\xi_{ij}^{*}(q_{i}, 1 - q_{i}) - q_{i}(1 - q_{i}))^{2}}$$

$$= \frac{2q_{i}(1 - q_{i}) - \xi_{ij}^{*}(q_{i}, 1 - q_{i})}{-(\xi_{ij}^{*}(q_{i}, 1 - q_{i}))^{2} + 2q_{i}(1 - q_{i})\xi_{ij}^{*}(q_{i}, 1 - q_{i})}$$

$$= \frac{1}{\xi_{ii}^{*}(q_{i}, 1 - q_{i})}.$$

(b) To compute the limit values of r_{ij}^+ , we require the limit values of ξ_{ij}^* . They have been computed in (Leisenberger et al., 2022), Lemma 2:

$$\lim_{q_i \to 0} \xi_{ij}^*(q_i, q_j) = 0 \tag{105}$$

$$\lim_{q_i \to 1} \xi_{ij}^*(q_i, q_j) = q_i \tag{106}$$

With this we have

$$\lim_{q_j \to 0} r_{ij}^+(q_i, q_j) = \lim_{q_j \to 0} \underbrace{\frac{\overbrace{q_j(1 - q_j) - \xi_{ij}^*(q_i, q_j) + q_i q_j}^{\to 0}}_{q_i q_j (1 - q_i)(1 - q_j) - \left(\xi_{ij}^*(q_i, q_j) - q_i q_j\right)^2}_{\to 0},$$

where both the numerator and the denominator tend to zero as q_j approaches zero. We thus apply de L'Hôspitals's rule and replace the above expression with the quotient of the derivatives:

$$\lim_{q_j \to 0} r_{ij}^+(q_i, q_j) = \lim_{q_j \to 0} \frac{\frac{\partial}{\partial q_j} \left(q_j (1 - q_j) - \xi_{ij}^*(q_i, q_j) + q_i q_j \right)}{\frac{\partial}{\partial q_i} T_{ij}(q_i, q_j)}$$
(107)

Using the formulas from Lemma 10, (a) yields

$$\lim_{q_{j}\to 0} \left[\frac{\partial}{\partial q_{j}} \left(q_{j} (1 - q_{j}) - \xi_{ij}^{*} (q_{i}, q_{j}) + q_{i} q_{j} \right) \right]$$

$$= \lim_{q_{j}\to 0} \left[1 - 2q_{j} - \frac{\partial \xi_{ij}^{*}}{\partial q_{j}} + q_{i} \right]$$

$$\stackrel{(43)}{=} \lim_{q_{j}\to 0} \left[1 - 2q_{j} - \frac{\alpha_{ij} (q_{i} - \xi_{ij}^{*}) + q_{i}}{1 + \alpha_{ij} (q_{i} + q_{j} - 2\xi_{ij}^{*})} + q_{i} \right]$$

$$\stackrel{(105)}{=} 1 - \frac{q_{i} (1 + \alpha_{ij})}{1 + \alpha_{ij} q_{i}} + q_{i}$$

$$= \frac{1 + \alpha_{ij} q_{i}^{2}}{1 + \alpha_{ij} q_{i}}$$

and

$$\lim_{q_{j} \to 0} \frac{\partial T_{ij}}{\partial q_{j}}$$

$$\stackrel{\text{(45)}}{=} \lim_{q_{j} \to 0} \left[(1 - 2q_{j})q_{i}(1 - q_{i}) - 2(\xi_{ij}^{*} - q_{i}q_{j})(\frac{\partial \xi_{ij}^{*}}{\partial q_{j}} - q_{i}) \right]$$

$$\stackrel{\text{(43)}}{=} \lim_{q_{j} \to 0} \left[(1 - 2q_{j})q_{i}(1 - q_{i}) - 2(\xi_{ij}^{*} - q_{i}q_{j})(\frac{\alpha_{ij}(q_{i} - \xi_{ij}^{*}) + q_{i}}{1 + \alpha_{ij}(q_{i} + q_{j} - 2\xi_{ij}^{*})} - q_{i}) \right]$$

$$\stackrel{\text{(105)}}{=} q_{i}(1 - q_{i}) - 2 \cdot 0 \cdot \left(\frac{q_{i}(1 + \alpha_{ij})}{1 + \alpha_{ij}q_{i}} - q_{i}\right)$$

$$= q_{i}(1 - q_{i}).$$

Then, (107) is further equal to

$$\frac{\frac{1+\alpha_{ij}q_i^2}{1+\alpha_{ij}q_i}}{q_i(1-q_i)} = \frac{1+\alpha_{ij}q_i^2}{(1+\alpha_{ij}q_i)q_i(1-q_i)},$$

which proves (56). An analogous calculation can be performed to compute the second limit value (57).

Proof [Proof of Theorem 13]

First, we consider the relation between $r_{ij}^{(+,0)}(q_i)$ and $r_{ij}^{(+,1)}(q_i)$. We use the derived formulas from Lemma 12, (b) to compute their difference as

$$r_{ij}^{(+,1)}(q_i) - r_{ij}^{(+,0)}(q_i)$$

$$= \lim_{q_j \to 1} r_{ij}^+(q_i, q_j) - \lim_{q_j \to 0} r_{ij}^+(q_i, q_j)$$

$$\stackrel{(56),(57)}{=} \frac{1 + \alpha_{ij}(1 - q_i)^2}{(1 + \alpha_{ij}(1 - q_i))q_i(1 - q_i)} - \frac{1 + \alpha_{ij}q_i^2}{(1 + \alpha_{ij}q_i)q_i(1 - q_i)}$$

$$= \underbrace{\frac{\sum_{j=0}^{0}}{\alpha_{ij}^2(1 - q_i)(1 - 2q_i)}}_{>0} \underbrace{\frac{\sum_{j=0}^{0}}{(1 + \alpha_{ij}q_i)}\underbrace{(1 + \alpha_{ij}(1 - q_i))}}_{>0}.$$

This expression is positive if $q_i \in (0,0.5)$, negative if $q_i \in (0.5,1)$, and zero if $q_i = 0.5$.

Second, we consider the difference between $r_{ij}^+(q_i, 1-q_i)$ and $r_{ij}^{(+,0)}(q_i)$:

$$r_{ij}^{+}(q_{i}, 1 - q_{i}) - r_{ij}^{(+,0)}(q_{i})$$

$$= r_{ij}^{+}(q_{i}, 1 - q_{i}) - \lim_{q_{j} \to 0} r_{ij}^{+}(q_{i}, q_{j})$$

$$\stackrel{(55)}{=} \frac{1}{\xi_{ij}^{*}(q_{i}, 1 - q_{i})} - \frac{1 + \alpha_{ij}q_{i}^{2}}{(1 + \alpha_{ij}q_{i})q_{i}(1 - q_{i})}$$

$$\stackrel{(24)}{=} \frac{2\alpha_{ij}}{1 + \alpha_{ij} - \sqrt{(1 + \alpha_{ij})^{2} - 4\alpha_{ij}(1 + \alpha_{ij})q_{i}(1 - q_{i})}} - \frac{1 + \alpha_{ij}q_{i}^{2}}{(1 + \alpha_{ij}q_{i})q_{i}(1 - q_{i})}$$

This expression is positive if and only if

$$2\alpha_{ij}(1 + \alpha_{ij}q_i)q_i(1 - q_i)$$

> $(1 + \alpha_{ij}q_i^2)(1 + \alpha_{ij} - \sqrt{(1 + \alpha_{ij})^2 - 4\alpha_{ij}(1 + \alpha_{ij})q_i(1 - q_i)})$

or

$$(1 + \alpha_{ij}q_i^2)\sqrt{(1 + \alpha_{ij})^2 - 4\alpha_{ij}(1 + \alpha_{ij})q_i(1 - q_i)}$$

> $(1 + \alpha_{ij}q_i^2)(1 + \alpha_{ij}) - 2\alpha_{ij}(1 + \alpha_{ij}q_i)q_i(1 - q_i).$

If the expression on the right-hand side is negative, then the inequality is trivially satisfied (since all terms on the left-hand side are positive). If the expression on the right-hand side is nonnegative, we can square both sides of the inequality to remove the root term and obtain the equivalent statement

$$(1 + \alpha_{ij}q_i^2)^2 ((1 + \alpha_{ij})^2 - 4\alpha_{ij}(1 + \alpha_{ij})q_i(1 - q_i))$$

> $((1 + \alpha_{ij}q_i^2)(1 + \alpha_{ij}) - 2\alpha_{ij}(1 + \alpha_{ij}q_i)q_i(1 - q_i))^2$

After simplifying and rearranging these terms, we arrive at the inequality

$$\alpha_{ij}q_i^6 - 4\alpha_{ij}q_i^5 + 6\alpha_{ij}q_i^4 - 4\alpha_{ij}q_i^3 + \alpha_{ij}q_i^2 > 0$$

which, in turn, is equivalent to

$$\alpha_{ij}q_i^2(1-q_i)^4 > 0,$$

a relation that is fulfilled unless $q_i \in \{0,1\}$. In summary, we have shown that $r_{ij}^+(q_i, 1-q_i)$ is greater than $r_{ij}^{(+,0)}(q_i)$, which proves another part of the Theorem. Moreover, the relation $r_{ij}^+(q_i, 1-q_i) > r_{ij}^{(+,0)}(q_i)$ (for all $q_i \in (0,1)$) follows analogously to the previous calculation and will therefore be omitted.

Finally, we conclude that the unique stationary point $q_j^* = 1 - q_i$ is a maximum of $r_{ij}^+(q_i, q_j)$ with respect to $q_j \in (0, 1)$, because its value in that point is greater than its limit values at the boundary points (otherwise $r_{ij}^+(q_i, q_j)$ would have another stationary point in that interval, which represents the line segment between $(q_i, 0)$ and $(q_i, 1)$ visualized in Figure 5).

Appendix B. Proofs of Sec. 3.3

Proof [Proof of Lemma 17]

To compute the infinite temperature limit of det $\mathbf{H}_{2\times 2}^{(i,j)}$, we require the limit values of ξ_{ij}^* and T_{ij} as $\beta \to 0$. First, note that

$$\lim_{\beta \to 0} \alpha_{ij} = \lim_{\beta \to 0} \left[e^{4\beta J_{ij}} - 1 \right] = 0, \tag{108}$$

where we have used the definition of α_{ij} from (24). Next, we use from (Welling and Teh, 2001) that ξ_{ij}^* is the (positive) solution of the quadratic equation

$$(1 + \alpha_{ij}(q_i + q_j))\xi_{ij}^* = \alpha_{ij}(\xi_{ij}^*)^2 + (1 + \alpha_{ij})q_iq_j.$$
(109)

We take the limit on both sides of (109) and obtain

$$\lim_{\beta \to 0} \left[\left(\underbrace{1 + \alpha_{ij}(q_i + q_j)}_{\to 1} \right) \xi_{ij}^* \right] = \lim_{\beta \to 0} \left[\underbrace{\alpha_{ij}(\xi_{ij}^*)^2}_{\to 0} \right] + \lim_{\beta \to 0} \left[\underbrace{(1 + \alpha_{ij})q_iq_j}_{\to q_iq_j} \right]$$
(110)

which, after using (108), becomes

$$\lim_{\beta \to 0} \xi_{ij}^* = q_i q_i. \tag{111}$$

With this and the definition (28) of T_{ij} , we further obtain

$$\lim_{\beta \to 0} T_{ij} = \lim_{\beta \to 0} \left[q_i q_j (1 - q_i) (1 - q_j) - \underbrace{(\xi_{ij}^* - q_i q_j)^2}_{\to 0} \right] = q_i q_j (1 - q_i) (1 - q_j). \tag{112}$$

Finally, we use (111) and (112) to derive the desired result (76):

$$\lim_{\beta \to 0} \left[(\det \mathbf{H}_{2 \times 2}^{(i,j)})(q_i, q_j) \right]$$

$$\stackrel{(75)}{=} \lim_{\beta \to 0} \left[\frac{d_i - 1}{d_i} \cdot \frac{d_j - 1}{d_j} \cdot \frac{1}{q_i q_j (1 - q_i)(1 - q_j)} + \frac{1}{T_{ij}} \left(1 - \frac{d_i - 1}{d_i} - \frac{d_j - 1}{d_j} \right) \right]$$

$$\stackrel{(112)}{=} \frac{d_i - 1}{d_i} \cdot \frac{d_j - 1}{d_j} \cdot \frac{1}{q_i q_j (1 - q_i)(1 - q_j)} + \frac{\left(1 - \frac{d_i - 1}{d_i} - \frac{d_j - 1}{d_j} \right)}{q_i q_j (1 - q_i)(1 - q_j)}$$

$$= \frac{1}{d_i d_j} \cdot \frac{1}{q_i q_j (1 - q_i)(1 - q_j)} > 0$$

Proof [Proof of Lemma 19]

We use the formula for det $\mathbf{H}_{2\times 2}^{(i,j)}$ from (75), in which we see that the term

$$\frac{d_i-1}{d_i} \cdot \frac{d_j-1}{d_j} \cdot \frac{1}{q_i q_j (1-q_i)(1-q_j)}$$

is independent from β and in the second term

$$\frac{1}{T_{ij}} \left(1 - \frac{d_i - 1}{d_i} - \frac{d_j - 1}{d_j} \right) \tag{113}$$

only T_{ij} depends – implicitly via ξ_{ij}^* – on β . Let us therefore first compute the partial derivatives of ξ_{ij}^* and T_{ij} (using the formulas (24) and (28)) with respect to β , starting with ξ_{ij}^* . As in the proof of Lemma 17, we use from (Welling and Teh, 2001) that ξ_{ij}^* is the (positive) solution of the quadratic equation

$$(1 + \alpha_{ij}(q_i + q_j))\xi_{ij}^* = \alpha_{ij}(\xi_{ij}^*)^2 + (1 + \alpha_{ij})q_iq_j.$$
(114)

Note that also α_{ij} (from (24)) depends on β . Its derivative is

$$\frac{\partial}{\partial \beta} \alpha_{ij} = \frac{\partial}{\partial \beta} \left(e^{4\beta J_{ij}} - 1 \right) = 4J_{ij} e^{4\beta J_{ij}}, \tag{115}$$

which is positive for a ferromagnetic edge $(J_{ij} > 0)$ and negative for an antiferromagnetic edge $(J_{ij} < 0)$. Now we compute the partial derivatives with respect to β on both sides of (114) and obtain

$$\left(\left(\frac{\partial}{\partial \beta} \alpha_{ij} \right) (q_i + q_j) \right) \xi_{ij}^* + \left(1 + \alpha_{ij} (q_i + q_j) \right) \frac{\partial}{\partial \beta} \xi_{ij}^*
= \left(\frac{\partial}{\partial \beta} \alpha_{ij} \right) (\xi_{ij}^*)^2 + 2\alpha_{ij} \xi_{ij}^* \frac{\partial}{\partial \beta} \xi_{ij}^* + \left(\frac{\partial}{\partial \beta} \alpha_{ij} \right) q_i q_j.$$
(116)

Rearranging this equation and expressing $\frac{\partial}{\partial \beta} \xi_{ij}^*$ through the other terms gives

$$\frac{\partial}{\partial \beta} \xi_{ij}^* = \frac{\left(\frac{\partial}{\partial \beta} \alpha_{ij}\right) \left((\xi_{ij}^*)^2 - (q_i + q_j) \xi_{ij}^* + q_i q_j \right)}{\left(1 + \alpha_{ij} (q_i + q_j) - 2\alpha_{ij} \xi_{ij}^* \right)}$$

or, equivalently,

$$\frac{\partial}{\partial \beta} \xi_{ij}^* = \left(\frac{\partial}{\partial \beta} \alpha_{ij}\right) \frac{(q_i - \xi_{ij}^*)(q_j - \xi_{ij}^*)}{1 + \alpha_{ij}(q_i + q_j - 2\xi_{ij}^*)}.$$
(117)

The terms $(q_i - \xi_{ij}^*)$ and $(q_j - \xi_{ij}^*)$ are elements from the joint probability table 1 and are therefore positive (and hence also the term $(q_i + q_j - 2\xi_{ij}^*)$). With (115), it follows that also $\frac{\partial}{\partial \beta} \xi_{ij}^*$ is positive if $J_{ij} > 0$, and negative if $J_{ij} < 0$. Next, we consider the partial derivative of T_{ij} with respect to β :

$$\frac{\partial}{\partial \beta} T_{ij} = \frac{\partial}{\partial \beta} \left(q_i q_j (1 - q_i) (1 - q_j) - (\xi_{ij}^* - q_i q_j)^2 \right) = -2(\xi_{ij}^* - q_i q_j) \left(\frac{\partial}{\partial \beta} \xi_{ij}^* \right) \tag{118}$$

According to Lemma 6 from Sec. 3.2, we know that $\xi_{ij}^* > q_i q_j$ for $J_{ij} > 0$, and $\xi_{ij}^* < q_i q_j$ for $J_{ij} < 0$. In each case (i.e., whether we consider a ferromagnetic or an antiferromagnetic edge) it follows together with (117) that $\frac{\partial}{\partial \beta} T_{ij}$ is negative (or, equivalently, that $\frac{\partial}{\partial \beta} \frac{1}{T_{ij}}$ is positive). Finally, note that

$$\left(1 - \frac{d_i - 1}{d_i} - \frac{d_j - 1}{d_j}\right)$$

is negative if we assume⁴² that both d_i, d_j are greater than 2. Then the statement of Lemma 19 follows, because

$$\frac{\partial}{\partial \beta} \det \mathbf{H}_{2 \times 2}^{(i,j)} \stackrel{(75)}{=} \underbrace{\left(1 - \frac{d_i - 1}{d_i} - \frac{d_j - 1}{d_j}\right)}_{\leq 0} \underbrace{\frac{\partial}{\partial \beta} \frac{1}{T_{ij}}}_{\geq 0} < 0. \tag{119}$$

Proof [Proof of Lemma 20]

We evaluate det $\mathbf{H}_{2\times 2}^{(i,j)}$ in (0.5,0.5), using the formula derived in (75):

$$\det \mathbf{H}_{2\times 2}^{(i,j)}(0.5,0.5) = 16 \cdot \frac{d_i - 1}{d_i} \cdot \frac{d_j - 1}{d_j} + \frac{1}{T_{ij}} \left(1 - \frac{d_i - 1}{d_i} - \frac{d_j - 1}{d_j} \right)$$
(120)

Recall that $T_{ij} = T_{ij}(q_i, q_j)$ is a function of q_i and q_j , which must be evaluated separately. For this we can use a result from (Leisenberger et al., 2022) (derived during the proof of Lemma 5), which says that

$$T_{ij}(0.5, 0.5) = \frac{1}{16\cosh^2(\beta J_{ij})}. (121)$$

^{42.} As we will see later in this section, $\mathbf{H}_{2\times 2}^{(i,j)}$ is always positive definite if $d_i \leq 2$ or $d_j \leq 2$. Therefore, this is a meaningful assumption at this point.

Substituting (121) in (120), and performing a few manipulations yields

$$\det \mathbf{H}_{2\times2}^{(i,j)}(0.5,0.5) = 16 \left(\frac{d_i - 1}{d_i} \cdot \frac{d_j - 1}{d_j} - \frac{d_i d_j - d_i - d_j}{d_i d_j} \cosh^2(\beta J_{ij}) \right)$$

$$= 16 \left(\frac{d_i d_j - d_i - d_j + 1 - \cosh^2(\beta J_{ij})(d_i d_j - d_i - d_j)}{d_i d_j} \right)$$

$$= 16 \left(\frac{(d_i d_j - d_i - d_j)(1 - \cosh^2(\beta J_{ij})) + 1}{d_i d_j} \right).$$
(122)

With the trigonometric identity

$$1 - \cosh^2(\beta J_{ij}) = \frac{1}{2} \left(1 - \cosh(2\beta J_{ij}) \right)$$

equation (122) is further equal to

$$16 \left(\frac{\frac{1}{2} \cdot (d_i d_j - d_i - d_j) (1 - \cosh(2\beta J_{ij})) + 1}{d_i d_j} \right)$$

$$= \frac{8}{d_i d_j} \cdot \left((d_i d_j - d_i - d_j) (1 - \cosh(2\beta J_{ij})) + 2 \right). \tag{123}$$

So far, we have found a relatively simple expression for det $\mathbf{H}_{2\times 2}^{(i,j)}(0.5,0.5)$. We now aim to determine its sign in dependence of β . To this end, let us make a couple of observations: First, note that the term $\frac{8}{d_i d_j}$ is only a positive scale factor which can be ignored. Second, we observe that the term

$$(d_i d_j - d_i - d_j) (1 - \cosh(2\beta J_{ij})) + 2$$
 (124)

is an even function of J_{ij} (i.e., we may exchange J_{ij} by $-J_{ij}$, without modifying the outcome), because the hyperbolic cosine is an even function of its argument. In other words, the sign of det $\mathbf{H}_{2\times2}^{(i,j)}(0.5,0.5)$ depends only on the absolute value of J_{ij} but not on its sign – we may thus replace J_{ij} by $|J_{ij}|$ in (124). Third, the hyperbolic cosine is lower bounded by one (and equals this lower bound if and only if its argument is zero), which implies that

$$1 - \cosh(2\beta |J_{ij}|) < 0.$$

Finally, the term $d_i d_j - d_i - d_j$ is always positive under our assumption that both $d_i, d_j > 2$. From these observations, we conclude that det $\mathbf{H}_{2\times 2}^{(i,j)}(0.5,0.5)$ is positive if and only if

$$(d_i d_j - d_i - d_j) (1 - \cosh(2\beta J_{ij})) > -2$$

or, equivalently,

$$\beta < \frac{1}{2|J_{ij}|}\operatorname{arccosh}\left(1 + \frac{2}{d_id_j - d_i - d_j}\right) \eqqcolon \beta^*.$$

Exchanging the less-than sign by the equals sign or the greater-than sign proves the complete statement of the Lemma.

Proof [Proof of Theorem 21]

We already know from Lemma 20 that (0.5, 0.5) is a solution to the equation

$$\det \mathbf{H}_{2\times 2}^{(i,j)}(q_i, q_j) = 0; \tag{125}$$

now we must prove that it is the unique solution. Afterwards, to prove that $\det \mathbf{H}_{2\times 2}^{(i,j)}$ is positive for all $(q_i,q_j) \neq (0.5,0.5)$, we compute the Hessian matrix of $\det \mathbf{H}_{2\times 2}^{(i,j)}$ and show that it is positive definite. Since $\det \mathbf{H}_{2\times 2}^{(i,j)}$ is a continuous function of (q_i,q_j) , this implies the statement.

Concretely, the proof consists of three parts: In Part 1, we modify equation (125) to bring it into a simpler form. In Part 2, we show that (0.5, 0.5) is the unique solution to this modified equation, and, by construction, the unique solution to the original equation. In Part 3, we finally show that $\det \mathbf{H}_{2\times 2}^{(i,j)}$ positive for all other points in the domain.

Part 1: In equation (125), we substitute the expression

$$\frac{d_i - 1}{d_i} \cdot \frac{d_j - 1}{d_j} \cdot \frac{1}{q_i q_j (1 - q_i) (1 - q_j)} + \frac{1}{T_{ij}} \left(1 - \frac{d_i - 1}{d_i} - \frac{d_j - 1}{d_j} \right) \tag{126}$$

for det $\mathbf{H}_{2\times 2}^{(i,j)}$, which has been derived in (75). Without loss of generality, we may assume that $J_{ij} > 0$ (i.e., we consider a ferromagnetic edge), because of the symmetry properties⁴³ of T_{ij} derived in the proof of Lemma 9 in Sec. 3.2. To abbreviate the notation, we define

$$c_1 := \frac{d_i - 1}{d_i} \cdot \frac{d_j - 1}{d_j},$$

$$c_2 := 1 - \frac{d_i - 1}{d_i} - \frac{d_j - 1}{d_j}, \quad \text{and}$$

$$q_{\pi} := q_i q_j (1 - q_i) (1 - q_j).$$

$$(127)$$

Then, after multiplying by T_{ij} , equation (126) is equivalent to

$$c_1 \frac{T_{ij}}{q_\pi} + c_2 = 0$$

or, using the definition (28) of T_{ii} ,

$$c_1 + c_2 - c_1 \frac{(\xi_{ij}^* - q_i q_j)^2}{q_\pi} = 0.$$
 (128)

Since

$$c_1 + c_2 \stackrel{\text{(127)}}{=} \frac{(d_i - 1)(d_j - 1) + d_i d_j - (d_i - 1) d_j - d_i (d_j - 1)}{d_i d_j} = \frac{1}{d_i d_j},$$

^{43.} More precisely, if we rotate det $\mathbf{H}_{2\times 2}^{(i,j)}$ by 90 degrees in its domain around the center point, we obtain det $\mathbf{H}_{2\times 2}^{(i,j)}$ which implicitly depends on a coupling with the same strength but an inverse sign. This transformation does not change the number of its roots, though. Hence, if (0.5,0.5) is the unique root of det $\mathbf{H}_{2\times 2}^{(i,j)}$ for $J_{ij} > 0$, it is also for $J_{ij} < 0$.

we can multiply equation (128) by $\frac{1}{d_i d_i q_{\pi}}$ and obtain

$$q_{\pi} - (d_i - 1)(d_j - 1)((\xi_{ij}^*)^2 - 2\xi_{ij}^* q_i q_j + q_i^2 q_i^2) = 0.$$
(129)

Next, we consider ξ_{ij}^* , using its definition (24). We have

$$\xi_{ij}^* = \frac{1}{2\alpha_{ij}} \left(Q_{ij} - \sqrt{Q_{ij}^2 - 4\alpha_{ij}(1 + \alpha_{ij})q_i q_j} \right), \tag{130}$$

where $Q_{ij} = 1 + \alpha_{ij}(q_i + q_j)$ with $\alpha_{ij} = e^{4\beta^* J_{ij}} - 1$ depending on the critical β^* . For simplicity, let us denote the square root term by $\sqrt{\cdots}$. Then

$$(\xi_{ij}^*)^2 = \frac{1}{4\alpha_{ij}^2} (Q_{ij}^2 - 2Q_{ij}\sqrt{\cdots} + Q_{ij}^2 - 4\alpha_{ij}(\alpha_{ij} + 1)q_iq_j)$$

and, after inserting the equations for ξ_{ij}^* and $(\xi_{ij}^*)^2$, equation (129) becomes

$$q_{\pi} - (d_{i} - 1)(d_{j} - 1) \left[\frac{1}{4\alpha_{ij}^{2}} (Q_{ij}^{2} - 2Q_{ij}\sqrt{\cdots} + Q_{ij}^{2} - 4\alpha_{ij}(\alpha_{ij} + 1)q_{i}q_{j}) - \frac{q_{i}q_{i}}{\alpha_{ij}} (Q_{ij} - \sqrt{\cdots}) + q_{i}^{2}q_{j}^{2} \right] = 0.$$

Further manipulations yield

$$q_{\pi} - (d_i - 1)(d_j - 1) \left[(Q_{ij} - \sqrt{\cdots}) \left(\frac{Q_{ij}}{2\alpha_{ij}^2} - \frac{q_i q_j}{\alpha_{ij}} \right) - \frac{(\alpha_{ij} + 1)}{\alpha_{ij}} q_i q_j + q_i^2 q_j^2 \right] = 0,$$

where we can isolate the radical according to

$$\frac{q_{\pi} - (d_{i} - 1)(d_{j} - 1)\left(Q_{ij}\left(\frac{Q_{ij}}{2\alpha_{ij}^{2}} - \frac{q_{i}q_{j}}{\alpha_{ij}}\right) - \frac{(\alpha_{ij} + 1)}{\alpha_{ij}}q_{i}q_{j} + q_{i}^{2}q_{j}^{2}\right)}{\left(\frac{Q_{ij}}{2\alpha_{ij}^{2}} - \frac{q_{i}q_{j}}{\alpha_{ij}}\right)(d_{i} - 1)(d_{j} - 1)} = (-1) \cdot \sqrt{\cdots}.$$

Now squaring both sides of this equation⁴⁴ and manipulating the result gives

$$q_{\pi}^{2} - 2q_{\pi}(d_{i} - 1)(d_{j} - 1)\left(Q_{ij}\left(\frac{Q_{ij}}{2\alpha_{ij}^{2}} - \frac{q_{i}q_{j}}{\alpha_{ij}}\right) - \frac{(\alpha_{ij} + 1)}{\alpha_{ij}}q_{i}q_{j} + q_{i}^{2}q_{j}^{2}\right) + \frac{(d_{i} - 1)^{2}(d_{j} - 1)^{2}}{4\alpha_{ij}^{4}}\left(Q_{ij}^{2} - 2Q_{ij}\alpha_{ij}q_{i}q_{j} + 2\alpha_{ij}^{2}q_{i}^{2}q_{j}^{2} - 2\alpha_{ij}^{2}q_{i}q_{j} - 2\alpha_{ij}q_{i}q_{j}\right)^{2} - \frac{(d_{i} - 1)^{2}(d_{j} - 1)^{2}}{4\alpha_{ij}^{4}}\left(Q_{ij} - 2\alpha_{ij}q_{i}q_{j}\right)^{2}(Q_{ij}^{2} - 4\alpha_{ij}q_{i}q_{j} - 4\alpha_{ij}^{2}q_{i}q_{j}) = 0,$$

^{44.} Note that the squaring operation might induce additional solutions to the resulting equation, which are not solutions to the original equation. Each solution to the new equation, however, is also a solution to the original equation. In the later proof, we show that (0.5, 0.5) is the unique feasible solution to the new equation, and thus the only candidate for a solution to the original equation.

where we substitute $Q_{ij} = 1 + \alpha_{ij}(q_i + q_j)$ and simplify the result:

$$q_{\pi}^{2} - \frac{2(d_{i} - 1)(d_{j} - 1)q_{\pi}}{2\alpha_{ij}^{2}} \left(\alpha_{ij}^{2}(2q_{i}^{2}q_{j}^{2} - 2q_{i}^{2}q_{j} - 2q_{i}q_{j}^{2} + q_{i}^{2} + q_{j}^{2}) + \alpha_{ij}(2q_{i} + 2q_{j} - 4q_{i}q_{j}) + 1\right)$$

$$+ \frac{(d_{i} - 1)^{2}(d_{j} - 1)^{2}}{4\alpha_{ij}^{4}} \left(\alpha_{ij}^{2}(2q_{i}^{2}q_{j}^{2} - 2q_{i}^{2}q_{j} - 2q_{i}q_{j}^{2} + q_{i}^{2} + q_{j}^{2}) + \alpha_{ij}(2q_{i} + 2q_{j} - 4q_{i}q_{j}) + 1\right)^{2}$$

$$+ \frac{(d_{i} - 1)^{2}(d_{j} - 1)^{2}}{4\alpha_{ij}^{4}} \left(\alpha_{ij}^{2}(q_{i}^{2} + q_{j}^{2} - 2q_{i}q_{j}) + \alpha_{ij}(2q_{i} + 2q_{j} - 4q_{i}q_{j}) + 1\right)$$

$$\cdot \left(1 + \alpha_{ij}(q_{i} + q_{j}) - 2\alpha_{ij}q_{i}q_{j}\right)^{2} = 0$$

This equation is the same as

$$q_{\pi}^{2} - \frac{(d_{i} - 1)(d_{j} - 1)q_{\pi}}{\alpha_{ij}^{2}} \left(\alpha_{ij}^{2}(2q_{i}^{2}q_{j}^{2} - 2q_{i}^{2}q_{j} - 2q_{i}q_{j}^{2} + q_{i}^{2} + q_{j}^{2}) + \alpha_{ij}(2q_{i} + 2q_{j} - 4q_{i}q_{j}) + 1\right) + (d_{i} - 1)^{2}(d_{j} - 1)^{2}q_{\pi}^{2} = 0$$

or

$$\frac{q_{\pi}}{\alpha_{ij}^{2}} \left[\alpha_{ij}^{2} q_{\pi} - (d_{i} - 1)(d_{j} - 1) \left(\alpha_{ij}^{2} (2q_{i}^{2} q_{j}^{2} - 2q_{i}^{2} q_{j} - 2q_{i} q_{j}^{2} + q_{i}^{2} + q_{j}^{2} \right) + \alpha_{ij} (2q_{i} + 2q_{j} - 4q_{i}q_{j}) + 1 + (d_{i} - 1)^{2} (d_{j} - 1)^{2} \alpha_{ij}^{2} q_{\pi} \right] = 0.$$

Recall that we have defined q_{π} in (127) as $q_i q_j (1 - q_i) (1 - q_j)$, which means that $q_i = 0$, $q_i = 1$, $q_j = 0$, and $q_j = 1$ are solutions to the above equation; however, they are not feasible (as the domain of det $\mathbf{H}_{2\times 2}^{(i,j)}$ is the open set $(0,1)\times(0,1)$) and therefore not relevant for our further considerations. Yet, we can multiply the previous equation by $\frac{\alpha_{ij}^2}{q_{\pi}}$, which leaves us with

$$\alpha_{ij}^{2}q_{\pi} - (d_{i} - 1)(d_{j} - 1)(\alpha_{ij}^{2}(2q_{i}^{2}q_{j}^{2} - 2q_{i}^{2}q_{j} - 2q_{i}q_{j}^{2} + q_{i}^{2} + q_{j}^{2}) + 2\alpha_{ij}(q_{i} + q_{j} - 2q_{i}q_{j}) + 1) + (d_{i} - 1)^{2}(d_{j} - 1)^{2}\alpha_{ij}^{2}q_{\pi} = 0.$$
(131)

Now we consider α_{ij} , in whose definition $\alpha_{ij} = e^{4\beta J_{ij}} - 1$ (from (24)) we substitute the critical inverse temperature β^* according to formula (78):

$$\alpha_{ij} = \exp\left(\frac{2J_{ij}}{|J_{ij}|}\operatorname{arccosh}\left(1 + \frac{2}{d_id_j - d_i - d_j}\right)\right) - 1 \tag{132}$$

With the trigonometric identity⁴⁵

$$\operatorname{arccosh}\left(1 + \frac{2}{d_i d_j - d_i - d_j}\right) = \log\left(\sqrt{\left(1 + \frac{2}{d_i d_j - d_i - d_j}\right)^2 - 1} + 1 + \frac{2}{d_i d_j - d_i - d_j}\right)$$

^{45.} This trigonometric identity is valid for a positive argument of arccosh, which is satisfied in our case as we assumed d_i , $d_i > 2$.

it follows that (132) is further equal to

$$\exp\left[\log\left(\sqrt{\left(1 + \frac{2}{d_id_j - d_i - d_j}\right)^2 - 1} + 1 + \frac{2}{d_id_j - d_i - d_j}\right)^2\right] - 1$$

$$= \frac{(2 + 2\sqrt{d_id_j - d_i - d_j + 1} + d_id_j - d_i - d_j)^2}{(d_id_j - d_i - d_j)^2} - 1$$

$$= 4\left(\frac{2(d_i - 1)(d_j - 1) + (2 + d_id_j - d_i - d_j)\sqrt{(d_i - 1)(d_j - 1)}}{(d_id_j - d_i - d_j)^2}\right),$$

where we have used our assumption $J_{ij} > 0$ made the beginning of this proof (i.e., $\frac{J_{ij}}{|J_{ij}|} = 1$). If we define

$$D := d_i d_j - d_i - d_j + 1 = (d_i - 1)(d_j - 1), \tag{133}$$

we get

$$\alpha_{ij} = 4 \left(\frac{2D + (D+1)\sqrt{D}}{(D-1)^2} \right). \tag{134}$$

We return to equation (131), into which we insert expression (134) for α_{ij} :

$$\frac{16D}{(D-1)^4} \left(4D + 4(D+1)\sqrt{D} + (D+1)^2\right) q_{\pi}$$

$$-D \left[\frac{16D}{(D-1)^4} \left(4D + 4(D+1)\sqrt{D} + (D+1)^2\right) \left(2q_i^2 q_j^2 - 2q_i^2 q_j - 2q_i q_j^2 + q_i^2 + q_j^2\right) \right.$$

$$+ 8 \left(\frac{2D + (D+1)\sqrt{D}}{(D-1)^2} \right) \left(q_i + q_j - 2q_i q_j\right) + 1 \right]$$

$$+ \frac{16D^3}{(D-1)^4} \left(4D + 4(D+1)\sqrt{D} + (D+1)^2\right) q_{\pi} = 0$$

We multiply this equation by $\frac{(D-1)^4}{D}$, rearrange a few terms, and arrive at

$$16(4D + 4(D+1)\sqrt{D} + (D+1)^{2})(1+D^{2})q_{\pi} - (D-1)^{4}$$

$$-16D(4D + 4(D+1)\sqrt{D} + (D+1)^{2})(2q_{i}^{2}q_{j}^{2} - 2q_{i}^{2}q_{j} - 2q_{i}q_{j}^{2} + q_{i}^{2} + q_{j}^{2})$$

$$-8(D-1)^{2}(2D + (D+1)\sqrt{D})(q_{i} + q_{j} - 2q_{i}q_{j}) = 0,$$
(135)

which is the final form of our equation that we will analyze in the second part of this proof.

<u>Part 2:</u> In this part, we show that the center point (0.5, 0.5) is the unique solution to the modified equation (135). However, instead of solving this equation directly, we apply an alternative strategy. Namely, we consider the left-hand side of (135) as a funtion of (q_i, q_j) and prove that it has a stationary point in (0.5, 0.5), in which it takes the value zero. Subsequently, we compute the limit values of this function at the boundary and show that they are all negative. We finally argue that this function is negative for all points $(q_i, q_j) \neq (0.5, 0.5)$

in $(0,1) \times (0,1)$ and that (0.5,0.5) must consequently be its unique global maximum (and thus the unique solution to equation (135)).

Let us define the left-hand side of (135) as

$$L'(q_{i}, q_{j}) := 16(4D + 4(D+1)\sqrt{D} + (D+1)^{2})(1 + D^{2})q_{\pi} - (D-1)^{4} - 16D(4D + 4(D+1)\sqrt{D} + (D+1)^{2})(2q_{i}^{2}q_{j}^{2} - 2q_{i}^{2}q_{j} - 2q_{i}q_{j}^{2} + q_{i}^{2} + q_{j}^{2}) - 8(D-1)^{2}(2D + (D+1)\sqrt{D})(q_{i} + q_{j} - 2q_{i}q_{j}),$$

$$(136)$$

considered as a function of (q_i, q_j) . To compute its stationary points (i.e., points where the gradient $\nabla L'(q_i, q_j)$ vanishes), we calculate its partial derivatives with respect to q_i and q_j , and set them both equal to zero:

$$\frac{\partial}{\partial q_i} L'(q_i, q_j)
= 16 (4D + 4(D+1)\sqrt{D} + (D+1)^2)(1 + D^2)(1 - 2q_i)q_j(1 - q_j)
- 32D (4D + 4(D+1)\sqrt{D} + (D+1)^2)(2q_iq_j^2 - 2q_iq_j - q_j^2 + q_i)
- 8(D-1)^2 (2D + (D+1)\sqrt{D})(1 - 2q_j) \stackrel{!}{=} 0$$
(137)

$$\frac{\partial}{\partial q_j} L'(q_i, q_j)
= 16 (4D + 4(D+1)\sqrt{D} + (D+1)^2)(1+D^2)q_i(1-q_i)(1-2q_j)
- 32D (4D+4(D+1)\sqrt{D} + (D+1)^2)(2q_i^2q_j - 2q_iq_j - q_i^2 + q_j)
- 8(D-1)^2 (2D+(D+1)\sqrt{D})(1-2q_i) \stackrel{!}{=} 0$$
(138)

This equation system is hard to solve directly, and therefore we compute the difference between the two partial derivatives which we then set to zero:

$$(\frac{\partial}{\partial q_i} L' - \frac{\partial}{\partial q_i} L')(q_i, q_j)$$

$$= 16(4D + 4(D+1)\sqrt{D} + (D+1)^2)(q_i - q_j)$$

$$\cdot \left[(1+D^2)(-1+q_i+q_j-2q_iq_j) - 2D(1+q_i+q_j-2q_iq_j) \right]$$

$$- 16(D-1)^2 (2D + (D+1)\sqrt{D})(q_i - q_j) \stackrel{!}{=} 0$$

$$(139)$$

Note that solutions to (139) are the only potential solutions to the equation system (137) + (138), and thus the only candidates for stationary points of L' (while, on the other hand, there might be solutions to (139) which are not stationary points of L'). We observe that in equation (139), the term $(q_i - q_j)$ occurs as a common factor in all terms which implies that all points (q_i, q_j) with $q_i = q_j$ are solutions to (139) (and thus candidates for stationary

points of L'). We need to check if there are other solutions to (139), i.e., for which the remaining equation (without the factor $16 \cdot (q_i - q_j)$)

$$(4D + 4(D+1)\sqrt{D} + (D+1)^{2})$$

$$\cdot \left[(1+D^{2})(-1+q_{i}+q_{j}-2q_{i}q_{j}) - 2D(1+q_{i}+q_{j}-2q_{i}q_{j}) \right]$$

$$-(D-1)^{2}(2D+(D+1)\sqrt{D}) = 0$$
(140)

is satisfied. We will show that (140) has no feasible solutions, by defining its left-hand side as another function

$$L''(q_i, q_j) := (4D + 4(D+1)\sqrt{D} + (D+1)^2) \cdot \left[(1+D^2)(-1+q_i+q_j-2q_iq_j) - 2D(1+q_i+q_j-2q_iq_j) \right] - (D-1)^2(2D+(D+1)\sqrt{D}),$$
(141)

and proving that L'' is negative for all (q_i, q_j) in $(0, 1) \times (0, 1)$. For that purpose, we first show that (0.5, 0.5) is the unique stationary point of L'' which, however, is a saddle point (i.e., both infimum and supremum of L'' are not taken by L'' but only approached as limit values at the boundary); afterwards, we compute the limit values of L'' at the boundary and show that they are all negative. From this, we conclude that L'' must be negative on its entire domain. We therefore compute the partial derivatives of L'' as

$$\frac{\partial}{\partial q_i} L''(q_i, q_j)
= (4D + 4(D+1)\sqrt{D} + (D+1)^2) \cdot (1-D)^2 \cdot (1-2q_j)$$
(142)

and

$$\frac{\partial}{\partial q_j} L''(q_i, q_j)
= (4D + 4(D+1)\sqrt{D} + (D+1)^2) \cdot (1-D)^2 \cdot (1-2q_i).$$
(143)

If we set both expressions to zero, we see that (0.5, 0.5) is the unique solution to the resulting equation system (since $(4D + 4(D+1)\sqrt{D} + (D+1)^2) \cdot (1-D)^2$ is positive, where D has been defined in (133)), and thus the only stationary point of L''. The Hessian matrix of L'' is

$$\nabla^2 L''(q_i, q_j) = \underbrace{\left(4D + 4(D+1)\sqrt{D} + (D+1)^2\right) \cdot (1-D)^2}_{>0} \cdot \begin{pmatrix} 0 & -2 \\ -2 & 0 \end{pmatrix},$$

which is indefinite for all (q_i, q_j) (because $\begin{pmatrix} 0 & -2 \\ -2 & 0 \end{pmatrix}$ has precisely one positive and one negative eigenvalue). In particular, (0.5, 0.5) (and any other point) is a saddle point of L''. To characterize the behavior of L'' as it approaches the boundary, we compute its corresponding limit values. Recall that L'' is defined on $(0,1) \times (0,1)$ (which is an open

subset of \mathbb{R}^2), and thus the boundary of its domain is precisely the union of the four line segments

$$\{(q_i, q_j) \in \mathbb{R}^2 \mid q_i = 0, 0 \le q_j \le 1\} \cup \{(q_i, q_j) \in \mathbb{R}^2 \mid q_i = 1, 0 \le q_j \le 1\}$$

$$\cup \{(q_i, q_j) \in \mathbb{R}^2 \mid 0 \le q_i \le 1, q_j = 0\} \cup \{(q_i, q_j) \in \mathbb{R}^2 \mid 0 \le q_i \le 1, q_j = 1\},$$

$$(144)$$

i.e., the four edges (and corners) of the unit square. Hence, for $0 \le k \le 1$, the limit values of L'' (defined in (140)) can be computed as

$$\lim_{\substack{q_i \to 0 \\ q_j \to k}} L''(q_i, q_j) = \underbrace{\left(4D + 4(D+1)\sqrt{D} + (D+1)^2\right)}_{>0} \left(\underbrace{\left(1 + D^2\right)(-1 + k)}_{\leq 0}\right) - \underbrace{2D(1+k)}_{\geq 0}\right) - \underbrace{\left(D - 1\right)^2\left(2D + (D+1)\sqrt{D}\right)}_{>0} < 0,$$

$$\lim_{\substack{q_i \to 1 \\ q_j \to k}} L''(q_i, q_j) = \underbrace{\left(4D + 4(D+1)\sqrt{D} + (D+1)^2\right)}_{>0} \left(\underbrace{\left(1 + D^2\right)(k - 2k)}_{\leq 0} - \underbrace{2D(2 + k - 2k)}_{\geq 0}\right) - \underbrace{\left(D - 1\right)^2 \left(2D + (D+1)\sqrt{D}\right)}_{>0} < 0,$$

and analogously for $\lim_{\substack{q_i \to k \\ q_j \to 0}} L''(q_i, q_j)$ and $\lim_{\substack{q_i \to k \\ q_j \to 1}} L''(q_i, q_j)$. Hence, all limit values of L''

at the boundary are negative. Since the only stationary point of L'' is a saddle point, this implies that L'' must be negative on its entire domain (otherwise, L'' would attain a maximum somewhere). In particular, L'' has no root in $(0,1) \times (0,1)$. With this, we have proven that equation (140) has no feasible solution and that points (q_i, q_j) with $q_i = q_j$ are consequently the only potential solutions to the equation system (137) + (138) (and thus the only candidates for stationary points of L'). With this knowledge, we return to equation (137), into which⁴⁶ we substitute $q_j = q_i$ to compute the actual stationary points of L':

$$\frac{\partial}{\partial q_i} L'(q_i, q_j = q_i)
= 16(4D + 4(D+1)\sqrt{D} + (D+1)^2)
\cdot \left[(1+D^2)q_i(1-q_i)(1-2q_i) - 2Dq_i(1-q_i)(1-2q_i) \right]
-8(D-1)^2(2D + (D+1)\sqrt{D})(1-2q_i) \stackrel{!}{=} 0$$
(145)

We observe that $(1-2q_i)$ is a common factor of all terms in (145). This means that $q_i = 0.5$ is a solution to the above equation, that (0.5, 0.5) is a solution to the equation system (137) + (138), and hence a stationary point of L'. To check whether equation (145) has other solutions, we must compute the solutions to the remaining equation

$$2(4D + 4(D+1)\sqrt{D} + (D+1)^2)(1-D)^2q_i(1-q_i) - (D-1^2)(2D + (D+1)\sqrt{D}) = 0,$$

^{46.} Note that we could also substitute $q_j = q_i$ into equation (138), but due to symmetry this is equivalent.

which is equivalent to the quadratic equation

$$q_i^2 - q_i + \frac{\sqrt{D}}{2(1+\sqrt{D})^2} = 0.$$
 (146)

We solve equation (146) and obtain the solutions

$$q_i^{(1)} = \frac{1}{2} - \sqrt{\frac{1}{4} - \frac{\sqrt{D}}{2(1 + \sqrt{D})^2}}$$
 and $q_i^{(2)} = \frac{1}{2} + \sqrt{\frac{1}{4} - \frac{\sqrt{D}}{2(1 + \sqrt{D})^2}}$. (147)

Then the points $(q_i^{(1)}, q_i^{(1)})$ and $(q_i^{(2)}, q_i^{(2)})$ are also solutions to the equation system (137) + (138) and thus, in principle, stationary points of L'; yet, we have not shown if they are feasible at all (i.e., if $q_i^{(1)}$ and $q_i^{(2)}$ are in (0,1)). To address this issue, we observe that $\frac{\sqrt{D}}{2(1+\sqrt{D})^2}$ is monotonically decreasing as D (defined in (133)) increases; i.e., if d_i or d_j or both – increases. As we have assumed $d_i > 2$ and $d_j > 2$, it follows that $D \ge 4$ (if $d_i = d_j = 3$), and hence $\frac{\sqrt{D}}{2(1+\sqrt{D})^2} \le \frac{\sqrt{4}}{2(1+\sqrt{4})^2} = \frac{1}{9}$. Thus, $q_i^{(1)}$ and $q_i^{(2)}$ are bounded by

$$q_i^{(1)} \le \frac{1}{2} - \sqrt{\frac{1}{4} - \frac{1}{9}} = \frac{1}{2} - \frac{\sqrt{5}}{6}$$
 and
$$q_i^{(2)} \ge \frac{1}{2} + \sqrt{\frac{1}{4} - \frac{1}{9}} = \frac{1}{2} + \frac{\sqrt{5}}{6}.$$
 (148)

On the other hand, if we consider the limit $D \to \infty$ (corresponding to infinitely many neighbors of node i or node j), the term $\frac{\sqrt{D}}{2(1+\sqrt{D})^2}$ converges (from above) to zero. This induces a lower (resp. upper) bound on $q_i^{(1)}$ (resp. $q_i^{(2)}$) by observing that

$$q_i^{(1)} > \frac{1}{2} - \sqrt{\frac{1}{4}} = \frac{1}{2} - \frac{1}{2} = 0$$
 and
$$q_i^{(2)} < \frac{1}{2} + \sqrt{\frac{1}{4}} = \frac{1}{2} + \frac{1}{2} = 1.$$
 (149)

The bounds (148) and (149) show that $q_i^{(1)}$ lies in the interval $(0,\frac{1}{2}-\frac{\sqrt{5}}{6})$ and $q_i^{(2)}$ lies in the interval $(\frac{1}{2}+\frac{\sqrt{5}}{6},1)$, which are both subsets of (0,1). Hence, $(q_i^{(1)},q_j^{(1)}=q_i^{(1)})$ and $(q_i^{(2)},q_j^{(2)}=q_i^{(2)})$ are feasible stationary points of L'. In summary, L' has precisely three stationary points in $(0,1)\times(0,1)$, which are the center point (0.5,0.5) and the two symmetrical points $(q_i^{(1)},q_j^{(1)}=q_i^{(1)})$ and $(q_i^{(2)},q_j^{(2)}=q_i^{(2)})$ (with $q_i^{(1)}$ and $q_i^{(2)}$ defined in (147)).

As the final step in this part, we need to determine which kind of stationary points they are, beginning with (0.5, 0.5). We therefore compute the Hessian matrix of L' and evaluate it in (0.5, 0.5). We use the first-order derivatives of L' derived in (137) and (138) to calculate

its second-order partial derivatives with respect to q_i and q_i :

$$\frac{\partial^{2} L'}{\partial q_{i}^{2}} = -32(4D + 4(D+1)\sqrt{D} + (D+1)^{2}) \left[(1+D^{2})q_{j}(1-q_{j}) + D(2q_{j}^{2} - 2q_{j} + 1) \right]$$

$$+ D(2q_{j}^{2} - 2q_{j} + 1) \left[(1+D^{2})(1-2q_{i})(1-2q_{j}) + (D+1)^{2} \right] \left[(1+D^{2})(1-2q_{i})(1-2q_{j}) + D(8q_{i}q_{j} - 4q_{i} - 4q_{j}) \right] + 16(D-1)^{2} \left(2D + (D+1)\sqrt{D} \right)$$

$$= \frac{\partial^{2} L'}{\partial q_{j} \partial q_{i}}$$

$$\frac{\partial^{2} L'}{\partial q_{j}^{2}} = -32(4D + 4(D+1)\sqrt{D} + (D+1)^{2}) \left[(1+D^{2})q_{i}(1-q_{i}) + D(2q_{i}^{2} - 2q_{i} + 1) \right]$$

Evaluating them in in the center point yields

$$\frac{\partial^2 L'}{\partial q_i^2}(0.5, 0.5) = -8(4D + 4(D+1)\sqrt{D} + (D+1)^2)(D+1)^2, \tag{150}$$

$$\frac{\partial^2 L'}{\partial q_i \partial q_j}(0.5, 0.5) = 32D(4D + 4(D+1)\sqrt{D} + (D+1)^2)$$
(151)

$$+16(D-1)^{2}(2D+(D+1)\sqrt{D})$$

$$= \frac{\partial^2 L'}{\partial q_i \partial q_i} (0.5, 0.5), \quad \text{and}$$
 (152)

$$\frac{\partial^2 L'}{\partial q_i^2}(0.5, 0.5) = -8(4D + 4(D+1)\sqrt{D} + (D+1)^2)(D+1)^2, \tag{153}$$

with the main diagonal entries (150) and (153) of the Hessian matrix being negative, and the off-diagonal entries (151) and (152) being positive. We aim to apply the diagonal dominance criterion (Sec. 2.1, (1)) to show that the negative of the Hessian is positive definite (and thus, the Hessian itself is negative definite). I.e., for the first row of the Hessian, we compute the difference between the magnitude of the diagonal entry (150) and the magnitude of the off-diagonal entry (151) as

$$\begin{split} &|\frac{\partial^2 L'}{\partial q_i^2}(0.5, 0.5)| - |\frac{\partial^2 L'}{\partial q_i \partial q_j}(0.5, 0.5)| \\ &= 8 \left(4D + 4(D+1)\sqrt{D} + (D+1)^2\right)(D+1)^2 \\ &- 32D \left(4D + 4(D+1)\sqrt{D} + (D+1)^2\right) - 16(D-1)^2 \left(2D + (D+1)\sqrt{D}\right) \\ &= 8(D-1)^2 \left(4D + 4(D+1)\sqrt{D} + (D+1)^2\right) - 16(D-1)^2 \left(2D + (D+1)\sqrt{D}\right) \\ &= 8(D-1)^2 \left[(D+1)^2 + 2(D+1)\sqrt{D}\right] \end{split}$$

which positive. For the second row of the Hessian, we can perform the same calculation. As the negatives of the diagonal entries (150) and (153) are positive, the negative of the

Hessian satisfies the diagonal dominance criterion and is thus positive definite. We conclude that the Hessian of L' is negative definite in (0.5, 0.5), and that the center point is a local maximum of L'.

To analyze of which kind the two remaining stationary points $(q_i^{(1)},q_i^{(1)}=q_i^{(1)})$ and $(q_i^{(2)},q_i^{(2)}=q_i^{(2)})$ $q_i^{(2)}$) are, we could perform a similar calculation; however, we choose a more elegant approach in which we argue that they can only be saddle points or minima of L' (but definitely no maxima). Concretely, we argue as follows: Suppose, without loss of generality⁴⁷, that $(q_i^{(1)}, q_j^{(1)} = q_i^{(1)})$ is a local maximum of L'. Then there must be some point (\hat{q}, \hat{q}) located on the line segment connecting the two maxima (0.5, 0.5) and $(q_i^{(1)}, q_i^{(1)} = q_i^{(1)})$, such that (\hat{q},\hat{q}) is the minimum of all points between these two maxima (otherwise they would not be maxima); more precisely, the directional derivative of L' along $(1,1)^T$ is zero in (\hat{q},\hat{q}) . On the other hand, (\hat{q}, \hat{q}) is also a minimum or a maximum with respect to the direction that is orthogonal to the main diagonal (i.e., the line segment that connects (0,0) and (1,1); in other words, the directional derivative of L' along $(1,-1)^T$ is zero in (\hat{q},\hat{q}) . This follows from the fact that L' is a symmetric function across any point that lies on the main diagonal with respect to that orthogonal direction, because q_i and q_j can be exchanged in the definition (136) of L' without changing its value. Hence, there exist two directions that are orthogonal to each other, for which the directional derivatives in (\hat{q}, \hat{q}) are zero. Consequently, (\hat{q}, \hat{q}) is another stationary point of L'. However, we know that this is not possible and thus a contradiction to our assumption that $(q_i^{(1)}, q_j^{(1)} = q_i^{(1)})$ is a maximum of L'. In summary, this shows that (0.5, 0.5) is the unique local maximum of L' in $(0, 1) \times (0, 1)$.

It remains to show that L' takes the value zero in (0.5, 0.5), and that it approaches negative limit values at the boundary. From this, we can then conclude that L' is negative for all $(q_i, q_j) \neq (0.5, 0.5)$, which implies that (0.5, 0.5) is the unique solution to our starting equation (135). Let us therefore evaluate L' in (0.5, 0.5) (using its definition (136)):

$$L'(0.5, 0.5) = \frac{16}{16} (4D + 4(D+1)\sqrt{D} + (D+1)^2)(1+D^2) - (D-1)^4$$
$$-\frac{16}{8} D(4D + 4(D+1)\sqrt{D} + (D+1)^2)$$
$$-\frac{8}{2} (D-1)^2 (2D + (D+1)\sqrt{D})$$
$$= (1-D)^2 (4D + (D+1)^2 - 8D) - (D-1)^4$$
$$= (1-D)^2 (D-1)^2 - (D-1)^4 = 0$$

Finally, we compute the limit values of L' at the boundary (144) as

$$\lim_{\substack{q_i \to 0 \\ q_j \to k}} L'(q_i, q_j) = -\underbrace{(D-1)^4}_{>0} - \underbrace{16D(4D + 4(D+1)\sqrt{D} + (D+1)^2)k^2}_{\geq 0}$$
$$-\underbrace{8(D-1)^2(2D + (D+1)\sqrt{D})k}_{>0} < 0,$$

^{47.} The argumentation regarding the symmetrical point $(q_i^{(2)}, q_i^{(2)} = q_i^{(2)})$ is the same.

$$\lim_{\substack{q_i \to 1 \\ q_j \to k}} L'(q_i, q_j) = -\underbrace{(D-1)^4}_{>0} - \underbrace{16D(4D + 4(D+1)\sqrt{D} + (D+1)^2)(1-k)^2}_{\geq 0} - \underbrace{8(D-1)^2(2D + (D+1)\sqrt{D})(1-k)}_{>0} < 0,$$

and analogously for $\lim_{\substack{q_i \to k \\ q_j \to 0}} L'(q_i, q_j)$ and $\lim_{\substack{q_i \to k \\ q_j \to 1}} L'(q_i, q_j)$ (where $0 \le k \le 1$). As described above, we have proven that (0.5, 0.5) is the unique solution to the modified equation (135), and thus the only candidate for solving the original equation (125). But, as we already know from Lemma 20, (0.5, 0.5) is actually a solution to (125), and consequently it must be its unique solution.

Part 3: As we already know from the first two parts, $\det \mathbf{H}_{2\times 2}^{(i,j)}$ has precisely one root in its domain which is the center point (0.5,0.5). In this third and final part of the proof, we verify the second statement of Theorem 21, namely that $\det \mathbf{H}_{2\times 2}^{(i,j)}$ is positive for all $(q_i,q_j)\neq (0.5,0.5)$. To this end, we first multiply $\det \mathbf{H}_{2\times 2}^{(i,j)}$ by the positive term $q_\pi\cdot T_{ij}$ to obtain a slightly modified version of $\det \mathbf{H}_{2\times 2}^{(i,j)}$, that we define as

$$H(q_i, q_j) := q_{\pi} T_{ij} \det \mathbf{H}_{2 \times 2}^{(i,j)} \stackrel{(75),(127)}{=} q_{\pi} T_{ij} \left(c_1 \frac{1}{q_{\pi}} + c_2 \frac{1}{T_{ij}} \right) = c_1 T_{ij} + c_2 q_{\pi}.$$
 (154)

The form (154) has the advantage that q_{π} and T_{ij} occur in the numerators instead of the denominators. At the same time, this modification does not change the sign of det $\mathbf{H}_{2\times 2}^{(i,j)}$, which is positive in a point (q_i, q_j) if and only if $H(q_i, q_j)$ is positive in (q_i, q_j) . In other words, to prove that det $\mathbf{H}_{2\times 2}^{(i,j)}$ is positive for all $(q_i, q_j) \neq (0.5, 0.5)$, we may equivalently prove this statement for $H(q_i, q_j)$. By construction, $H(q_i, q_j)$ has a unique root in (0.5, 0.5), and therefore it is sufficient to prove that $H(q_i, q_j)$ is positive definite in (0.5, 0.5). This implies that $H(q_i, q_j)$ is positive on its entire domain (otherwise it would have multiple roots). We thus calculate its second-order partial derivatives with respect to q_i and q_j as

$$\frac{\partial^2 H}{\partial q_i^2} = c_1 \frac{\partial^2 T_{ij}}{\partial q_i^2} - 2c_2 q_j (1 - q_j), \tag{155}$$

$$\frac{\partial^2 H}{\partial q_i \partial q_i} = c_1 \frac{\partial^2 T_{ij}}{\partial q_i \partial q_j} + c_2 (1 - 2q_i) (1 - 2q_j), \tag{156}$$

$$\frac{\partial^2 H}{\partial q_j^2} = c_1 \frac{\partial^2 T_{ij}}{\partial q_j^2} - 2c_2 q_i (1 - q_i), \tag{157}$$

with the second-order derivatives of T_{ij} calculated in Lemma 10, (b). To evaluate (155) - (157) in (0.5, 0.5), we first need to evaluate the second-order derivatives of T_{ij} and all involved sub-functions in (0.5, 0.5). From Lemma 1 in (Leisenberger et al., 2022), we know the value of ξ_{ij}^* in the center point which is

$$\xi_{ij}^*(0.5, 0.5) = \frac{\sigma(2\beta J_{ij})}{2}.$$
(158)

Here we have used the logistic sigmoid function which is defined as

$$\sigma(2\beta J_{ij}) := \frac{1}{1 + e^{-2\beta J_{ij}}}. (159)$$

Earlier in this paper (in equation (121)) we have already provided the value for T_{ij} in the center point (also as a result from (Leisenberger et al., 2022)) which is given by

$$T_{ij}(0.5, 0.5) = \frac{1}{16\cosh^2(\beta J_{ij})}. (160)$$

Next, we evaluate the first-order derivatives of ξ_{ij}^* and T_{ij} in (0.5, 0.5), that have been derived in Lemma (10), (a). Substituting (158) and (160) into the corresponding equations (42) - (45) yields

$$\frac{\partial \xi_{ij}^*}{\partial q_i}(0.5, 0.5) = \frac{\partial \xi_{ij}^*}{\partial q_j}(0.5, 0.5) = \frac{\alpha_{ij}\left(\frac{1}{2} - \frac{\sigma(2\beta J_{ij})}{2}\right) + 0.5}{1 + \alpha_{ij}(1 - \sigma(2\beta J_{ij}))} \stackrel{(159)}{=} \frac{1}{2}$$
(161)

and

$$\frac{\partial T_{ij}}{\partial q_i}(0.5, 0.5) = \frac{\partial T_{ij}}{\partial q_i}(0.5, 0.5) = -2\left(\frac{\sigma(2\beta J_{ij})}{2} - \frac{1}{4}\right)\left(\frac{1}{2} - \frac{1}{2}\right) = 0.$$
 (162)

Subsequently, we evaluate the second-order derivatives of ξ_{ij}^* and T_{ij} in (0.5, 0.5), that have been derived in Lemma (10), (b). We substitute (158) - (162) into the corresponding equations (48) - (53) and, using the definition (24) of $\alpha_{ij} = e^{4\beta J_{ij}} - 1$ and the trigonometrical identities

$$\sinh(2\beta J_{ij}) = \frac{1}{2} (e^{2\beta J_{ij}} - e^{2\beta J_{ij}}),$$

$$\cosh(2\beta J_{ij}) = \frac{1}{2} (e^{2\beta J_{ij}} + e^{2\beta J_{ij}}), \text{ and}$$

$$\tanh(2\beta J_{ij}) = \frac{\sinh(2\beta J_{ij})}{\cosh(2\beta J_{ij})},$$
(163)

obtain

$$\frac{\partial^{2} \xi_{ij}^{*}}{\partial q_{i}^{2}}(0.5, 0.5) = \frac{\partial^{2} \xi_{ij}^{*}}{\partial q_{i}^{2}}(0.5, 0.5)$$

$$= \frac{\alpha_{ij}(-\frac{1}{2})\left(1 + \alpha_{ij}(1 - \sigma(2\beta J_{ij}))\right)}{\left(1 + \alpha_{ij}(1 - \sigma(2\beta J_{ij}))\right)^{2}} = -\sinh(2\beta J_{ij}), \qquad (164)$$

$$\frac{\partial^{2} \xi_{ij}^{*}}{\partial q_{i} \partial q_{j}}(0.5, 0.5) = \frac{\partial^{2} \xi_{ij}^{*}}{\partial q_{j} \partial q_{i}}(0.5, 0.5)$$

$$= \frac{\left(\frac{\alpha_{ij}}{2} + 1\right)\left(1 + \alpha_{ij}(1 - \sigma(2\beta J_{ij}))\right)}{\left(1 + \alpha_{ij}(1 - \sigma(2\beta J_{ij}))\right)^{2}} = \cosh(2\beta J_{ij}), \qquad (165)$$

and

$$\frac{\partial^{2} T_{ij}}{\partial q_{i}^{2}}(0.5, 0.5) = \frac{\partial^{2} T_{ij}}{\partial q_{i}^{2}}(0.5, 0.5)$$

$$= -\frac{1}{2} + 2\left(\left(\frac{\sigma(2\beta J_{ij})}{2} - \frac{1}{4}\right)(\sinh(2\beta J_{ij}))\right) = \frac{1}{2}\left(\cosh(2\beta J_{ij}) - 2\right), \tag{166}$$

$$\frac{\partial^{2} T_{ij}}{\partial q_{i}\partial q_{j}}(0.5, 0.5) = \frac{\partial^{2} T_{ij}}{\partial q_{j}\partial q_{i}}(0.5, 0.5)$$

$$= -2\left(\left(\frac{\sigma(2\beta J_{ij})}{2} - \frac{1}{4}\right)\left(\cosh(2\beta J_{ij}) - 1\right)\right) = -\sinh^{2}(\beta J_{ij})\tanh(\beta J_{ij}). \tag{167}$$

With the prepared second-order derivatives of T_{ij} , we are now ready to compute the Hessian matrix of the function $H(q_i, q_j)$ (defined in (154)) in the center point. We thus insert the expressions from (166) and (167) into the equations for the second-order derivatives of $H(q_i, q_j)$ (computed in (155) - (157)) and get

$$\frac{\partial^2 H}{\partial q_i^2}(0.5, 0.5) = \frac{c_1}{2} \left(\cosh(2\beta J_{ij}) - 2\right) - \frac{c_2}{2},\tag{168}$$

$$\frac{\partial^2 H}{\partial q_i \partial q_i}(0.5, 0.5) = c_1 \left(-\sinh^2(\beta J_{ij}) \tanh(\beta J_{ij})\right), \quad \text{and}$$
(169)

$$\frac{\partial^2 H}{\partial q_j^2}(0.5, 0.5) = \frac{c_1}{2} \left(\cosh(2\beta J_{ij}) - 2\right) - \frac{c_2}{2}.$$
 (170)

Now recall that we are considering det $\mathbf{H}_{2\times 2}^{(i,j)}$ (and thus $H(q_i,q_j)$) for $\beta=\beta^*$, i.e., at the critical inverse temperature. We thus substitute β^* (from (78) and with D defined in (133)) into (168) - (170):

$$\frac{\partial^2 H}{\partial q_i^2}(0.5, 0.5) = \frac{\partial^2 H}{\partial q_i^2}(0.5, 0.5) = \frac{1}{2} \left(c_1 \frac{2}{D-1} - 2 - c_2\right) \tag{171}$$

$$\frac{\partial^2 H}{\partial q_i \partial q_j}(0.5, 0.5) = \frac{\partial^2 H}{\partial q_j \partial q_i}(0.5, 0.5) = -\frac{c_1}{D - 1} \frac{1}{\sqrt{D}}$$
(172)

In the computation of (172), we have used the trigonometrical identities

$$\sinh(\beta^* J_{ij}) = \sinh\left(\frac{1}{2}\operatorname{arccosh}(1 + \frac{2}{D-1})\right) = \sqrt{\frac{1 + \frac{2}{D-1} - 1}{2}} = \frac{1}{\sqrt{D-1}},$$

$$\tanh(\beta^* J_{ij}) = \tanh\left(\frac{1}{2}\operatorname{arccosh}(1 + \frac{2}{D-1})\right) = \sqrt{\frac{1 + \frac{2}{D-1} - 1}{1 + \frac{2}{D-1} + 1}} = \frac{1}{\sqrt{D}}.$$

To finally prove that the Hessian of $H(q_i, q_j)$ is positive definite in (0.5, 0.5), we apply the diagonal dominance criterion (Sec. 2.1, (1)). Note that the main diagonal entries (171) are positive (because $|c_1| > |c_2|$, with c_1, c_2 being defined in (127)) and the off-diagonal entries (172) are negative (because $c_1 > 0$). For both rows of the Hessian, the difference

between the magnitude of the main diagonal entry and the magnitude of the off-diagonal entry is

$$\frac{1}{2}\left(c_1\frac{2}{D-1}-2-c_2\right) - \frac{c_1}{D-1}\frac{1}{\sqrt{D}} = \frac{1-\frac{1}{\sqrt{D}}}{2d_id_j(1+\frac{1}{\sqrt{D}})} > 0. \tag{173}$$

Hence, the Hessian of $H(q_i, q_j)$ is diagonally dominant and therefore positive definite in (0.5, 0.5). Then $H(q_i, q_j) > 0$ for all $(q_i, q_j) \neq (0.5, 0.5)$ (as (0.5, 0.5) is its only root) and consequently this is also true for det $\mathbf{H}_{2\times 2}^{(i,j)}(q_i, q_j)$. This completes the final part and thus the proof of Theorem 21.

Appendix C. Algorithm BETHE-MIN

Algorithm 1 describes our proposed method BETHE-MIN for minimizing the Bethe free energy that we have applied in our experiments in Sec. 4.2. It requires an initialization $q^{(0)}$ of the parameter vector which contains estimates of the singleton marginals. Until convergence, BETHE-MIN iterates through the following steps: Update of the search direction according a quasi-Newton scheme, i.e., with the inverse Hessian being replaced by an approximation; projecting the largest possible step back into \mathbb{B} ; optimizing the step size via an adaptive Wolfe line search (WOLFE-LS, described in Algorithm 2); updating the parameter vector according to (89); and updating the current approximation to the inverse Hessian (we use the BFGS update rules for approximating the inverse Hessian, Nocedal and Wright (2006)). For checking convergence, we compute the gradient norm with respect to the current parameter vector $q^{(t)}$. After BETHE-MIN has converged, it returns a stationary point q^* (usually a minimum) of \mathcal{F}_B .

The Wolfe conditions used in the adaptive line search stategy are as follows:

$$\mathcal{F}_{B}(\boldsymbol{q}^{\mathrm{tail}} + \rho^{\mathrm{W}} \cdot (\boldsymbol{q}^{\mathrm{head}} - \boldsymbol{q}^{\mathrm{tail}})) \leq \mathcal{F}_{B}(\boldsymbol{q}^{\mathrm{tail}}) + \tau_{1} \cdot \rho^{\mathrm{W}} \cdot \boldsymbol{d}^{T} \nabla \mathcal{F}_{B}(\boldsymbol{q}^{\mathrm{tail}})$$
 (W1)

$$\boldsymbol{d}^{T} \nabla \mathcal{F}_{B} (\boldsymbol{q}^{\text{tail}} + \rho^{W} \cdot (\boldsymbol{q}^{\text{head}} - \boldsymbol{q}^{\text{tail}})) \geq \tau_{2} \cdot \boldsymbol{d}^{T} \nabla \mathcal{F}_{B} (\boldsymbol{q}^{\text{tail}})$$
(W2)

The parameter vectors \mathbf{q}^{tail} and \mathbf{q}^{head} specify the search interval. Condition (W1) ensures that there is a sufficient decrease of the energy function after each iteration. This can be achieved by sufficiently reducing the step size ρ^{W} to prevent \mathcal{F}_B from increasing again (which may happen if the step is too large). Conversely, condition (W2) ensures that we do not stop moving along the search direction \mathbf{d} , as long as the energy function descends sufficiently steeply. Hence, the step size must not be chosen too small. Both conditions together guarantee that the step size is neither chosen too great nor too small. The parameters τ_1 and τ_2 control how 'strict' the individual conditions are. Following a recommendation of Nocedal and Wright (2006), we have selected numerical values of $\tau_1 = 10^{-4}$ and $\tau_2 = 0.9$ for our experiments in Sec. 4.2. The detailed procedure of computing a step size satisfying the Wolfe conditions is described in Algorithm 2. It is used as subroutine in Algorithm 1.

Algorithm 1 BETHE-MIN (Projected quasi-Newton for minimizing \mathcal{F}_B)

```
Input: Parameter vector \boldsymbol{q}^{(0)} in \mathbb{B}
Output: Stationary point q^* of \mathcal{F}_B
    \boldsymbol{q}^{(t)} \leftarrow \boldsymbol{q}^{(0)}
    Initialize \mathbf{B}^{(t)} randomly as a matrix of size |\mathbf{X}| \times |\mathbf{X}|
    while \|\nabla \mathfrak{F}_B(\boldsymbol{q}^{(t)})\| > \epsilon do
                                                                                                                                                     ▷ Check for convergence
            oldsymbol{q}^{	ext{old}} \leftarrow oldsymbol{q}^{(t)}
                                                                                                                                  oldsymbol{d}^{(t)} \leftarrow -ig(\mathbf{B}^{(t)}ig)^T \, 
abla \mathfrak{F}_Big(oldsymbol{q}^{(t)}ig)
                                                                                                                                                  ▶ Update search direction
            oldsymbol{q}^{\pi} \leftarrow oldsymbol{q}^{(t)} + oldsymbol{d}^{(t)}
            while q^{\pi} \notin \mathbb{B} do
                                                                                                                                                    \triangleright Project q^{\pi} back into \mathbb{B}
                    \rho^{\max} \leftarrow 0.9 \cdot \rho^{\max}
                    \boldsymbol{q}^{\pi} \leftarrow \boldsymbol{q}^{(t)} + \rho^{\max} \cdot \boldsymbol{d}^{(t)}
            end while
            \rho^{(t)} \leftarrow \mathtt{WOLFE-LS}(\boldsymbol{q}^{(t)}, \boldsymbol{q}^{\pi})
                                                                                                                         ▷ Compute step size via Algorithm 2
            \mathbf{q}^{(t)} \leftarrow \mathbf{q}^{(t)} + \rho^{(t)} \cdot (\mathbf{q}^{\pi} - \mathbf{q}^{(t)})
                                                                                                                                               ▶ Update parameter vector
            \hat{m{s}}^{(t)} \leftarrow \hat{m{q}}^{(t)} - \hat{m{q}}^{	ext{old}}
            \mathbf{y}^{(t)} \leftarrow \nabla \mathcal{F}_B(\mathbf{q}^{(t)}) - \nabla \mathcal{F}_B(\mathbf{q}^{\text{old}})
                                                                                                                                                            ▶ BFGS update rules
            \gamma^{(t)} \leftarrow (\boldsymbol{s}^{(t)})^{\hat{T}} \boldsymbol{y}^{(t)}
                                                                                                                                                             ▷ for approximating
            \mathbf{B}^{(t)} \leftarrow \mathbf{B}^{(t)'} + \frac{1}{\left(\gamma^{(t)}\right)^2} \left(\gamma^{(t)} + (\boldsymbol{y}^{(t)})^T \mathbf{B}^{(t)} \boldsymbol{y}^{(t)}\right)

    b the inverse Hessian

                              +rac{1}{\gamma^{(t)}}(\mathbf{B}^{(t)}\mathbf{y}^{(t)}(s^{(t)})^T+s^{(t)}(\mathbf{y}^{(t)})^T\mathbf{B}^{(t)})
    end while
    return q^{(t)}
```

Algorithm 2 WOLFE-LS (Adaptive line search with Wolfe conditions)

```
Input: Endpoints q^{\text{tail}}, q^{\text{head}} of search interval Output: Step size \rho^{\text{W}} satisfying the Wolfe conditions (W1) and (W2)
  oldsymbol{d} \leftarrow oldsymbol{q}^{	ext{head}} - oldsymbol{a}^{	ext{tail}}
                                                                                            ▶ Search direction
  Initialize step size \rho^{W} randomly between zero and one
   while (W1) is satisfied and (W2) is not satisfied do
       \rho^{W} = 1.1 \cdot \rho^{W}
                                                                ▶ Expand interval of potential step sizes
   end while
   if (W1) and (W2) are satisfied then
       return \rho^{W}
                                                             ▷ STOP. Feasible step size has been found
   else
       l \leftarrow 0
                                                     ▶ Define new search interval for feasible step size
       r \leftarrow \rho^{\mathrm{W}}
                                                                   ▶ Upper bound of new search interval
       while (W1) or (W2) is not satisfied do
                                                                                         Pick \rho^{W} randomly from interval (l, r)
           if (W1) is not satisfied then
                r \leftarrow \rho^{W}
                                                           ▶ Upper bound of search interval is reduced
           else
                l \leftarrow \rho^{W}
                                                          ▶ Lower bound of search interval is increased
           end if
       end while
   end if
   return \rho^{W}
```

References

- Vitaly Aksenov, Dan Alistarh, and Janne H. Korhonen. Relaxed scheduling for scalable belief propagation. In *Proceedings of NeurIPS*, 2020.
- Hans A. Bethe. Statistical theory of superlattices. *Proceedings of the Royal Society A*, 150 (871):552–575, 1935.
- Kurt Binder. Finite size effects on phase transitions. Ferroelectrics, 73(1):43-67, 1987.
- Edouard Brezin and Jean Zinn-Justin. Finite size effects in phase transitions. *Nuclear Physics*, B257(FS14):867–893, 1985.
- Michael Chertkov and Vladimir Y. Chernyak. Loop series for discrete statistical models on graphs. *Journal of Statistical Mechanics: Theory and Experiment*, 2006(6):P06009, 2006.
- Gregory F. Cooper. The computational complexity of probabilistic inference using Bayesian belief networks. *Artificial intelligence*, 42(2-3):393–405, 1990.
- Thomas Cover and Joy Thomas. Elements of Information theory. John Wiley & Sons, 1991.
- Roland L. Dobrushin. The description of the random field by its conditional distributions and its regularity conditions. *Theory of Probability and its Applications*, 13(2):197–224, 1968.
- Paul Erdos and Alfred Renyi. On random graphs I. *Publicationes Mathematicae*, 6(3–4): 290–297, 1959.
- Brendan J. Frey and David J.C. MacKay. A revolution: Belief propagation in graphs with cycles. In *Proceedings of NIPS*, 1997.
- Robert G. Gallager. Low-density parity-check codes. *IEEE Transactions on Information Theory*, 8(1):21–28, 1962.
- Hans-Otto Georgii. Gibbs measures and phase transitions. De Gruyter, 1988.
- Gene H. Golub and Charles F. Van Loan. *Matrix Computations*. The Johns Hopkins University Press, 4th edition, 2013.
- Tom Heskes. Stable fixed points of loopy belief propagation are minima of the Bethe free energy. In *Proceedings of NIPS*, 2003.
- Tom Heskes. On the uniqueness of loopy belief propagation fixed points. *Neural Computation*, 16(11):2379–2413, 2004.
- Tom Heskes. Convexity arguments for efficient minimization of the Bethe and Kikuchi free energies. *Journal of Artificial Intelligence Research*, 26(1):153–190, 2006.
- Kerson Huang. Statistical mechanics. John Wiley & Sons, 2nd edition, 1987.
- Alexander T. Ihler. Accuracy bounds for belief propagation. In *Proceedings of UAI*, 2007.

- Alexander T. Ihler, John W. Fisher, and Alan S. Willsky. Loopy belief propagation: convergence and effects of message errors. *Journal of Machine Learning Research*, 6(1):905–936, 2005.
- Ernst Ising. Beitrag zur Theorie des Ferromagnetismus. Zeitschrift für Physik, 31(1):253–258, 1925.
- Michael I. Jordan, Zoubin Ghahramani, Jaakkola Tommi S., and Lawrence K. Saul. An Introduction to Variational Methods for Graphical Models. *Machine Learning*, 37:183–233, 1999.
- Ryoichi Kikuchi. A theory of cooperative phenomena. *Physical Review*, 81(6):988–1003, 1951.
- Dongmin Kim, Suvrit Sra, and Inderjit S. Dhillon. Tackling box-constrained optimization via a new projected quasi-Newton approach. SIAM Journal on Scientific Computing, 32 (6):3548–3563, 2010.
- Christian Knoll and Franz Pernkopf. On loopy belief propagation Local stability analysis for non-vanishing fields. In *Proceedings of UAI*, 2017.
- Christian Knoll and Franz Pernkopf. Belief propagation: accurate marginals or accurate partition function where is the difference? *Journal of Statistical Mechanics: Theory and Experiment*, 2020(12):124009, 2020.
- Christian Knoll, Michael Rath, Sebastian Tschiatschek, and Franz Pernkopf. Message Scheduling Methods for Belief Propagation. In *Machine Learning and Knowledge Discovery in Databases*, pages 295–310. Springer, 2015.
- Daphne Koller and Nir Friedman. Probabilistic Graphical Models: Principles and Techniques. MIT press, 2009.
- Steffen L. Lauritzen and David J. Spiegelhalter. Local computations with probabilities on graphical structures and their application to expert systems. *Royal Statistical Society*, 50 (2):157–224, 1988.
- Harald Leisenberger, Franz Pernkopf, and Christian Knoll. Fixing the Bethe approximation: How structural modifications in a graph improve belief propagation. In *Proceedings of UAI*, 2022.
- David J. C. MacKay. *Information Theory, Inference, and Learning Algorithms*. Cambridge University Press, 6th edition, 2003.
- Ofer Meshi, Ariel Jaimovich, Amir Globerson, and Nir Friedman. Convexifying the Bethe free energy. In *Proceedings of UAI*, 2009.
- Marc Mezard and Andrea Montanari. *Information, Physics, and Computation*. Oxford University Press, 2009.
- Joris Mooij and Bert Kappen. Validity estimates for loopy belief propagation on binary real-world networks. In *Proceedings of NIPS*, 2004.

- Joris M. Mooij and Hilbert J. Kappen. On the properties of the Bethe approximation and loopy belief propagation on binary networks. *Journal of Statistical Mechanics: Theory and Experiment*, 2005(11):P11012, 2005.
- Joris M. Mooij and Hilbert J. Kappen. Sufficient conditions for convergence of the sumproduct algorithm. *IEEE Transactions on Information Theory*, 53(12):4422–4437, 2007.
- Joris M. Mooij and Hilbert J. Kappen. Bounds on marginal probability distributions. In *Proceedings of NIPS*, 2008.
- Kevin P. Murphy, Yair Weiss, and Michael I. Jordan. Loopy belief propagation for approximate inference: An empirical study. In *Proceedings of UAI*, 1999.
- Jorge Nocedal and Stephen J. Wright. Numerical optimization. Springer, 2006.
- Lars Onsager. Crystal statistics. I. A two-dimensional model with an order-disorder transition. *Physical Review, Series II*, 65(3–4):117–149, 1944.
- Payam Pakzad and Venkat Anantharam. Estimation and marginalization using the Kikuchi approximation methods. *Neural Computation*, 17(8):1836–1873, 2005.
- Giorgio Parisi. Statistical Field Theory. Addison-Wesley, 1988.
- Judea Pearl. Probabilistic Reasoning in Intelligent Systems: Networks of Plausible Inference. Morgan Kaufmann Publishers, 1988.
- Rudolf E. Peierls. Statistical theory of superlattices with unequal concentrations of the components. *Proceedings of the Royal Society A*, 154(881):207–222, 1936.
- Alessandro Pelizzola. Cluster variation method in statistical physics and probabilistic graphical models. *Journal of Physics A: Mathematical and General*, 38(33):R309–R339, 2005.
- Frederick Reif. Fundamentals of statistical and thermal physics. McGraw-Hill, 1965.
- R. Tyrrell Rockafellar. Convex Analysis. Princeton University Press, 1970.
- Nicholas Ruozzi. Beyond log-supermodularity: lower bounds and the Bethe partition function. In *Proceedings of UAI*, 2013.
- Jinwoo Shin. Complexity of Bethe approximation. In Proceedings of AISTATS, 2012.
- Barry Simon. A remark on dobrushin's uniqueness theorem. Communications in Mathematical Physics, 68(2):183–185, 1979.
- Charles Sutton and Andrew McCallum. Improved dynamic schedules for belief propagation. In *Proceedings of UAI*, 2007.
- Nobuyuki Taga and Shigeru Mase. Error bounds between marginal probabilities and beliefs of loopy belief propagation algorithm. In *Proceedings of MICAI*, 2006a.
- Nobuyuki Taga and Shigeru Mase. Applications of Gibbs measure theory to loopy belief propagation algorithm. In *Proceedings of MICAI*, 2006b.

- Sekhar C. Tatikonda. Convergence of the sum-product algorithm. In *Proceedings of IEEE Information Theory Workshop*, 2003.
- Sekhar C. Tatikonda and Michael I. Jordan. Loopy belief propagation and Gibbs measures. In *Proceedings of UAI*, 2002.
- Joseph M. Thomas. Sturm's theorem for multiple roots. *National Mathematics Magazine*, 15(8):391–394, 1941.
- Gerard Toulouse. Theory of the frustration effect in spin glasses: I. Communications on Physics, 2(4):115–119, 1977.
- Leslie G. Valiant. The complexity of computing the permanent. Theoretical Computer Science, 8(2):189–201, 1979.
- Pascal O. Vontobel. Counting in graph covers: A combinatorial characterization of the Bethe entropy function. *IEEE Trans. on Information Theory*, 59(9):6018–6048, 2013.
- Martin J. Wainwright, Tommi S. Jaakkola, and Alan S. Willsky. A new class of upper bounds on the log partition function. *IEEE Transactions on Information Theory*, 51(7): 2313–2335, 2005.
- Martin J. Wainwright, Michael I. Jordan, et al. Graphical models, exponential families, and variational inference. Foundations and Trends in Machine Learning, 1(1–2):1–305, 2008.
- Yusuke Watanabe and Kenji Fukumizu. Graph zeta function in the Bethe free energy and loopy belief propagation. In *Proceedings of NIPS*, 2009.
- Yair Weiss. Correctness of local probability propagation in graphical models with loops. Neural Computation, 12(1):1–41, 2000.
- Adrian Weller and Tony Jebara. Bethe bounds and approximating the global optimum. In *Proceedings of AISTATS*, 2013.
- Adrian Weller and Tony Jebara. Approximating the Bethe partition function. In *Proceedings* of UAI, 2014a.
- Adrian Weller and Tony Jebara. Clamping variables and approximate inference. In *Proceedings of NIPS*, 2014b.
- Adrian Weller, Kui Tang, Tony Jebara, and David Sontag. Understanding the Bethe approximation: When and how can it go wrong? In *Proceedings of UAI*, 2014.
- Max Welling and Yee W. Teh. Belief optimization for binary networks: A stable alternative to loopy belief propagation. In *Proceedings of UAI*, 2001.
- Alan S. Willsky, Erik B. Sudderth, and Martin J. Wainwright. Loop series and Bethe variational bounds in attractive graphical models. In *Proceedings of NIPS*, 2007.
- Philip Wolfe. Convergence conditions for ascent methods. SIAM Review, 11(2):226–235, 1969.

- Chen Yanover and Yair Weiss. Approximate inference and protein-folding. In *Proceedings* of NIPS, 2002.
- Jonathan S. Yedidia, William T. Freeman, and Yair Weiss. Bethe free energy, Kikuchi approximations, and belief propagation algorithms. In *Proceedings of NIPS*, 2001.
- Jonathan S. Yedidia, William T. Freeman, and Yair Weiss. Constructing free energy approximations and generalized belief propagation algorithms. *IEEE Transactions on Information Theory*, 51(7):2282–2312, 2005.
- Julia M. Yeomans. Statistical mechanics of phase transitions. Oxford University Press, 1992.
- Alan L. Yuille. CCCP algorithms to minimize the Bethe and Kikuchi free energies: Convergent alternatives to belief propagation. *Neural Computation*, 14(7):1691–1722, 2002.
- Lenka Zdeborová and Florent Krzakala. Statistical physics of inference: Thresholds and algorithms. Advances in Physics, 65(5):453–552, 2016.